UNIVERSITY OF CALIFORNIA,
IRVINE

Effects of Dung and Biomass Emissions on Macrophage Defenses, Gene Regulation, and Cellular Metabolism

DISSERTATION

submitted in partial satisfaction of the requirements
for the degree of

DOCTOR OF PHILOSOPHY

in Environmental Health Sciences

by

Jessica Estefania Monterrosa Mena

Dissertation Committee:
Professor Rufus Edwards, Chair
Adjunct Professor Michael T. Kleinman
Professor Masashi Kitazawa

2023

DEDICATION

To

my partner, Cecilia, my mother, and my siblings

in recognition of their support, encouragement, and love

TABLE OF CONTENTS

LIST OF FIGURES

LIST OF TABLES

LIST OF ABBREVIATIONS

5,5’-dithiobis-2-nitrobenzoic acid (DTNB)

3-(4, 5-dimethylthiazolyl-2)-2, 5-diphenyltetrazolium bromide (MTT)

9, 10 phenanthrenequinone (PQN)

Adenosine triphosphate (ATP)

Analysis of variance (ANOVA)

Area under the curve (AUC)

Bromodeoxyuridine (BrdU)

Carbon dioxide (CO_2)

Carbon monoxide (CO)

Coefficient of variance (CV)

Complementary deoxyribonucleic (cDNA)

Chronic obstructive pulmonary disease (COPD)

Deionized water (DI)

Deoxyribonuclease (DNase)

Dithiothreitol (DTT)

Dimethyl sulfoxide (DMSO)

Elemental carbon (EC)

Ethanol (etOH)

Ethylenediaminetetraacetate (EDTA)

Fetal Bovine Serum (FBS)

Fine particulate matter ($PM_{2.5}$)

Glucose-6-phosphate dehydrogenase (G6pd)

Glutathione (GSH)

Glutathione peroxidase enzyme (Gpx)

Glutathione peroxidase-1 (Gpx1)

Glutathione reductase (Gsr)

Glyceraldehyde 3-phosphate dehydrogenase (Gapdh)

High-performance liquid chromatography–photodiode array–high resolution mass spectrometry (HPLC-PDA-HRMS)

High temperature to low temperature VOC ratio (high/low VOC ratio)

Humic-like substances (HULIS)

Lactate dehydrogenase (LDH)

Lipopolysaccharide (LPS)

Microgram (µg)

Microliter (µL)

Micrometer (µm)

Micromolar (µM)

Milligram (mg)

Milliliter (mL)

Millimolar (mM)

Minutes (Min)

Modified combustion efficiency (MCE)

Messenger RNA (mRNA)

NADPH oxidase (NOX)

NAD(P)H: quinone oxidoreductase 1 (Nqo1)

Nanospray desorption electrospray ionization–high resolution mass spectrometry (nano-DESI-HRMS)

Nicotinamide adenine dinucleotide (NADH)

Nicotinamide adenine dinucleotide phosphate (NADPH)

Nuclear factor erythroid 2–related factor 2 (Nrf2)

Organic carbon (OC)

Oxidative potential (OP)

Oxidized glutathione disulfide (GSSG)

P-value (P)

Particulate matter (PM)

Phorbol 12-myristate 13-acetate (PMA)

Phosphate buffered saline (PBS)

Picomole (pmol)

Polycyclic aromatic hydrocarbons (PAHs)

Polytetrafluoroethylene (PTFE)

Propidium Iodine (PI)

Quantitative real time polymerase chain reaction (qRT-PCR)

Reduction-oxidation (redox)

Residual oil fly ashes (ROFAs)

Ribonucleic acid (RNA)

Reactive oxygen species (ROS)

Standard Deviation (SD)

Standard error of the mean (SEM)

Standard reference material 1648a (SRM 1648a)

Secondary organic aerosols (SOAs)

Summed 16 PAHs (ΣPAH)

Time (t)

Tris(hydroxymethyl)aminomethane (TRIS)

Volatile organic compounds (VOCs)

ACKNOWLEDGEMENTS

I would like to acknowledge all the friends, family, and loved ones who cheered me on over the seven-year pursuit of my Ph.D. I express my deepest gratitude to my partner, Cecilia, for unwaveringly urging me to embrace the lessons from my errors, to maintain a positive outlook throughout this research journey, and offering an abundance of heartfelt encouragement.

I would also like to thank the many friends and colleagues whose encouragement and kind companionship have been invaluable throughout these years. Special thanks to Samantha Renusch, my first acquaintance at the Kleinman lab, who adeptly guided me through the intricacies of the air pollution lab and introduced me to the fundamentals of macrophage cell culture. My heartfelt gratitude extends to all my colleagues at Kleinman lab- Dr. David Herman, Dr. Rebecca Johnson Arechavala, Elizabeth Choy, Jayvee Bautista, Bishop Bliss, Irene Hasan, Amanda Ting, and many more- for their unwavering camaraderie, continuous assistance, and abundant wellspring of inspiration. I would also like to thank Dr. Robert Weltman for his assistance with this project, particularly his expertise in particle collection and chemical analytical methods, which were invaluable in the completion of this project. Lastly, a sincere thank you to my cohort members, the most fun and brilliant study companions one could ask for.

I would like to acknowledge the support received from my committee co-chairs, Professor Edwards and Professor Kleinman, for their invaluable mentorship and consistent support. Their guidance, feedback, and dedication to my professional growth have been instrumental. Their expertise in air pollution science laid the foundation for my journey through this advanced degree.

I extend my gratitude to various collaborators whose assistance, provision of lab equipment, cell lines, and diverse reagents were invaluable to this endeavor. I extend my thanks to Professor Kitazawa, a member of my committee, as well as to Dr. Sharon Lim and Dr. Jay Hsu from the Kitazawa lab for their support. I also owe a debt of gratitude to Professor Manabu Shiraiwa and Dr. Ting Fang for guiding me through atmospheric and particle chemistry-based experiments. My appreciation also goes to Professor Angela Fleischman and Dr. Gaja Ramanathan for their guidance with flow cytometry-based experiments. The expertise, mentorship, and optimism from these collaborators were crucial, and I'm grateful for their enduring support over the years.

This research received support from EPA STAR R83503601- Characterization of Emissions for Small, Variable, Solid Fuel Combustion Sources for Determining Global Emissions and Climate Impact and R835425- Impacts of Household Sources on Outdoor Pollution at Village and Regional Scales in India. The contents are solely the responsibility of the authors and do not necessarily represent the official views of the U.S EPA. The U.S. EPA does not endorse the purchase of any commercial products or services mentioned in the publication.

VITA

Jessica Estefania Monterrosa Mena

Education

2023	Doctor of Philosophy in Environmental Health Sciences. University of California- Irvine. Department of Environmental and Occupational Health. Environmental Toxicology track.
2014	Bachelor of Arts. Williams College. Honors in Chemistry. Biochemistry and Molecular Biology concentration.

Experience

2016-2023	Graduate Student Researcher. U.C. Irvine, Air Pollution Health Effects Laboratory
2021-2023	Associate Instructor; Teaching Assistant. U.C. Irvine, Department of Public Health
2014-2016	Research Associate I. Cedars-Sinai Medical Center, Los Angeles, CA
2012-2014	Chemistry Teaching Assistant. Williams College, MA
2013	Neuroscience Research Summer Intern. University of Miami Miller Medical School, FL
2011-2014	Chemistry Research Assistant and Student Fellow. Williams College, MA
2010-2011	Biology Research Assistant**.** Williams College, MA

Fellowships and Professional Honors

2020-2023	Rose Hill Foundation Science & Engineering Fellowship
2020-2022	U.C. Irvine Department of Environmental and Occupational Health Research Fellowship
2016	U.C. Irvine Graduate Opportunity Fellowship
2016	U.C. Irvine DECADE Competitive Edge Program Member *Certification: Mentoring Excellence, U.C. Irvine Graduate Division*
2013	Williams College Guadino Travel Fellowship
2010	Heart of Los Angeles Scholarship

Appointments and Activities

2021-2022	American Heart Association FIT& Early Career Blog Author
2020	Decade Competitive Edge summer Mentor
2018-2020	The Loh Down on Science Scriptwriter and Student Fellow
2017-2021	The BIOTA Project Content Creator
2017-2018	Brews and Brains Event Organizer
2012-2013	Williams College Biochemistry and Molecular Biology 1960's Scholar
2010-2018	Heart of Los Angeles Alumni Association Mentor

Professional Memberships

2020-2022	Society of Toxicology Member,
2021	American Heart Association Member
2014 *(elected)*	Sigma Xi Scientific Research Society

Peer-Reviewed Publications

Ramanathan G, Chen JH, Mehrotra N, Trieu T, Huang A, Mas E, Monterrosa Mena JE, Bliss B, Herman DA, Kleinman MT, Fleischman AG. Cigarette smoke stimulates clonal expansion of Jak2V617F and Tet2-/- cells. *Front Oncol*. 2023;13:1210528. doi:10.3389/fonc.2023.1210528

Fang, T., Huang, Y. K., Wei, J., Monterrosa Mena, J. E., Lakey, P. S. J., Kleinman, M. T., Digman, M. A., & Shiraiwa, M. Superoxide Release by Macrophages through NADPH Oxidase Activation Dominating Chemistry by Isoprene Secondary Organic Aerosols and Quinones to Cause Oxidative Damage on Membranes. *Environ Sci Technol*. 2022;56(23):17029-17038. doi:10.1021/acs.est.2c03987

Shi, J., Dai, W., Chavez, J., Carreno, J., Zhao, L., Kleinman, MT., Arechavala, RJ., Hasen, I., Ting, A., Bliss, B., Monterrosa Mena, JE., Kloner, RA. One Acute Exposure to E-Cigarette Smoke Using Various Heating Elements and Power Levels Induces Pulmonary Inflammation. *SSRN Journal*. Published online 2022. doi:10.2139/ssrn.4010908

Liang J., Liu N., Xue L., Monterrosa Mena J, Xie T., Geng Y., Huan C., Zhang Y., Taghavifar F., Huang G., Kurkciyan A., Barron V., Jiang D, Noble P.W. Mitogen-activated Protein Kinase–activated Protein Kinase 2 Inhibition Attenuates Fibroblast Invasion and Severe Lung Fibrosis. *Am J Respir Cell Mol Biol*. 2019;60(1):41-48. doi:10.1165/rcmb.2018-0033OC

Cheng H, Dove NC, Mena JM, Perez T, Ul-Hasan S. The Biota Project: A Case Study of a Multimedia, Grassroots Approach to Scientific Communication for Engaging Diverse Audiences. *Integrative and Comparative Biology*. 2018;58(6):1294-1303. doi:10.1093/icb/icy091

Liang J, Zhang Y, Xie T, Liu N, Chen H, Geng Y, Kurkciyan A, Mena JM, Stripp BR, Jiang D, Noble PW. Hyaluronan and TLR4 promote surfactant-protein-C-positive alveolar progenitor cell renewal and prevent severe pulmonary fibrosis in mice. *Nat Med*. 2016;22(11):1285-1293. doi:10.1038/nm.4192

Li Y, Liang J, Yang T, Monterrosa Mena J, Huan C, Xie T, Kurkciyan A, Liu N, Jiang D, Noble PW. Hyaluronan synthase 2 regulates fibroblast senescence in pulmonary fibrosis. *Matrix Biology*. 2016;55:35-48. doi:10.1016/j.matbio.2016.03.004

Huan C, Yang T, Liang J, Xie T, Cheng L, Liu N, Kurkciyan A, Monterrosa Mena J, Wang C, Dai H, Noble PW, Jiang D. Methylation-mediated BMPER expression in fibroblast activation in vitro and lung fibrosis in mice in vivo. *Sci Rep*. 2015;5(1):14910. doi:10.1038/srep14910

Select Scientific Abstracts

JE. Monterrosa Mena, H. Hsu, RJ. Arechavala, I. Hasen, A. Ting, B. Bliss, J. Shi, W. Dai, JN Chavez, J. Carreno, L.Zhao, R. Kloner, MT. Kleinman. Inflammatory Gene Expression Changes and Immune System Depression in Rats Exposed to a Single 4-hr Exposure to Electronic Cigarette Vapor. University of California, Irvine. American Heart Association Scientific Sessions 2022.

J. E. Monterrosa Mena, M. Kleinman, and R. Edwards. Source-Specific Particle Matter Chemical Characteristics Influences RAW 264.7 Macrophage Immune Function and Cell Cycle Progression. University of California Irvine, Irvine, CA. Society of Toxicology 61st Annual Meeting, 2022.

J. E. Monterrosa Mena, F. Khalaj, C. Faiola, and M. T. Kleinman. Characterizing Atmospheric Particle Toxicity from Biogenic and Anthropogenic Sources Using In Vitro Assays. University of California Irvine, Irvine, CA. Society of Toxicology 59th SOT Annual Meeting, 2020.

J. Monterrosa Mena, M.T. Kleinman. Lung Inflammation Mediates Hepatic Pro-Inflammatory Responses Leading to Altered Lipid Metabolism. University of California-Irvine 2016 Research Symposium Day.

ABSTRACT OF THE DISSERTATION

Effects of Dung and Biomass Emissions on Macrophage Defenses, Gene Regulation, and Cellular Metabolism

by

Jessica Estefania Monterrosa Mena

Doctor of Philosophy in Environmental Health Sciences

University of California, Irvine, 2023

Professor Rufus Edwards, Chair

Introduction: Human exposure to biomass smoke particulate matter has been documented to induce immunomodulatory effects that can promote respiratory and cardiovascular injuries. Despite the prevalent use of solid fuels and the potential detrimental impact on global health, the effects of specific solid biomass fuels on innate immune cell function remains poorly understood. Therefore, I aimed to begin to fill this gap by studying the effects of acute exposure to particulate matter emissions from dung and mixtures of dung with brushwood used with chulha and angithi traditional cookstoves commonly used in India, collected from in-field sampling.

Methods: Particles collected on to Teflon filters in-field were extracted into aqueous suspension for cell-free and cellular *in vitro* toxicity assessment. The intrinsic cell-free oxidative capacity of particulate matter samples was compared to urban particulate matter and a single diesel quinone compound using dithiothreitol measures. Biological toxicity was assessed using submerged culture exposure with the macrophage-like RAW 264.7 cell line. Biological dose response changes in viability and innate immune function were assessed following four-hour exposures. Biochemical approaches were used to evaluate respiratory burst, metabolic activity, cell cycling

dynamics, and gene expression changes. Associations between combustion emission factors, particle oxidative potential, and biological effects were evaluated using multivariate analysis to explore how particle toxicity is influenced by combustion processes.

Results: PM emissions from dung-angithi combustion had higher oxidative potential measures than emissions from solid fuel use with chulha cookstoves. The oxidative potential of emissions from dung-chulha cookstoves were lower compared to all other sources of PM including urban dust and quinone compounds. Acute four-hour exposure to solid biomass particles altered critical innate immune respiratory burst function but did not reduce cell viability. Gene expression changes were observed following acute exposures in macrophages exposed to all the air pollutants studied here, including the downregulation of antioxidant response element transcription factor *Nrf2* and antioxidant *Gpx*1, yet an upregulation of detoxifying enzyme *Nqo1*. However, differential gene expression patterns were observed for antioxidant *Gsr*, and metabolic housekeeping gene *G6pd*. The degree of particle reduction-oxidation (redox) activity, and biological respiratory burst dynamics and gene expression changes were associated with pyrolysis combustion processes that influence the generation of volatile organic compounds.

Conclusions: In summary, this dissertation describes differences in the toxicity of air pollution particles from distinct sources. Particles generated by the combustion dung fuel and dung brushwood mixtures combustion commonly used with chulha and angithi cookstoves, induce innate immune cell changes through distinct mechanisms compared to urban dust and quinone. This study provides valuable insight into flaming, smoldering, and pyrolysis combustion processes that contribute to air pollution compositional differences and particle toxicity related to household cooking with solid biomass fuels.

1. Introduction

1.1 Overview of solid fuel use

More than 3 billion people worldwide rely on solid biomass fuels such as firewood, crop residues, charcoal, and animal waste as a main source of energy for the home [1,2]. Solid biomass fuels are commonly used for daily cooking, heating, and lighting in low- and middle-income countries and rural communities because the materials tend to be readily available and cheaper alternatives to cleaner fuels, such as liquid petroleum gas. While estimates vary, over 80% of people in sub-Saharan Africa, more than 60% of people in Southeast Asia, and upwards of 50% of people in Latin America rely on solid fuels [3–5]. Wood, crop residue, and dung materials are commonly burned inside households' living quarters without proper ventilation leading to pollutant levels that exceed the World Health Organizations' (WHO) guidelines for indoor air quality and have major global health impacts. Epidemiological studies have reported strong associations between indoor solid fuel use and adverse health effects. Exposure to pollutants from solid fuel smoke has been linked to chronic heart and lung diseases, cancers, immune defense dysfunctions, pneumonia, tuberculosis, low birth weight, diabetes mellitus, and premature death [2]. These detrimental health effects are particularly concerning for individuals who spend most of their time in the kitchen and indoors, such as such as women and children. Household air pollution from the use of solid fuels for cooking stands as a primary risk factor for global disease burden, with the WHO estimating that exposure to household air pollution was responsible for 3.2 million deaths in 2020 from heart disease, stroke, lower respiratory infection, chronic obstructive pulmonary disease (COPD) and lung cancer globally [2].

Although economic growth has led to reduced reliance on solid biomass fuels in certain global regions and the fraction of the population using solid fuels has declined, the expanding human population has resulted in an increase in households persistently utilizing solid biomass fuels [6–8]. The most populous countries, India, and China, which see some of the world's highest ambient air pollution concentrations, together account for about 30% of the world's population or about 3 billion people. In 2010, it was estimated that these regions accounted for nearly 90% of the estimated global deaths from household air pollution attributed to cooking with solid fuels [9]. Most of the black carbon and organic carbon emissions in India and China can be attributed to residential coal and solid biomass fuel use, as opposed to other countries such as the United states where industrial and mobile emission are the dominant contributor of black carbon and organic carbon [10]. In India, wood, crop residues, and dung cake fuels fulfill about 75% of the nation's domestic energy needs and citizens there experience the highest levels of air pollution related fatalities and disease burden globally; exposure to solid biomass fuel emissions is attributed to causing 662,000 annual deaths annually [11,12]. Dung serves as the predominant household cooking fuel in the Indian subcontinent, with India reported to have the highest population utilizing dung fuels for cooking compared to any other country [13]. Solid fuels are expected to continue playing a crucial role as a significant source of household energy in India, China, and sub-Saharan Africa, stressing the significance of discerning the components of solid biomass fuel emissions that are most hazardous to human health and identifying solutions to protect poor households that rely on solid fuels.

1.2 Adverse health outcomes from solid fuel smoke exposure

Inhalable PM deposits in the respiratory tract and damages lung tissues by directly impairing cell membranes, and promoting oxidative stress and inflammation, which are well known

mechanisms associated with air pollution related pathologies [14]. PM from combustion sources (fuel oil burning and diesel exhaust) in addition to causing effects in the lung, also cause significant effects on the cardiovascular system [15]. Women in rural Indian villages who are exposed to indoor air pollution from solid biomass fuels use with traditional cookstoves have a greater prevalence of hypertension and tachycardia compared to those who cook in liquid petroleum gas (LPG) [16]. These cardiovascular effects were linked to systemic inflammation and oxidative stress biomarkers, contributing to evidence that solid biofuel smoke predisposes women to cardiovascular disease development [16]. Higher levels of pro-inflammatory cytokines and systemic oxidative stress markers were found in blood collected from solid biomass fuel users, but the differences between the chemical components of solid biomass fuel smoke and LPG emissions that contribute to these differences in cardiopulmonary function were not identified. In a follow up study, this research team also found higher numbers of pulmonary airway and immune cells, increased levels pro-inflammatory cytokines and chemokines, and markers of oxidative stress in the sputum of women who cook with solid biomass fuels compared to those who use LPG [17]. The health effects and cellular-level changes reported in solid biomass fuel users provide insight into the mechanisms of toxicity from indoor air pollution, but few studies compare the toxicity and health impacts arising from specific fuel and stove combinations and how these combinations influence smoke composition.

A major limitation of human health effects exposure studies is that households usually rely on whichever mixture of solid biomass fuels are readily available and those vary over time. However, fuel type and stove combinations are likely a critical factor contributing to poor health outcomes from household air pollution. In an investigation comparing the respiratory impact of chronic smoke exposure in women who used either solid biomass fuels with traditional indoor

cookstoves or LPG stoves, spirometry assessments indicated that nearly 30% of solid fuel users had reduced lung function compared to only 16% of LPG users [18]. The prevalence of reduced lung function and a diagnosis of COPD was highest amongst women who used dung fuels compared to those who primarily use wood or crop residues. The findings imply that specific fuels contribute to unique mechanisms promoting upper and lower respiratory symptoms and dyspnea, but detailed chemical characterization of the cookstoves emissions associated with these fuel-specific health effects remain unknown. In addition, few studies provide insight into how dung fuel emissions contribute to disease and toxicity.

1.3 Toxicity of specific components in solid fuel emissions

Fine particulate matter, particles with a median aerodynamic diameter smaller of 2.5 microns ($PM_{2.5}$), emitted from solid mass burning stoves can remain elevated in homes for many hours following cooking events and indoor air concentrations often exceed the WHO's Indoor Air Quality annual average concentration guideline of 5 $\mu g/m^3$ for $PM_{2.5}$ emissions [19]. $PM_{2.5}$ can infiltrate deep into the lungs and deposit in the alveoli, where it can penetrate the body's defenses. Smoke emitted from burning solid biofuels is a complex mixture of respirable pollutants, including carbon monoxide (CO), carbon dioxide (CO_2), coarse (Dp > 2.5 μm), fine (Dp ≤2.5 μm), and ultrafine PM (Dp ≤ 0.1 μm), nitrogen and sulfur oxides, volatile organic compounds (VOCs), and polycyclic aromatic hydrocarbons (PAHs), all of which are associated with morbidity and mortality [14]. In addition, the combustion of solid biomass fuels results in the release of thousands of individual pollutants. The emission factors, a metric linking pollutant quantity released to an associated activity (typically expressed as pollutant weight per unit of fuel burned), and the chemical composition of these biomass burning emissions are significantly influenced by fuel source, stove type, and burn rates, adding complexity to our comprehension of

the biological toxicity resulting from solid biomass smoke. Emission factors of $PM_{2.5}$ from smoldering combustion, which refers to the prolonged, low temperature, and flameless burning of fuels, are more than double the values observed in flaming combustion processes [20]. This inefficient burning of solid biomass fuels also results in emissions of higher amounts of incomplete combustion compounds, such as CO, compared to more efficient flaming processes. Flaming combustion converts more of the biomass fuels to complete combustion products such as CO_2 and water vapor. Solid biomass fuel emissions vary drastically due to factors such as temperature fluctuations during burning events, surface to volume ratios of fuels, and moisture content of fuels, which may explain the diversity of health effects and biological toxicity from solid biomass fuels observed in biological studies. Chemicals found on the PM surface likely initiate disease promoting cellular mechanisms that result in the unique cellular toxicity and differences in adverse health effects arising from diverse air pollutant sources.

The toxicity of PM from distinct types of wood can vary greatly and combustion conditions strongly impact differences in toxicity even for the same fuel source [21–25]. Rodent exposure studies comparing the toxicity of laboratory biomass emissions produced by various American forest biomass fuels have established that combustion conditions (flaming or smoldering) influence the concentration and composition of pollutants generated, as well as the degree of pulmonary toxicity from red oak, peat, pine needles, eucalyptus, and pine materials. Kim *et al*. showed that smoldering combustion has higher emission factors of PM compared to flaming combustion, and biological toxicity of emissions for each biomass material varies. For instance, differential *in vitro* immune and pro-inflammatory responses in the lung and bacterial mutagenicity were observed based on the distinct combustion phase from which the particles originated [22,23]. Bolling *et al*. reported that combustion temperature may influence *in vitro*

immune cell toxicity. Cultures of mixed monocyte and pneumocyte cells exposed to particles released from the medium temperature (500-800 ºC) combustion of birch and fir wood mixtures using a cast-iron woodstove demonstrate reduced cell numbers (indicated by cell death) and higher releases of lactate dehydrogenase (an indicator of cell membrane permeability and cellular toxicity), compared to cells exposed to wood emissions from high-temperature (700-1000 ºC) combustion or particles representative of traffic related PM [21]. This study also revealed complex trends in the induction of various pro-inflammatory markers with traffic related particles and medium-temperature wood particles inducing a higher release of specific inflammatory markers like, IL-6 that are usually produced concurrently with other inflammatory cytokines (IL-1 and TNF-α), compared to high-temperature wood. Surprisingly, different patterns for cytokines such as IL-8 were observed, which is a chemoattractant agent that attracts and activates inflammatory cells. In summary, *in vivo* and *in vitro* studies demonstrate that pollutant emission factors, which vary according to fuel type and the specific combustion conditions during the burning event are determining factors in the toxicity profiles of solid biomass fuels, but the specific toxicological effects of distinct solid fuels such as dung is currently not well studied.

1.4 Identifying biochemical markers to relate stove-fuel combinations to toxicity

1.4.1 Oxidative potential

One of the main underlying chemical characteristics of particulate matter thought to drive biological toxicity is oxidative potential. Oxidative potential (OP) refers to the ability of PM to trigger reactive oxygen species (ROS) formation and induce cellular oxidative stress. Oxidative stress occurs when cellular ROS generation overwhelms the innate antioxidant responses and can result in deteriorated cell functions. OP can be evaluated using acellular and cellular methods to

determine the rate of ROS generation and antioxidant consumption by various air pollutants. PM is known to promote biological ROS generation, in part due to the absorbed chemical species on the particle surface. $PM_{2.5}$ is composed of elemental carbon and organic carbon, and components such as metals that can adhere to the particle surface. Compounds such as metals and quinones can directly participate in Fenton and redox-cycling reaction, while some PAHs can undergo oxidative reaction on the particle surface and result in increased redox activity. This ability of surface-bounds PAHS to undergo oxidative reactions and form surface-bound quinone-like species with high redox potential has been observed for soot, which are fine black carbon-based particles and are characteristic of incomplete combustion [26]. Soot particles are highly enriched with PAHs, which drive their carcinogenic effects [27]. Although OP has some limitations in predicting biological toxicity, it provides a metric relevant to health effect mechanisms associated with PM induced diseases.

Regional OP of ambient PM is associated with distinct sources of atmospheric pollutants. In Delhi, India, atmospheric air samples from regional events occurring in 2019 such as post monsoon dry season, Diwali holiday festivals with firework activity, and a winter fog period demonstrated different average mass concentrations of $PM_{2.5}$, distinct volume normalized PM OP measures, and chemical patterns linked to each of those events. The mass concentration of $PM_{2.5}$ and their intrinsic OP normalized by volume were highest during the winter fog period when atmospheric inversions intensify ambient PM concentrations at a time when biomass burning is prevalent. Additionally, each event had a unique chemical signature attributed to different air pollutant sources such as elevated chloride and potassium ions attributed to biomass burning during the winter fog period, while secondary sulfates and crustal elements associated with traffic and resuspended dust sources were more common during the post monsoon season.

A high OP in atmospheric air samples from cities with high levels of biomass burning has been reported in multiple studies, particularly in the winter time when residential solid biomass fuel burning is common [28–30].

Ambient PM oxidative properties contribute to poor health outcomes for those in Atlanta, Georgia, with a high OP positively correlating with emergency department visits for wheezing, asthma, and congestive heart failure [31]. Biomass burning activity in Georgia accounted for the elevated OP assessed with the dithiothreitol (DTT) assay, a commonly used measure of particle redox activity. Biomass burning activity contributed the largest fraction of total historical OP within the nearly 10-year study period, contributed to 45% of the overall DTT activity, which was higher than the contribution of light-duty gasoline vehicles and heavy-duty diesel vehicles. The high DTT activity values occurred in the wintertime when prescribed burns occur in the region. In India, episodic pollution events from fireworks in Delhi cause elevated levels of ambient PM and have been associated with excess cases of mortalities and hospital admissions [32]. In Latin America and South America, high levels of biomass smoke from prescribed burn episodes have also led to increased hospital admission and morbidity amongst sugar cane workers [33,34]. The OP of pollutants and their links to excess hospitalization from episodic events with high atmospheric pollutants, suggests that particle induced oxidative stress contributes to poor health outcomes, and therefore it is important to understand the oxidative properties unique to solid biomass burning emissions that initiate toxic mechanisms and promote respiratory and cardiovascular damage.

1.4.2 Cellular mechanisms associated with solid fuel toxicity

Source-specific chemical composition and physical properties of PM likely drive the unique toxicity of specific biofuels. However, while higher OP measures have been reported for rice straw particles compared to pine stem particles, higher *in vitro* cellular inflammatory responses are observed for pine stem particles compared to rice straw particles [35]. Variations in chemical composition such as the presence of trace element (copper, zinc) and organic carbon content have been attributed to result in differences in OP among specific solid fuel types and may also influence the differences in toxicity once PM is inhaled or in *in vitro* cellular toxicity studies. Smoke generated from the low temperature combustion (550 ºC) of coal has been reported to have greater biological toxicity compared to smoke from high temperature combustion (1100 ºC) , likely due to the higher output of carbonaceous compounds and PAHs at lower temperatures [35], but changes in elemental composition may also play a role. Studies using both acellular and cell toxicity approaches provide insight into how various solid biomass fuel sources activate different biological pro- and anti-inflammatory response pathways and promote different extents of cellular toxicity. There may be multiple components of solid biomass fuel smoke contributing to altered cell function or compromised viability in specific cell types. Cow dung is generally understood to produce PM with higher OP and more PM per mass of fuel burned, but the biological implication of these differences among distinct solid biomass fuel sources remains understudied [36–38].

Airway immune cells such as alveolar macrophages are part of the innate immune system and serve as the first defense response in the lung against foreign substances, infectious organisms, and inhaled PM. Macrophages internalize foreign material through phagocytosis and release antimicrobial mediators such as superoxide and hydrogen peroxide through a “respiratory burst”

process involving transient oxygen consumption and nicotinamide adenine dinucleotide phosphate oxidase, illustrated in Figure 1. Alveolar macrophages are also involved in maintaining redox homeostasis, initiating (and later resolve) inflammation, tissue repair, and airway remodeling signaling processes.

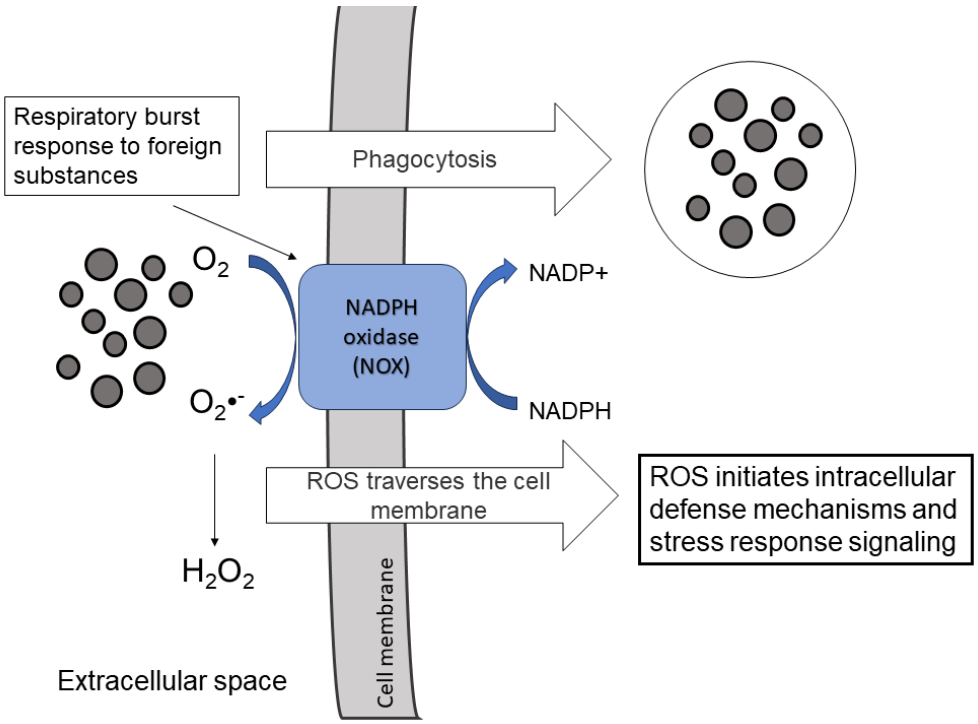

Figure 1: Respiratory burst and phagocytosis functions in macrophage cells.

Particulate carbon has been observed in the alveolar macrophages of people exposed to solid biomass fuel smoke, and can serve as a graphic indicator of personal cumulative exposure to combustion-derived PM [39,40]. Some of the soot-containing macrophages are removed by mucociliary clearance and are swallowed. Others migrate to the lymph nodes where they are retained for years and can release toxic constituents that affect distal organs. For example, the sputum of Ethiopian women and children exposed who regularly cook with biomass fuels contained alveolar macrophages with significantly more carbonaceous particles compared to

sputum from reference participants [41]. The elevated carbon loading observed in people exposed to high levels of PM suggests that once internalized by phagocytic cells, PM can remain in innate immune cells for prolonged periods that may contribute to direct PM-mediated and indirect cellular-mediated ROS generation processes that promote oxidative stress and detrimental cellular outcomes. Alveolar macrophages exposed to wood PM and fine carbon black particles *in vitro* have reduced phagocytic activity and reduced oxidative burst capacity in response to bacterial pathogens [42]. The reduced capacity to produce an effective antibacterial response was directly related to intracellular particulate loading and might be a factor in the increased incidences of pneumonia and other respiratory system disease observations in epidemiological studies of individuals exposed to high levels of smoke from indoor cooking activities [43,44]. A limited body of work has also demonstrated that viral defenses are compromised humans airway epithelial cells exposed to in dung smoke and in mice expose to dung smoke [38,45].

Studies examining the immunomodulatory effects of solid dung fuel pollutants remain limited, and much less has been done to describe macrophage antioxidant and metabolic gene expression changes following exposure to solid biomass fuels. This study approached this gap by addressing three specific aims. The first aim of this work is to relate fuel and stove conditions to the composition of smoke PM by characterizing the OP of PM emissions from cookstoves and solid fuels that are predominantly used in rural households in the Indo-Gangetic Plain. The second aim of this work is to relate toxicity effects to specific fuel and combustion characteristics. Immune cell viability, respiratory burst function, oxidative stress, metabolic homeostasis, and gene expression of metabolic and glutathione maintenance genes responses were examined using *in vitro* methods with the RAW 264.7 macrophage-like monocyte cell line to model acute exposures to solid biomass fuel smoke. The third aim of this study is to conduct a systematic

multivariate analysis of the fuel type and combustion conditions against the outcomes explored in this study (OP, cytotoxicity, and oxidative stress and metabolic responses). Fuel source and cookstove properties were expected to play a meaningful role in particle toxicity due to the formation of aromatic compounds and unsaturated bonds with reactive oxidizing and electrophilic properties during inefficient combustion processes. PM emissions demonstrating high oxidative capacities were thought to exacerbate the negative effects following exposure *in vitro* due to the promotion of intracellular oxidative stress and possible direct inhibition of enzymatic processes. Furthermore, cellular exposure to PM with low oxidative properties were expected to produce less adverse outcomes due to sustained intracellular homeostasis and stress-response capabilities.

2. Field site and particulate matter collection

The sample collection and characterization of PM emissions were the focus of students Robert Weltman's [46] Master's thesis and Lauren Fleming's [47] Ph.D. dissertation work. Extensive details of the collection methods, emission factors, and the molecular composition of the biomass burning emissions have been described in detail in previous publications [48–50], but are summarized herewith for completeness.

2.1 Particulate matter source

The $PM_{2.5}$ emissions used in this study were sampled from partially controlled testing from a village in Khatela in the Palwal district of Haryana, India. A local cook was hired to prepare traditional meals of *roti* or rice and vegetables for four people carried out in traditional mud chulha or angithi cookstoves, pictured in Figure 2. The chulha is a U-shaped cookstove made of bricks and a clay covering and is typically used to cook family meals. Chulha stoves have an open front design allowing sufficient supply of oxygen that results primarily in flaming combustion with a high modified combustion efficiency (MCE). MCE is a simplified proxy value for combustion efficiency calculated by the concentration ratios of CO_2 to the sum of CO_2 and CO, defined in equation (1), where ΔCO_2 and ΔCO is the change in the measured mixing ration of the emission versus the background.

$$\boldsymbol{MCE = \frac{\Delta CO_2}{\Delta CO + \Delta CO_2}} \qquad \boldsymbol{(1)}$$

With complete combustion where all carbon is converted to CO_2 the MCE is 1. Flaming combustion has an MCE of 0.99, while smoldering combustion is in the range of 0.8-0.88 [47]. The

angithi cookstove is made of mud and a clay bowl and is largely smoldering with relatively low MCE and is primarily used for cooking animal fodder and simmering milk. The fuels used in the chulha stoves were brushwood in the form of branches and twigs, and/or buffalo and cow dung cakes. The fuel used in the angithi cookstoves was exclusively dung.

Figure 2: Photograph of traditional mud cookstoves used in India. *An angithi stove is pictured on the left and a chulha stove loaded with dung cakes is pictured on the right.*

2.2 Particle matter emission factors and chemical constituent analysis

Three-pronged metal probes were hung 60 cm above each cookstove and emissions from independent cooking events were sampled using PCXR8 pumps (SKC Inc. Universal, PA). $PM_{2.5}$ emissions were collected onto polytetrafluoroethylene (PTFE) filters with polymethylpentene support rings (2.0 μm, 47 mm, SKC Inc., Fullerton, CA) during meal preparations using cyclone

fractionators (2.5 μm, URG Corporation). Concentrations of CO_2 and CO were analyzed for all samples using a TSI Q-Trak 7575 (TSI, Shoreview, MN) and adjusted for background ambient concentrations. The total mass of each fuel type consumed was calculated by weighing the total fuel before and after each cooking event, while fuel moisture content was assessed using a 9-volt digital moisture meter (model: 50270, SONIN Inc., China). The reported emissions factors and PM samples collected by the research team reflect the actual usage in local homes, which differ from conditions in controlled laboratory studies.

$PM_{2.5}$ from independent cooking events were analyzed via nanospray desorption electrospray ionization–high resolution mass spectrometry (nano-DESI-HRMS) and high-performance liquid chromatography–photodiode array–high resolution mass spectrometry (HPLC-PDA-HRMS) techniques to generate an inventory of the numerous compounds present in the particle phase. Parallel studies were conducted on the gas-phase emissions as well.

2.2.1 Chemical composition of dung $PM_{2.5}$ emissions

In general, dung fuels used with traditional Indian oven-type angithi stoves yield higher amounts of $PM_{2.5}$, volatile organic compounds (VOCs) and secondary organic aerosols (SOAs) compared to brushwood or wood-dung mixtures from chulha stoves. Weltman and Fleming's studies identified differences in the chemical composition of volatile and PM emissions from dung or brushwood emissions. MCE and different fuel-stove combinations were shown to influence the emission factors of sulfur-containing compounds, halogen-containing compounds, organo-nitrates, alkanes, alkenes, alkynes, aromatics, terpenes, and oxygenated compounds. Other factors such as pyrolysis temperature and fuel moisture may also lead to variability in biomass burning emissions, but Weltman and Fleming's did not find a significant relationship between

specific compound emissions and fuel moisture content or meal cooked. However, angithi stoves, characterized by lower MCE values compared to chulha stoves, release higher amounts of $PM_{2.5}$ per kilogram of dry fuel burned. Measures using nano-DESI HRMS also detected a greater chemical complexity from dung-angithi cookfires (262 compounds) compared brushwood only-chulha cookfires, as detailed in Table 1.

Table 1: Average emission factors and standard deviation of $PM_{2.5}$ for cook fire events.

Stove Type	chulha	chulha	chulha	angithi
Fuel	cow dung	brushwood	mixed fuels	cow dung
Emission Factor: $PM_{2.5g}$ g/kg dry fuel	19.2 ± 7.1 (N = 18)	7.4 ± 5.7 (N = 14)	11.0 ± 2.0 (N = 13)	33.2. ± 7.6 (N = 10)
MCE	0.865 ± 0.014	0.937 ± 0.035	0.892 ± 0.021	0.819 ± 0.031
Molecular complexity of $PM_{2.5}$	212 compounds	93 compounds	Not included	262 compounds

Values represented as the mean of (N) filters for each stove-fuel combination ± standard deviation. (Adopted from Fleming et al. [48,49]*).*

The nano-DESI HRMS analysis revealed that the compounds arising from dung and brushwood combustion predominantly consist of complex nitrogenated and oxygenated heterocyclic compounds, as summarized in Figure 3. Dung emissions from either chulha or angithi stoves are primarily composed of nitrogen containing aromatic hydrocarbons (N-HC), with few or no oxygen atoms, and exhibit a high degree of unsaturation. The presence of nitrogen containing hydrocarbon compounds in dung emissions may be a result of the herbivore diet and digestive processes, and the lower combustion efficiencies of dung fuels compared to brushwood [51]. Oxygen and nitrogen containing hydrocarbons (N,O-HC) are also more abundant in dung combustion emission than in brushwood emissions. In contrast, emissions from brushwood burning are largely composed of oxygenated hydrocarbons (O-HC), which is typical of woody materials that naturally contain lignin. Potassium salts are a well-known flaming biomass burning tracer, and are observed in chulha stoves, but are absent from angithi cookfires. The

source of potassium salts may be from flaming combustion processes, the potassium content of the fuel, but also the specific stove materials and food items cooked.

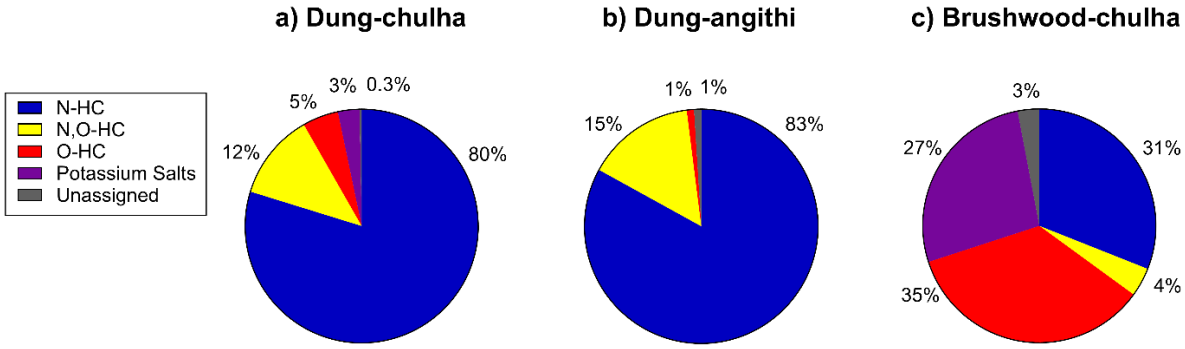

Figure 3: Relative abundance of distinct chemicals in solid biomass fuel PM emissions. *Pie chart describing results from nano-DESI-HRMS and illustrate the elemental makeup of PM emissions generated from a) dung-chulha, b) dung-angithi, and c) brushwood-chulha fuel-stove combinations. Compounds detected include nitrogen containing aromatic hydrocarbons (N-HC, blue), oxygen, and nitrogen containing hydrocarbons (N,O-HC, yellow), oxygenated hydrocarbons (O-HC, red), potassium salts (purple), or other unassigned compounds (gray). (Adopted from Fleming et al.* [49]*)*

2.3 Post-site collection toxicology assessment strategy

The relative toxicity of emission from burning dung and mixed brushwood-dung fuels, with varying moisture contents, generated under varying combustion conditions has been understudied and warrants further investigation. A systematic analysis of the relationship of stove type, fuels, and PM emissions toxicity in macrophage cells following acute exposures was the focus of this dissertation. Prior studies have established that the diversity of compounds emitted from biofuel combustion vary according to fuel type and combustion efficiency. Based on the chemical analyses and emission factor estimations conducted in our laboratory, we expect the *in vitro* biological toxicity of cook fire emissions to be influenced by the combustion conditions unique to the fuel-stove combination.

This dissertation work was conducted using a subset of the cookstove emission Teflon filter samples previously used for chemical analysis. A total of 18 individual emission samples were used across the toxicology studies, which included five filter extracts from dry dung samples from chulha stoves, four wet dung samples from chulha stoves, six mixed fuel (wood-dung) samples from chulha stoves, and three dung samples from angithi stoves. Reference compounds were also included in the experiments to ascertain if cellular toxicity from solid fuels is comparable to that of urban dust and a single quinone compound. The National Institute of Standards and Technology (NIST, Gaithersburg, MD) Standard Reference Material 1648a (SRM 1648a), which is an urban air particulate matter sample collected over a 2-year between 1974 to 1976, in St. Louis, MO, was used as positive control. It is considered "total suspended particle" material with about 50% of particles being less than 10 μm in mean diameter (NIST, Certificate of Analysis). SRM 1648a is commonly used for method development, cross-laboratory comparisons, and *in vitro* studies because its chemical composition is well-characterized [52,53]. *In vitro* cellular exposures to SRM 1648a is known to induce oxidative stress and DNA damage due to the presence of metals like iron [52]. A stock solution of SRM 1648a was prepared by weighing out and resuspending 1 mg of the powder into cell culture grade water. The chemical standard 9, 10 phenanthrenequinone (PQN) was also included in this study. This compound is an oxygenated derivative of the PAH phenanthrene, produced through photooxidation or chemical oxidation. It is a known redox active compound and represents a prominent quinone in diesel exhaust and is present in ambient air samples both in the particle-phase and the gas-phase [54]. *In vitro* experiments indicate that PQN exerts cytotoxic effects on cells through promoting excess ROS formation triggering apoptosis [55]. A 5 mM PQN stock solution was prepared in dimethyl sulfoxide (DMSO) and was further diluted to a 0.03 μM working concentration using deionized

water (DI) immediately preceding experiments. Both SRM 1648a and PQN reference compound solutions were stored at -20 °C when not in use.

2.3.1 Aqueous particle suspension preparations

Particle suspensions were prepared by extracting the particles from the PTFE filters using a combination of sonication and shaker techniques. First, filters were placed face down onto a 16-ounce glass amber jar prefilled with 4 mL of ultrapure cell culture grade water and coated with 60 µL of 95% ethanol (etOH). The jars were placed in an ultrasonic bath and sonicated for 30 minutes to dislodge particles. The jars were then placed on a rotary shaker for 15 minutes. This process was repeated two more times to maximize particle removal from the filters. To determine the extraction efficiency and particle concentration in the aqueous extract, the PTFE filters were dried, and the mass of particles was assessed with a microbalance (Cahn C-31 Microbalance, Thermo). Mass normalized aliquots of the aqueous particle extracts (cookstove filter samples and SRM 1648a control) were sonicated for 30 minutes in a water bath prior to use for cell-free assays and *in vitro* cell exposures. All PM extract stocks were stored at -20 °C when not in use.

2.3.2 Particle extraction efficiency

Extraction efficiency was determined by mass, which was assessed by the gravimetric mass loading of particles on the Teflon filter during the emission sampling and subtracting the mass of the filter after aqueous extraction as summarized in equation (2).

$$\boldsymbol{Extraction\ efficiency}\ (\%) = \frac{\boldsymbol{mass\ extracted}\ (\boldsymbol{mg})}{\boldsymbol{mass\ collected}\ (\boldsymbol{mg})} \times \mathbf{100} \qquad \textbf{\textit{(2)}}$$

Table 2 shows the extraction efficiency for all 18 filters used in this study ranged from. The aqueous filter extracts were used for DTT experiments, and for *in vitro* cell-based experiments when the concentration was sufficiently high for dosage. While extraction efficiencies for the filter samples used for experiments 55% - 100% as described in Table 2, there was a strong correlation observed between high particulate mass loading and extraction of particles from filters indicating a favorable extraction procedure, Figure 4. Differences in extraction efficiency may be attributed to mass lost from evaporation due to long term storage and errors associated with weighing filters, and variations in room humidity and temperature.

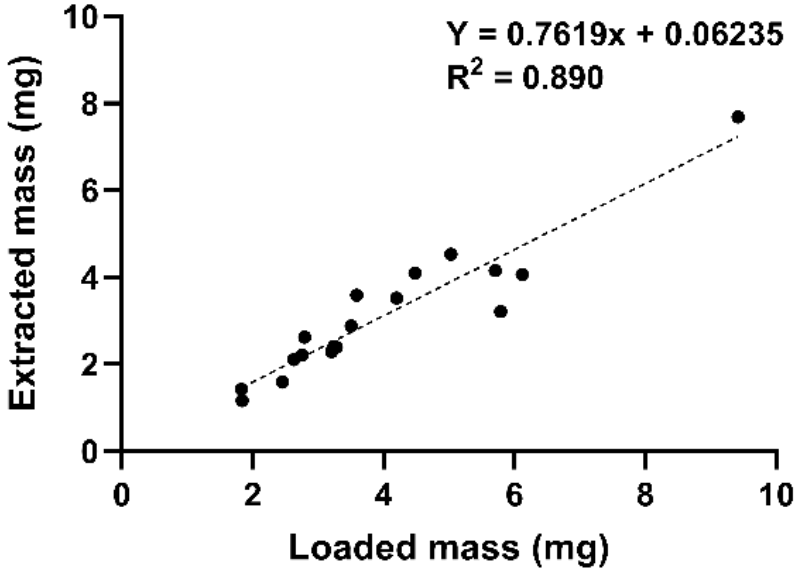

Figure 4: Correlation between particle mass loading and extraction of particles *from 18 filters used for toxicity experiments.*

Table 2: Extraction efficiency for 18 filters used for toxicity experiments.

Stove	Fuel type	Moisture	Meal	Filter ID	Blank filter pre-weight	Mass loaded (mg)	Loaded filter weight (mg)	Post-extraction filter weight (mg)	Extracted mass (mg)	Extraction efficiency (%)
Chulha	dung	dry	roti	1	81.63	5.03	86.66	82.13	4.53	90%
		dry	rice	2	83.33	3.59	86.93	83.33	3.59	100%
		dry	roti	3	85.34	4.20	89.54	86.02	3.52	84%
		dry	rice	4	80.41	9.42	89.82	82.13	7.69	82%
		dry	rice	5	81.96	2.76	84.72	82.52	2.20	80%
Chulha	dung	wet	roti	1	83.60	3.28	86.89	84.50	2.39	73%
		wet	rice	2	80.70	3.51	84.22	81.34	2.88	82%
		wet	roti	3	84.06	5.71	89.77	85.62	4.15	73%
		wet	rice	4	78.32	6.12	84.44	80.38	4.06	66%
Chulha	dung + brushwood	wet + dry	rice	1	79.31	2.46	81.77	80.18	1.59	65%
		dry + dry	roti	2	82.00	2.80	84.80	82.18	2.62	94%
		dry + dry	roti	3	81.71	2.63	84.34	82.24	2.10	80%
		wet + dry	roti	4	82.35	3.24	85.59	83.19	2.40	74%
		wet + dry	roti	5	80.19	1.83	82.02	80.61	1.42	77%
		wet + dry	roti	6	80.48	3.21	83.69	81.40	2.29	71%
Angithi	dung	wet	animal food	1	77.91	1.84	79.75	78.59	1.16	63%
		dry	animal food	2	81.85	4.48	86.34	82.23	4.10	92%
		dry	animal food	3	81.30	5.79	87.09	83.88	3.21	55%

3. Oxidative potential of solid biomass fuel particulate matter emissions

3.1 Introduction

Biological oxidative stress is an important mechanism implicated in PM induced toxicity, which occurs when the excessive generation of ROS *in vivo* overwhelms natural antioxidant defenses. The ability of redox active PM species to generate ROS *in vivo*, referred to as the OP of particles, can be assessed by various acellular techniques. The DTT assay is commonly used to measure the depletion of free sulfhydryl groups in DTT over time by redox active compounds such as PQN, which catalyze the transfer of electrons from DTT to oxygen thereby producing superoxide and converting DTT to its disulfide form [56]. Numerous investigations focus on the DTT activity in water-soluble aerosol sample extracts, which may be the most biologically relevant due to the solubility and capacity for absorption in the respiratory tract. DTT acts as a surrogate for biological reductants such as reduced nicotinamide adenine dinucleotide (NADH) or nicotinamide adenine dinucleotide phosphate (NADPH) involved in the generation of cellular superoxide and oxidative stress processes [57,58]. The linear rate of DTT depletion over time is proportional to the concentration of redox active constituents in PM extracts, such as black carbon and transition metals, and to a lesser extent electrophile compound, providing insight into the constituents that generate ROS and oxidize biological molecules to promote oxidative stress [59,60]. The use of DTT assays has gained popularity due to its strong association with adverse health outcomes, while similar associations using alternative OP methods involving the acellular depletion of physiologically relevant antioxidants such as ascorbic acid are inconsistent [61,62].

The aim of this study was to characterize the DTT activity (rate of depletion of DTT normalized by mass) by $PM_{2.5}$ emissions derived from dung and mixed dung-brushwood solid biofuels used with traditional cookstoves commonly used in India to assess the OP of particles from distinct sources. We hypothesized that PM emissions from angithi smoldering combustion cookstoves would have higher OP (higher DTT depletion rate) properties than PM emissions from chulha flaming combustion cookstoves due to the formation of different reactive chemicals from inefficient burning of solid biofuels. This study also sheds light on how fuel moisture content influences the redox properties of PM emissions from solid fuel cookstoves and compared the OP between PM from different sources including chemical standards PQN representing a major quinone in diesel, as well as urban dust material SRM 1648a. The analysis aimed to evaluate the OP variations of $PM_{2.5}$ emissions from distinct stove-fuel sources and how combustion parameters influence particle reactivity.

3.2 Materials and methods

3.2.1 Oxidative potential using a semi-automated DTT system

Mass normalized aqueous extracts of biomass PM emissions were used to measure the PM-dependent decay of DTT over a 40-minute period. PQN solution (0.3 µM) as a blank control and a blank PTFE filter extract as a negative control were included for each daily experimental batch to assess reproducibility, while each cookstove filter extract sample was run in duplicate. The blank PTFE filter extract was further diluted 1:10 in cell culture grade water to mimic the highest dilution scheme performed with the field sample filter extract stock solutions.

Methods from Gao, Fang, and Weber [60,63] were adapted to conduct the water-soluble DTT assay measuring the depletion of 100 µM of DTT by PM extracts from cookstove emissions over a 40-minute period. Stock solutions of PM aqueous extracts were diluted to a concentration of 50 µg/mL and 0.7 mL of the extract was incubated at 37ºC with continuous shaking with 0.2 mL potassium phosphate buffer (0.5 mM) and 0.1 mL DTT (1 mM) in 15 mL polypropylene centrifuge tubes. Aliquots (50 µL) were withdrawn at time (t) = 5, 10, 20, 30, and 40 minutes, and mixed with 0.5 mL trichloroacetic acid (1% w/v) to quench the consumption of DTT. The quenched solution was further mixed with 1 mL Tris buffer (0.08 M Tris buffer with 4 mM EDTA (ethylenediaminetetraacetate)) and 0.25 mL of DTNB (0.2 mM, 5,5'-dithiobis-(2-nitrobenzoic acid) and then diluted with 9.2 mL of Milli Q water. The resulting solution was immediately measured for absorbance at 412 nm and a background wavelength at 700 nm using the Liquid Waveguide Capillary Cell with an optical path length of 10 cm (World Precision Instruments, Inc.) coupled to the ultraviolet-visible spectrophotometer (DH-MINI, Ocean Optics, Inc.) and the multi-wavelength light detector (FLAME-T-UV-VIS-ES, Ocean Optics, Inc.). The rate of DTT consumption was calculated from the linear regression of absorbance versus time. The final oxidative capacity of the PM sample was calculated after subtracting blank filter values from the sample values and further normalized by total PM mass in the reaction vial, presented as the water-soluble, mass normalized DTT oxidation activity (DTTm, pmol min^{-1} μg^{-1}). The total cookstove PM mass in each reaction vial was calculated to be 35 µg (0.7 mL aliquot × 50 µg mL^{-1} liquid concentration).

3.2.2 Statistical analysis

All data were expressed as means ± standard error of the mean (SEM), unless otherwise stated. To determine the statistical significance of the differences between groups six independent

groups: dry dung-chulha, wet dung chulha, mixed fuels with chulha, dung with angithi, PQN, and SRM 1648a, the Kruskal-Wallis non-parametric one-way analysis of variance (ANOVA) was performed following a normality test. The Dunn multiple comparison post hoc test was used to assess pairwise differences between groups. The significance level was set at a =0.05 to determine statistical significance. All statistical analyses were performed using GraphPad Prism (version 10.1.0 for Windows, GraphPad Software, San Diego, CA, USA, www.graphpad.com).

3.3 Results

3.3.1 Oxidative potential differences between angithi and chulha stove PM emissions

To assess the oxidative potential of particles from different emission sources, we conducted a DTT assay using $PM_{2.5}$ emissions from biomass combustion with traditional cookstoves, PQN standard, and SRM 1648a urban dust. The mean OP of PQN from eight replicate measures was determined to be 35.7 pmol min^{-1} μg^{-1}, while the mean OP of urban dust sample SRM 1648a from four replicate measures had a lower value of 21.9 pmol min^{-1} μg^{-1}. Angithi dung samples (N= 3 filters) had an average OP at 50.6 pmol min^{-1} μg^{-1}, higher than any other PM source tested. In contrast, emissions from chulha cookstoves exhibit a lower mean OP than both PQN and SRM 1648a. Mixed wood-dung fuel emissions used with chulha (N = 6 filters) had a mean OP of 15.2 pmol min^{-1} μg^{-1}, which was comparable to the mean OP observed in wet dung chulha emission samples (N = 4 filters) of 17.5 pmol min^{-1} μg^{-1}. Dry dung chulha samples (N = 5 filters) exhibited the lowest OP among the PM sources studied, with a mean OP of 10.3 pmol min^{-1} μg^{-1}. The mean OP of the PM samples tested are summarized in Table 3.

Table 3: Summary of mean oxidative potential in PQN and SRM 1648a standards and biomass combustion PM from traditional cookstoves

Sample	N (filters tested; repeat measures *)	DTT Activity ± SD
PQN	8*	35.7 ± 7.9
SRM 1648a	4*	21.9 ± 7.2
Dry dung-chulha	5	10.3 ± 7.8
Wet dung-chulha	4	17.5 ± 11
Mixed fuels-chulha	6	15.2 ± 11
Dung-angithi	3	50.6 ± 28

DTT activity values represent pmol of DTT consumed, min^{-1}, μg^{-1} of PM. Values represented as the mean ± standard deviation (SD) from different filters used (N) differed for each stove-fuel combination. Mean DTT activity values were attained by averaging duplicate or triplicate measures of each filter when possible.

3.3.2 Fuel source and stove combustion efficiency influence oxidative potential

Overall, the PM emissions from angithi stoves were demonstrated to have the highest OP, but PM emissions from chulha stoves were lower than PQN and urban dust chemical standard SRM 1648a. Statistically significant group differences (H = 26.2, P <.001) in the mean OP of particles from these sources were observed, summarized in Figure 5. A pairwise post-hoc Dunn's test showed that PM from angithi cookstoves displayed a significantly higher OP (50.6 pmol min^{-1} μg^{-1}) compared to chulha dry dung (10.3 pmol min^{-1} μg^{-1}, P <.001) and chulha mixed fuel extracts (15.2 pmol min^{-1} μg^{-1}, P =.025). Statistically significant differences were also observed between PQN (35.7 pmol min^{-1} μg^{-1}) and dry dung chulha PM (P =.002). However, no statistical difference was observed between the OP of dung samples obtained from angithi cookstoves, which encompassed both dry and wet moisture content, and the wet dung emissions from chulha cookstoves with a lower OP (17.5 pmol min^{-1} μg^{-1}), likely attributable to the inherent variability in the OP across individual filters.

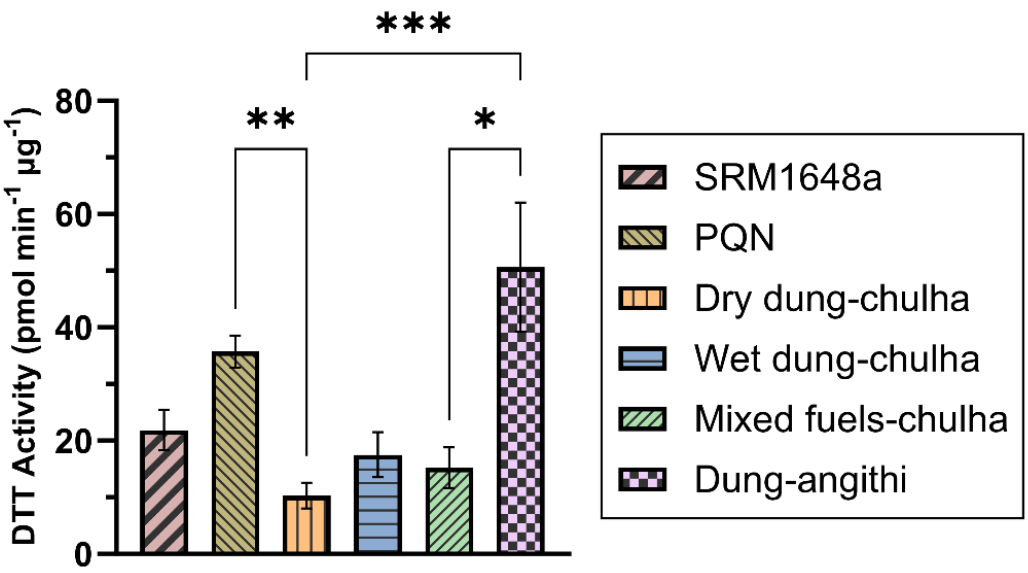

Figure 5: Oxidative potential of PQN, SRM 1648a, and solid fuel PM emissions. *Mean DTT activity ± SEM for 15 filters from chulha stoves (N =* 5 dry dung samples, *N = 4 wet dung samples, and N = 6 mixed wood-dung fuel samples) and three filters from dung combustion with angithi cookstoves measured in duplicate or triplicate when possible. * P <0.033, ** P <0.003, *** P <0.001.*

3.3.3 Variability of oxidative potential measures

The DTT decay rate varied between filters from the same stove and fuel type, but also between replicates of the same filter extract, as summarized in Table 4. Three out of the five chulha dry dung filter extracts had a low OP of less than 6 pmol min^{-1} μg^{-1}. The coefficient of variation (CV) for replicate measures of any single dry dung chulha stove filter extract ranged from 30 % to 73%. For the four wet dung chulha filter extracts tested, three filters had an OP range between 11 and 18 pmol min^{-1} μg^{-1} and only one filter had a high OP of 32 pmol min^{-1} μg^{-1}. The CV for replicate measures of any single wet dung filter extract ranged from 2 % to 26 %. The chulha mixed fuel extracts exhibited similar variation in OP, with only one out six filters having a high OP of 34 pmol min^{-1} μg^{-1} and the other five filters having an OP of less than 14 pmol min^{-1} μg^{-1}. The CV for replicate measures of any single mixed fuel chulha filter ranged from 14 % to 50 %. Only three dung angithi stove filters were assessed, and all these filter extracts had a high OP

exceeding 34 pmol min^{-1} μg^{-1}. The highest OP average measure for single dung angithi filter was 76 pmol min^{-1} μg^{-1} with the CV for filters extracts of this fuel stove type ranging from 44-48 %. The CV for PQN was determined to be 22 %, whereas the CV for SRM 1648a was calculated to be 33 %.

Table 4: Summary of filter samples used for DTT experiments and oxidative potential results

Sample Type	**Filter ID**	**N (filters tested; repeat measures *)**	**Oxidative potential ± CV, pmol min^{-1} μg^{-1}**
Redox active control	PQN	8*	35.7 ± 22%
Urban dust	SRM 1648a	4*	21.9 ± 33%
Dry dung chulha	1	3	14.5 ± 41%
	2	2	4.0 ± 46%
	3	2	5.4 ± 47%
	4	3	5.9 ± 73%
	5	2	21.9 ± 30%
Wet dung chulha	1	2	11.2 ± 2%
	2	2	13.0 ± 25%
	3	2	18.7 ± 23%
	4	2	32.4 ± 26%
Mixed fuels chulha	1	1	5.7
	2	2	7.5 ± 14%
	3	2	11.3 ± 24%
	4	1	12.0
	5	2	14.2 ± 50%
	6	2	34.3 ± 30%
Dung angithi	1	3	34.3 ± 44%
	2	1	48.7
	3	2	76.1 ± 48%

Oxidative potential of individual solid biomass fuel PM emission filter extracts. The mean DTT consumption ± coefficient of variance (CV) for each filter extract was determined from 2-3 independent experiments except for two mixed fuels-chulha filters (ID 1,4), and one dung-angithi filter (ID 2) that were only tested once due to limited sample volumes.

3.4 Discussion

3.4.1 Variable oxidative capacity of particulate matter from distinct sources

The DTT activities for the samples used in this study range from 4 – 76 pmol min^{-1} μg^{-1}. The PM emissions from angithi stoves demonstrated the highest mean OP, followed by PQN and SRM 1648a, while PM emissions from chulha stoves had the lowest OP amongst all the samples in this study. The lower OP of flaming chulha stove emissions compared to smoldering angithi stoves were expected because flaming combustion results in the formation of complete oxidation products such as carbon dioxide, while smoldering combustion results in incompletely oxidized products such as carbon monoxide and other redox active compounds [64].

The results in this study fall in line with previous literature describing that cooking and biofuel burning emissions are relatively high. Cooking related organic aerosols and biomass burning organic aerosols have been associated with higher DTT activity than ambient particulate matter. In fact, one study using a combination of DTT experiments and Positive Matrix Factorization mathematical modeling found the DTT activity of biomass burning emissions to be 151 ± 20 pmol min^{-1} μg^{-1}, while that of urban cities in the United States ranges from be 10 - 70 pmol min^{-1} μg^{-1}, based on data from the water soluble fractions of these samples [65]. Other studies have reported similar values, with values ranging from about 60-150 pmol min^{-1} μg^{-1} for cooking and biomass burning related sources [65–67]. The exact methodology for conducting DTT experiments vary greatly in the literature and can be difficult to compare among various studies. One study by Conte *et al.*, reported the DTT activity of SRM 1648a to be 0.0005 nmol min^{-1} μg^{-1}, which was higher than the OP of ash wood pellet combustions using a pellet stoves reported at 0.0003 nmol min^{-1} μg^{-1} [58]. A different study by McWhinney *et al.*, reported the DTT activity value of SRM

1648a to be less than 10 pmol min^{-1} μg^{-1} and have a relatively lower DTT activity than PM from diesel exhaust or vehicle sources [68]. However, a different study by De Jesus *et al*., found the DTT activity of SRM 1649b (a modern batch of the NIST SRM 1648a sample [69]) measured 0.0242 nmol min^{-1} μg^{-1} which is comparable to the values reported in this study of 21.9 ± 7.2 pmol min^{-1} μg^{-1} [70]. Additionally, the rate of DTT consumption observed in this study for the same concentration of PQN is 1.7 nmol min^{-1}, which is similar to the values reported by Fang *et al* [63].

A relatively understudied aspect that may influence the OP of solid biomass fuel sources is the moisture content. The fuel moisture content of solid fuels have been shown to influence the amounts of carbon and nitrogen species emitted during burning [64]. The presence of wet biofuel is also known to enhance the formation of compounds that promote oxidative reactions and reactive hydrocarbon precursor compounds are more readily the formed under humid conditions as opposed to arid conditions [66]. While not statistically significant, we observed a trend of wet dung emissions from chulha stoves having a higher mean OP than either dry dung or mixed emissions from chulha cookstoves. The higher OP in wet dung samples may reflect the formation of products formed from the inefficient combustion of the wet fuels. While the moisture content of emissions from mixed fuels used with chulha stoves varied, the mean OP was more similar to the wet dung emissions than to dry dung emissions. The OP results from dung-angithi emission samples may reflect the generation of reactive chemicals generated by both wet and dry moisture contents of the fuel, as well as the formation of reactive chemicals from smoldering combustion.

Studies comparing the chemical composition differences of PM emissions from anthropogenic (man-made emission sources such as vehicle fuel combustion) or biogenic (plant-based emissions sources such as solid biofuel burning) sources and their associations with OP have

identified secondary organic aerosols (SOAs) chemicals bound to PM to play an important role. The presence of chemical species on the PM source such as conjugated polyaromatic precursor compounds or nitroaromatics precursor compounds may drive strong OP effects. Other chemicals that vary among particulate matter source, such as metals, PAHs, and OC may also influence OP [71–73]. Biomass burning is also known to contribute significantly to the production of humic-like substances (HULIS), a complex class of incomplete combustion products exhibiting both nonpolar and polar chemical characteristics. These compounds encompass water-soluble nitrogen -containing compounds such as pyridine and imidazole, which exhibit high redox activity, possibly facilitated by the unshielded nitrogen atom's electron accepting capacity [74]. The biomass samples used in this study include dung samples which contain higher levels of nitrogenated aromatic species than brushwood samples, while brushwood samples contain more oxygenated aromatics and potassium salts. While this study did not include emission samples strictly from brushwood combustion, the DTT activity of mixed fuels PM source did not statistically differ from dung only sources. This study adds to the growing evidence showing that the oxidative potential of particles generated during cooking with traditional cookstoves highly influenced by the fuel source and that particle redox activity is associated with the OC emission compositions [75].

3.4.2 Limitations

The DTT experiments described in this study were conducted using aqueous extracts containing the carbonaceous material from cookstove emissions. Carbonaceous material is known to contain reactive compounds that participate in redox reactions [76]. The variability in observed OP values for any single filter likely arose from differences in the amounts of these particles in the reaction solution. These particulates were not filtered and the differing ability of PM materials to break

apart during sonication or mixing during pipetting preparation may contribute to the variation for replicate assays. Additionally, the low number of samples used in this study limits the conclusions that can be made regarding the associations between fuel-specific chemical composition, such as for brushwood contribution and moisture content, and the OP of particles.

4. Macrophage respiratory burst and viability following exposure to particulate matter emissions from solid biomass fuels

4.1 Introduction

Alveolar macrophages residing in the pulmonary alveoli serve as the first responders to inhaled pollutants, maintaining local immunologic and tissue homeostasis in the lung. Microbes or inhaled contaminants activate cell surface receptors (such as toll-like receptors and pathogen-associated molecular receptors), which promote engulfment and clearance of the foreign material by phagocytosis. This process initiates a respiratory burst in which reduced NADPH oxidase enzymes (NOX) generates superoxide and other downstream ROS effector molecules such as hydrogen peroxide to clear pathogens and initiate immune defense responses and tissue repair [77].

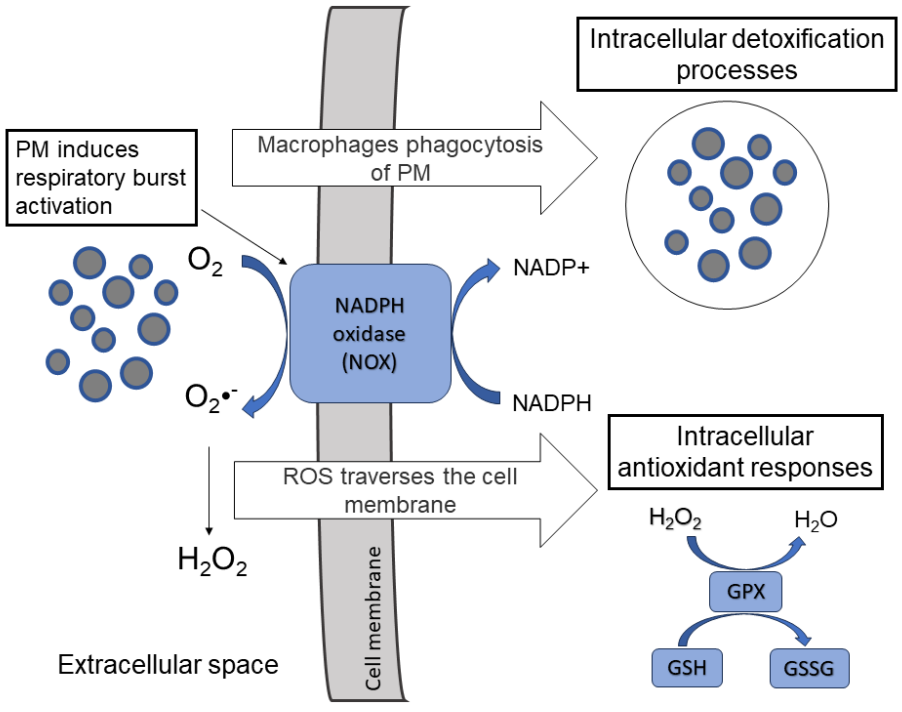

Figure 6: Macrophage respiratory burst and phagocytosis in response to PM exposure induces intracellular detoxification and antioxidant activity. *Particle surface properties including the presence of oxidant, electrophile, and complex PAH compounds directly introduce ROS. Respiratory burst and phagocytosis activity also contribute to cellular mediated ROS generation.*

While respiratory burst is an essential macrophage function, *in vitro* exposure to inhaled pollutants can alter innate immune cell respiratory burst functions and induce oxidative stress, which are linked to air pollutant induced adverse human health outcomes such as COPD [78]. PM is known to indirectly induce cellular mediated ROS generation by altering NOX activity. Macrophage respiratory burst function is commonly assessed with fluorescent and chemiluminescent probes that measure the rate of ROS production *in vitro*. Respiratory burst can be rapidly stimulated in macrophages by exposure to zymosan yeast cell wall particles that initiate phagocytosis and NOX activity or through treatment with phorbol 12-myristate 13-acetate (PMA) which alters the molecular inhibition processes associated with NOX regulation [79]. One study by Becker *et al*., explored ROS generation by in various human inflammatory immune cells including neutrophils, eosinophils, monocytes, and alveolar macrophages after a 20-minute co-exposure with zymosan and either residual oil fly ashes (ROFAs), coal fly ash, diesel, silicon dioxide, titanium dioxide, or fugitive dust. The researchers observed that the various sources of particulate matter stimulate stimulates ROS generation, but the strength of the oxidant response was both cell specific and unique for each type of particle [80]. Additional treatment of cells with molecular inhibitors that target oxidant radical formation altered the levels of ROS generated in the mitochondria cellular compartment or through NOX activity, providing an explanation to the observed variability in cellular oxidative stress responses following PM exposures. Such studies partially indicate that different immune cell types may exhibit unique oxidative stress responses to particles from different sources due to the contribution of distinct cellular signaling processes that promote ROS formation.

PM also directly promotes cellular oxidative stress via respiratory tract interactions with particle-bound chemical oxidants such as hydroperoxides which catalyze ROS generation. The impact of

direct chemical oxidation and indirect cellular mediated oxidative stress was the focus of a study by Fang *et al*. exploring macrophage responses exposed to either PQN or isoprene SOA. The rate of cell-free superoxide generation is higher in PQN compared to isoprene. Macrophages exposed to PQN or isoprene generate superoxide immediately following exposure, but lower concentrations of PQN were required to activate the superoxide formation cellular process while higher concentrations were needed for isoprene indicating that anthropogenic aromatic quinone compounds are more toxic to macrophages than biogenic isoprene compounds. Co-exposure with apocynin (a specific NOX inhibitor) reduced the levels of superoxide generated by cells, indicating that NOX is a significant source of cellular superoxide. Furthermore, cells exposed to either PQN, isoprene SOA, or PMA showed indications of higher membrane fluidity due to lipid peroxidation processes, demonstrating that inhaled toxicants could induce superoxide generation by NOX that promotes cellular oxidative stress and cytotoxicity.

In this chapter, the impact of PM emissions from solid biomass fuel use on macrophage superoxide production from NOX activity was evaluated. Macrophages are widely used *in vitro* models to explore the cytotoxic effects of air pollutants. The RAW 264.7 is an immortalized cell line and is well-characterized in regard to immune, metabolic and phagocytic functions making them attractive for toxicity studies comparing diverse air pollutants [81]. Respiratory burst was stimulated using PMA in cells that had been previously exposed to solid biomass fuel PM emission extracts to assess whether biomass PM emissions modulates normal macrophage immune activity and identify whether oxidative stress results from excessive superoxide radical formation via NOX. PQN was used as a positive control, since it has shown to promote cytotoxicity via redox cycling mechanisms [82]. Higher particle OP was hypothesized to influence the extent of a respiratory burst in microphages exposed to PM and dose-responses were assessed

to evaluate whether exposure to higher PM mass yielded stronger cell responses. Changes in cell viability were also assessed to determine whether changes in respiratory burst function could be explained by differences in cytotoxicity. To our knowledge, no other studies have explored the effects of exposure to dung combustion emissions on macrophage respiratory burst capacity and oxidative stress.

4.2 Materials and methods

4.2.1 Cell culture and PM exposures

RAW 264.7 macrophage-like cells (ATCC TIB-71) were passaged in complete Dulbecco's Modified Eagle Medium (DMEM) supplemented with 10% fetal bovine serum (FBS) and 1% penicillin streptomycin until >80% confluent. Cell counts were determined by either using a hemocytometer or flow cytometry (BD Accuri C6 Flow Cytometer). Cells were seeded at a density of 2.5×10^4 cells per well into 96-well plates with 200 µL complete media and incubated at 37 °C and 5% CO_2 in an incubator overnight.

Cell media was replaced with complete media containing 100 µL of PM extracts for exposures. An exposure time of four hours was used for all cell-based studies, as this time point has been shown to be sufficient to induce stress response activation [83]. Sterile cell culture water was used as a mock treatment for all biological studies. Cells were treated with one of four dosages ranging from 31 µg/cm^2, 16 µg/cm^2, 8 µg/cm^2, and 3 µg/cm^2 of PM. A single dosage of a 0.3 µM PQN solution (0.1 µg/ mL; 0.03µg/cm^2) was used as a positive control. To investigate whether acute exposure to PM compromises oxidative burst function, cells were allowed to rest overnight for 18 hours before performing respiratory burst measurements using the superoxide

chemiluminescent enhancing Diogenes Assay (National Diagnostics, Atlanta GA) according to the manufacturer's instructions.

4.2.2 Respiratory burst superoxide measurements

Cells in clean media 18-hours post the acute exposure event were coated with 100 µL Diogenes reagent and placed inside a temperature controlled luminometer (Centro LB 960 Chemiluminescent Instrument, Berthold Technologies, Bad Wildbad, Germany) at 37 ºC. Cells were stimulated with 100 µM phorbol 12-myristate 13-acetate (PMA), an artificial stimulator used to induce macrophage respiratory burst at t = 3 minutes. The chemiluminescent signal was continuously monitored for two hours or until all the luminol in the system was consumed. Assays were conducted twice using two replicate wells to obtain average endpoint values. The total amount of superoxide generated was quantified by calculating the area under the curve (AUC) over the 90-minute monitoring period. The rate of superoxide production was assessed by finding the time point at which superoxide production peak, or the maximum point over the 90-minute monitoring period. The final superoxide generation values (AUC and peak) were expressed as fold change from mock treated controls.

4.2.3 Viability assessment with MTT cell proliferation assay

Cells were seeded at an optimal density of 1×10^5 cells per well into 96-well plates with 200 µL complete media and incubated at 37 °C and 5% CO_2 in an incubator overnight. The media was then replaced with complete media containing 100 µL of PM extracts. Sterile cell culture water was used as a mock treatment for all biological studies. Cells were treated with dosages ranging from 31 µg/cm^2, 16 µg/cm^2, 8 µg/cm^2, and 3 µg/cm^2 of PM. Two concentrations of PQN at either 0.3 µM (0.1 µg/ mL; 0.03µg/cm^2) or 0.02 nM (4 µg/ mL; 12.5µg/cm^2) were used to determine

whether the redox activity of phenanthrenequinone influences cell viability. Cell viability was assessed immediately following the 4-hour exposure using the 30-1010K MTT Cell Proliferation Assay (ATCC®). Cell viability was determined based on the ability of metabolically active cells with intact with mitochondrial oxidoreductase enzymes to reduce the yellow 3-(4, 5-dimethylthiazolyl-2)-2, 5- diphenyl- tetrazolium bromide (MTT) reagent to form a purple formazan product. The exposure media was replaced with fresh cell media and cells were incubated with MTT reagent for two hours before proceeding to the detergent incubation step. The final absorbance was read using a plate reader (Opsys MR, Thermo Lab Systems, Vantaa, Finland) at 570 nm and a background of 630 nm. Assays were conducted using two replicate wells and two duplicate plates to obtain average values. The final metabolic activity values were expressed as fold change from mock treated controls.

4.2.4 Apoptosis detection with Annexin V staining

Cells were seeded in 12-well plates at a density of 2.5 x 10^5 cells per well and exposed to 14 µg/cm^2 of PM extracts for four hours before harvesting cells for apoptosis detection using a commercially available apoptosis kit (Annexin V: FITC Apoptosis Detection Kit, BD Biosciences). Staining and blocking were performed according to the manufacturer's instructions. In brief, cells were washed with PBS and then counted. A total of 1 x 10^5 cells were incubated with 5 µL of FITC Annexin- V and 2 µL of propidium iodide (0.1 mg/mL solution) in a total of 100 µL Annexin V binding buffer. Cells were incubated for 15 minutes in the dark and resuspended in an additional 400 µL of Annexin V binding buffer before acquiring data using a BD Accuri C6 Flow cytometer and FlowJo software.

4.2.5 Statistical analysis

All data were expressed as means ± SEM, unless otherwise stated. Different sample size filters (N) were used across experiments, due to sample volume limitations. For respiratory burst experiments, N = 5 dry dung-chulha filters, N = 4 wet dung-chulha filters, N = 5 mixed fuels-chulha filters, and N = 1 dung-angithi filters were used. For MTT experiments, N = 3 dry dung-chulha filters, N = 3 wet dung-chulha filters, N = 3 mixed fuels-chulha filters, and N = 1 dung-angithi filters were used. For respiratory burst outcomes and MTT assays, values are normalized to the fold-change of 1 for mock controls. For apoptosis experiments, N = 5 dry dung-chulha filters, N = 4 wet dung-chulha filters, N = 6 mixed fuels-chulha filters, and N = 3 dung-angithi filters were used. For apoptosis analysis, values represent percentage of cells positive for the outcome evaluated, from the total cell population analyzed. For respiratory burst and apoptosis studies, the statistical significance was assessed using the non-parametric Kruskal-Wallis test performed with Dunn's correction for multiple comparisons following a normality test using a significance level of a=0.05. All statistical analyses were performed using GraphPad Prism (version 10.1.0 for Windows, GraphPad Software, San Diego, CA, USA, www.graphpad.com).

4.3 Results

4.3.1 Changes in respiratory burst activity following acute exposures to PM

Respiratory burst is characterized by a rapid increase in superoxide that peaks and slowly returns to baseline levels. A rapid increase in chemiluminescence is observed after PMA stimulation in all cells exposed to PM, indicating that macrophages retain immunocompetent activity following exposures. Chemiluminescent readings returned to baseline values by t = 90 minutes, as illustrated in Figure 7. The results from this study demonstrate that exposure to PM reduced total

superoxide generation and rate of superoxide generation, with changes observed in the maximal superoxide levels measures and time to reach the peak superoxide levels. This inhibition of macrophage respiratory burst function occurred after an 18-hour resting period in clean media following the single 4-hour exposure with particle-spiked media.

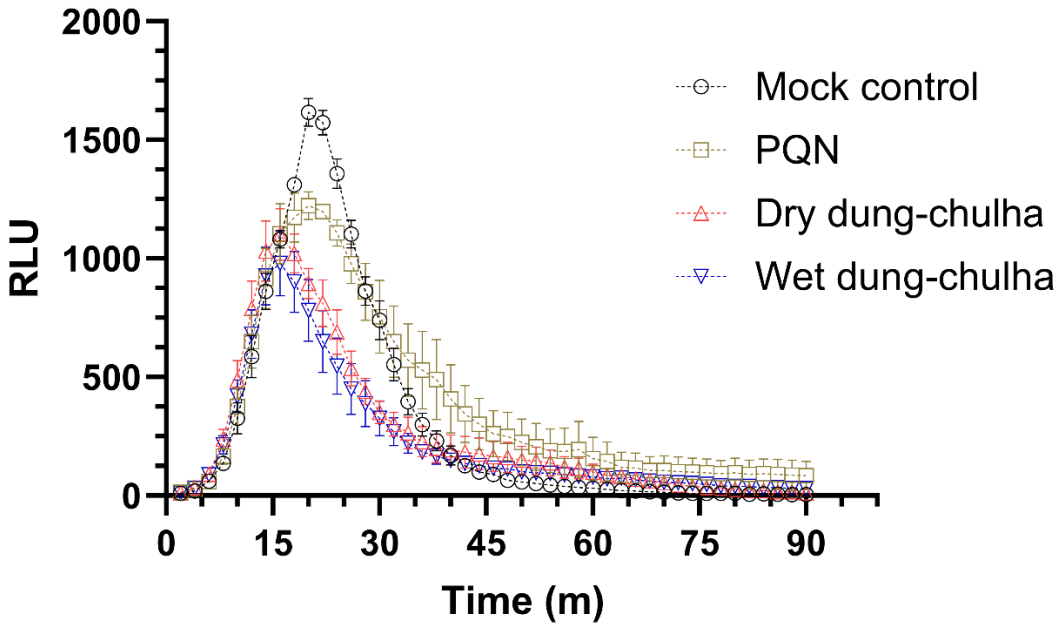

Figure 7: Representative time course of macrophage respiratory burst response following acute exposure to PM. *Macrophages exposed to 31 µg/cm^2 of PM from either dry dung or wet dung or single dose of PQN (0.03µg/cm^2) were stimulated with PMA to induce superoxide generation.*

4.3.2 Peak superoxide response inhibition in innate immune cells

Statistically significant reductions in maximal peak superoxide generation and total superoxide production were observed in all cells treated with biomass PM at all concentrations, with values ranging from 0.51-fold to 0.86-fold change, Figure 7. Statistically significant group differences in peak superoxide levels for all exposure treatments ($H = 32$, $P < .001$ for dosage of 31 µg/cm^2) were observed. The rate of superoxide generation is markedly different between cells exposed to PQN and cells treated with solid biomass fuel PM emissions. Cells exposed to PQN had a mean

1.2-fold increase in total superoxide generation compared to mock treated control cells, while the mean peak superoxide level decreased by 0.90-fold compared to mock controls. The discrepancy between increased total superoxide generation and diminished peak response level is explained by the different rates of superoxide generated towards the end of the observation period, where PQN exposed cells generated superoxide levels that surpass mock controls, Figure 7.

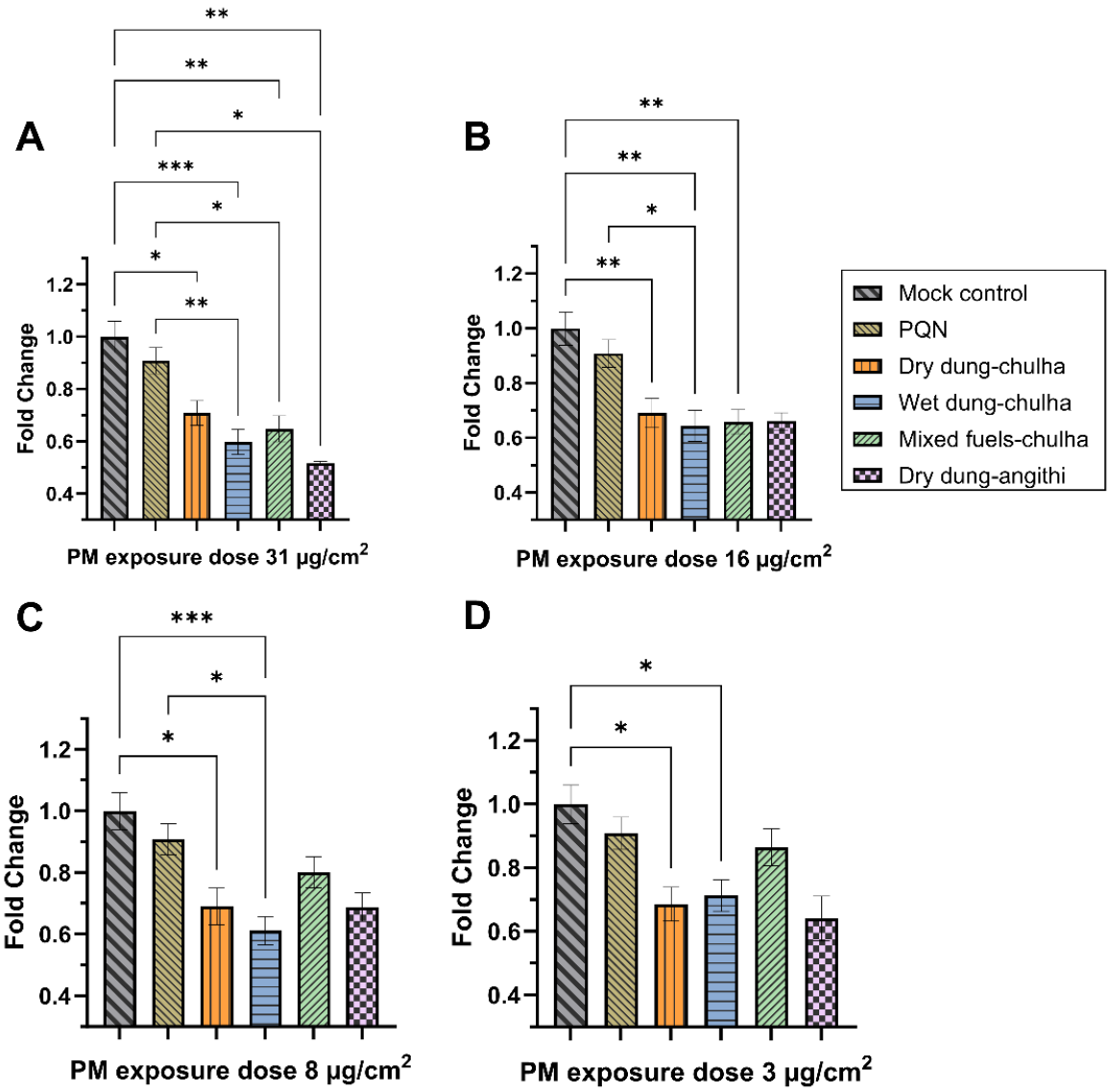

Figure 8: Peak superoxide levels during respiratory burst in PM macrophages exposed to biomass PM *concentrations of (A) 31 µg/cm2 (B) 16 µg/cm2 (C) 8 µg/cm2 and (D) 3 µg/cm2. A single dose of PQN (0.03µg/cm^2) was used as a positive control. * P <0.033, ** P <0.003, *** P <0.001.*

Cells exposed to dry dung PM from angithi stoves exhibited the strongest reduction of peak superoxide levels after exposure to the highest dosage of 31 μg/cm^2 exhibiting a 0.51-fold decrease in the maximal peak response, which was significantly lower than peak response observed for mock control cells or PQN (P =.004; P =.019 respectively) as illustrated in Figure 8A. Less severe reduction nearing 0.7-fold change in peak response compared to control were observed at lower concentrations of dung PM from angithi stoves, which were not statistically different from mock control values, illustrated in Figure 8 B,C,D. A gradual decrease in peak superoxide levels was also observed in cells exposed to wet dung emissions from chulha stoves. A statistically significant 0.60-fold decrease in peak superoxide level compared to mock controls was observed at the highest dose (p <.001), while the lowest dosage of wet dung PM from chulha stoves induced a statistically significant 0.71-fold reduction in peak superoxide level compared to mock treatments (P =.031) indicated in Figure 8D. The least pronounced effects were observed for chulha dry dung exposures, which induced a consistent statistically significant reduction response of nearly 0.70-fold reduction across all dosages compared to mock controls. Cells exposed to mixed fuel PM emissions from chulha stoves demonstrated linear dose responses. At the higher dosages of 31 μg/cm^2 and 16 μg/cm^2, strong reduction in maximal peak response of 0.65-fold change were observed in cells exposed to mixed fuel PM compared to mock treated cells (P =0.003; P =0.004 respectively), while a less pronounced 0.86-fold change was observed for the 3 μg/cm^2 dosage.

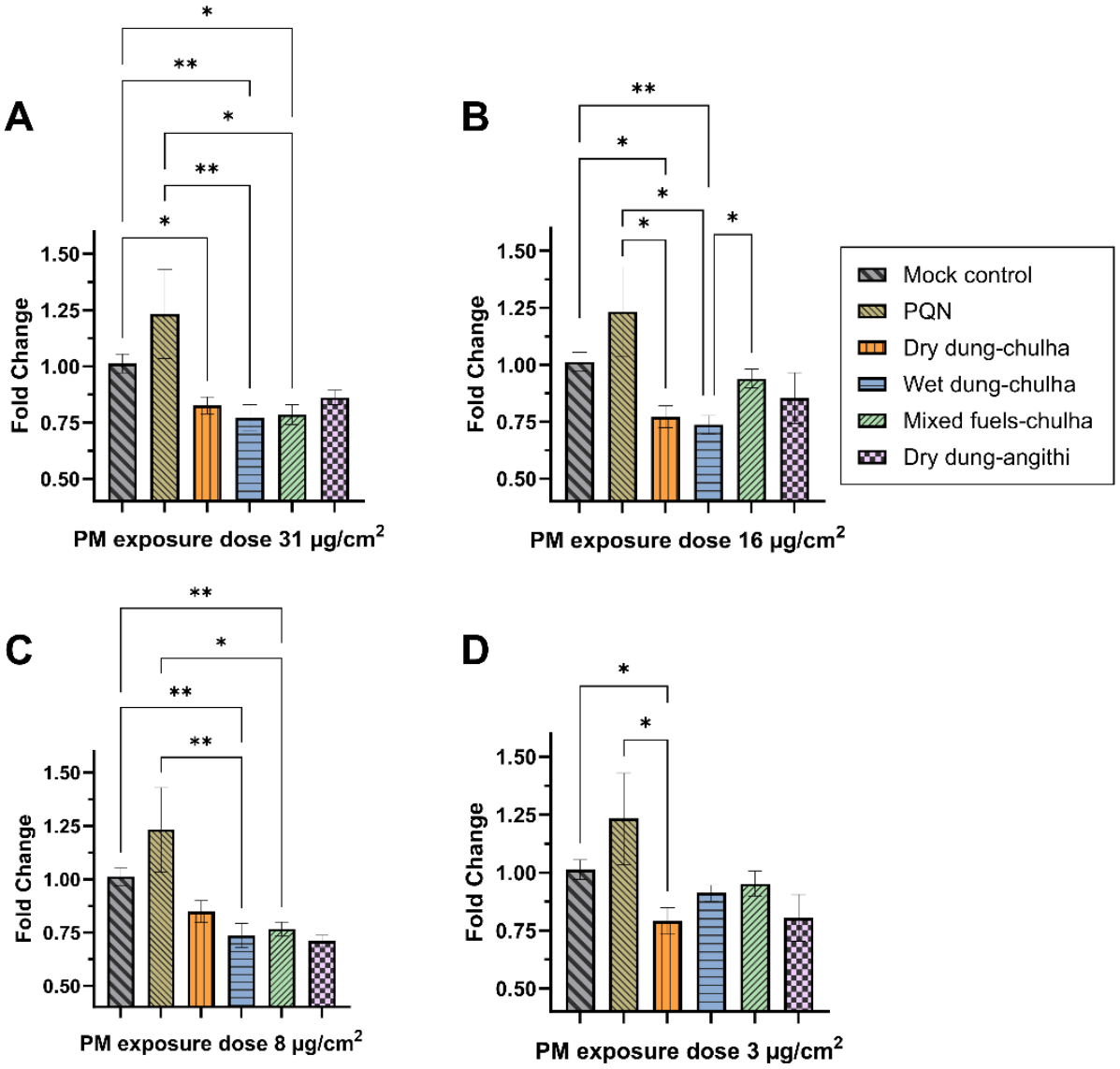

Figure 9: Total superoxide generation during respiratory burst in PM macrophages exposed to biomass PM. *Values were assessed by area under the curve. Cells were treated to concentrations of (A) 31 µg/cm², (B) 16 µg/cm² (C) 8 µg/cm², and (D) 3 µg/cm² of solid biomass fuel PM. A single dose of PQN (0.03µg/cm²) was used as a positive control. * P <0.033, ** P <0.003, *** P <0.001.*

Reductions in total superoxide generation were observed for all cells exposed to biomass PM, with values ranging from 0.71-fold to 0.95-fold change for all treatments and dosages studied. Statistically significant group differences in total superoxide generation for all exposure

treatments (H = 24, P <.001 for dosage of 31 μg/cm^2) were observed, illustrated in Figure 9A. Cells exposed to PM from dry dung angithi exhibited the least pronounced effects of 0.86-fold reduction of total superoxide generation at the higher dosages of 31 μg/cm^2 and 16 μg/cm^2 compared to mock control cell and non-linear dose responses were observed at lower dosages, illustrated in Figure 9B, C, D. For example, cells exposed to dry dung angithi exposed exhibited the strongest reduction in total superoxide generation by 0.71-fold change from mock control at the 8 μg/cm^2 exposure dose but did not reach statistical significance, Figure 9C. Statistically significant reductions in peak superoxide levels were observed in cells exposed to biomass particles generated from chulha cookstoves compared to mock controls but exhibited non-linear dose responses. Maximal superoxide levels were observed at an average time point of t = 11 minute for mock control exposures and PQN exposed cells. Superoxide levels peaked earlier with chulha sourced biomass PM at all doses studied (31 μg/cm^2, 16 μg/cm^2, 8 μg/cm^2, and 3 μg/cm^2) and generally occurred at t = 8 minutes, as described in Figure 10A-D. A summary of all Diogenes results is described in Table 5.

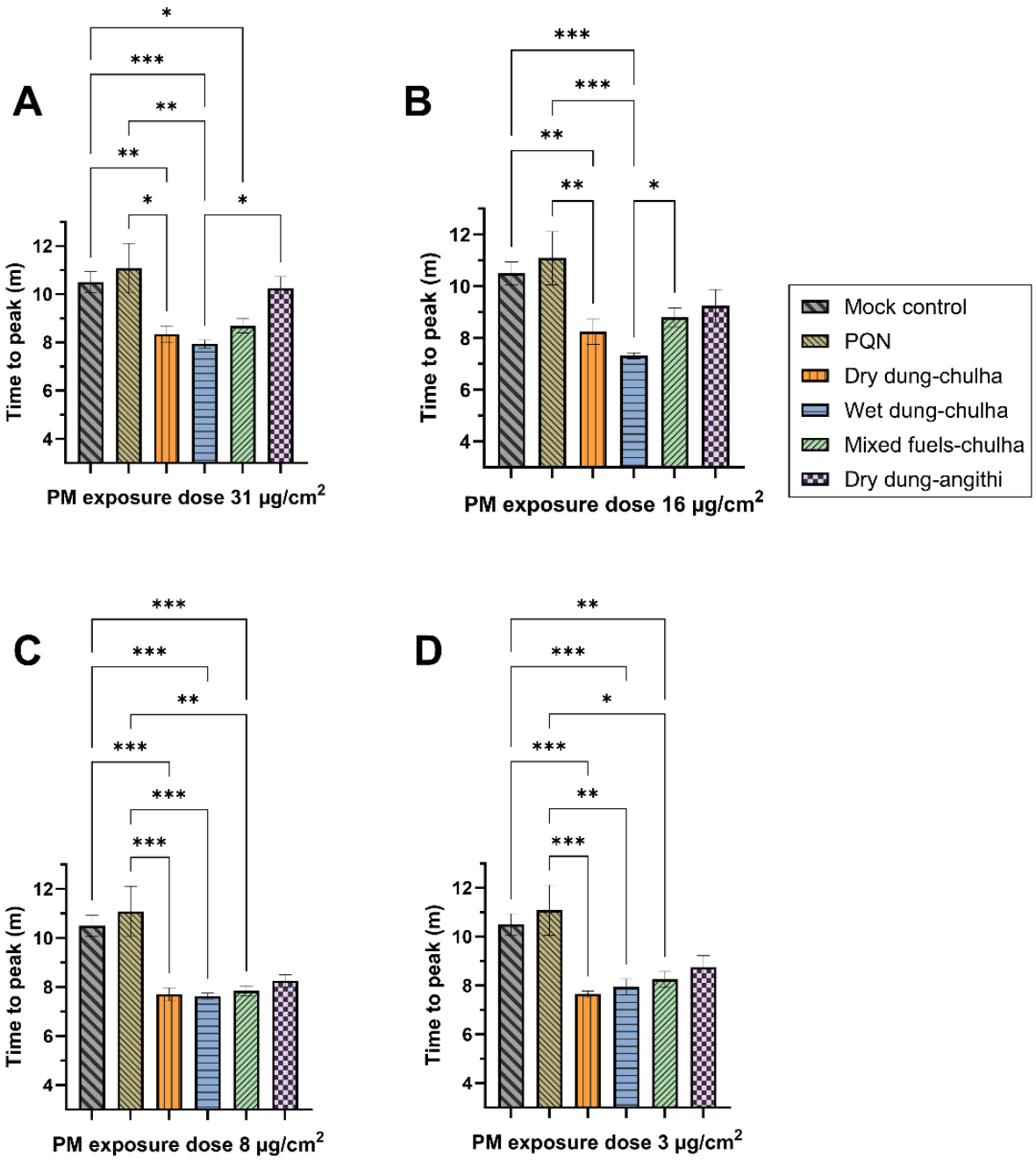

Figure 10: PM source influences mean time at which respiratory burst superoxide generation levels peak. *The minutes until the peak respiratory burst responses was assessed in macrophages treated with either (A) 31 µg/cm^2 (B) 16 µg/cm^2 (C) 8 µg/cm^2 and (D) 3 µg/cm^2 of solid biomass fuel PM. A single dose of PQN (0.03µg/cm^2) was used as a positive control. * P <0.033, ** P <0.003, *** P <0.001.*

Table 5: Summary of Diogenes results

			Total superoxide release		Maximum superoxide level		Time to reach peak value
Dose µg/cm^2	**Treatment**	**N filters; replicate measures***	**Mean AUC ± CV**	**Fold change vs. control**	**Mean Peak value ± CV**	**Fold change vs. control**	**Mean min at peak ± SD**
0	Mock control *	3	28181 ± 14%		1725 ± 20%		10.5 ± 1.4
0.03	PQN *	3	34392 ± 54%	1.2	1568 ± 18%	0.91	11.1 ± 3.4
31	Dry dung-chulha	5	23545 ± 27%	0.83	1194 ± 30%	0.71	8.4 ± 1.5
	Wet dung-chulha	4	20324 ± 30%	0.72	987 ± 26%	0.60	7.9 ± 0.7
	Mixed fuels-chulha	5	21190 ± 18%	0.78	1062 ± 33%	0.65	8.7 ± 1.3
	Dung-angithi	1	19409 ± 7%	0.86	786 ± 3%	0.51	10.3 ± 0.8
16	Dry dung-chulha	5	22844 ± 20%	0.77	1156 ± 31%	0.69	8.3 ± 2.1
	Wet dung-chulha	4	21290 ± 29%	0.74	1064 ± 30%	0.64	7.3 ± 0.5
	Mixed fuels-chulha	5	21658 ± 25%	0.94	1087 ± 30%	0.65	8.8 ± 1.6
	Dung-angithi	1	23497 ± 6%	0.86	1006 ± 8%	0.66	9.3 ± 1.1
8	Dry dung-chulha	5	21287 ± 27%	0.84	1155 ± 37%	0.69	7.7 ± 1.2
	Wet dung-chulha	4	20306 ± 22%	0.73	1018 ± 27%	0.61	7.6 ± 0.5
	Mixed fuels-chulha	5	25898 ± 8%	0.77	1308 ± 25%	0.80	7.9 ± 0.9
	Dung-angithi	1	23139 ± 23%	0.71	1054 ± 11%	0.68	8.3 ± 0.4
3	Dry dung-chulha	5	21901 ± 31%	0.79	1145 ± 32%	0.69	7.7 ± 0.6
	Wet dung-chulha	4	25179 ± 15%	0.91	1187 ± 26%	0.71	7.9 ± 1.3
	Mixed fuels-chulha	5	26277 ± 24%	0.95	1408 ±26%	0.86	8.3 ± 1.4
	Dung-angithi	1	21818 ± 22%	0.80	979 ± 19%	0.64	8.8 ± 0.8

Values represented as the mean ± coefficient of variance (CV) or standard deviation (SD) from (N) filters used for each stove-fuel combination. Fold change is normalized to 1 for mock controls. Solid biomass fuel samples were measured in duplicate wells and represent two biological replicate values, while mock control and PQN were measured in quadruplicate wells and represent three biological replicate values.

4.3.3 Cell viability dose-responses

MTT reduction activity in cells immediately following a 4-hours of incubation with biomass PM did not change from mock treated control cells as described in Figure 11. Cells exposed to 31 µg/cm^2, 16 µg/cm^2, 8 µg/cm^2, and 3 µg/cm^2 of biomass PM showed non-significant fold change ranging between 0.98 to 1.08 compared to mock treated cells. Two dosages of PQN were used for this study (100 µL of either a 0.02 mM or a 0.3 µM solution of PQN). In comparison to controls, a significant reduction of 0.8-fold-change was observed in cells treated with high doses of PQN (0.02 mM) compared to mock controls (P <.001), but not to exposures with lower concentrations of PQN (0.3 µM)

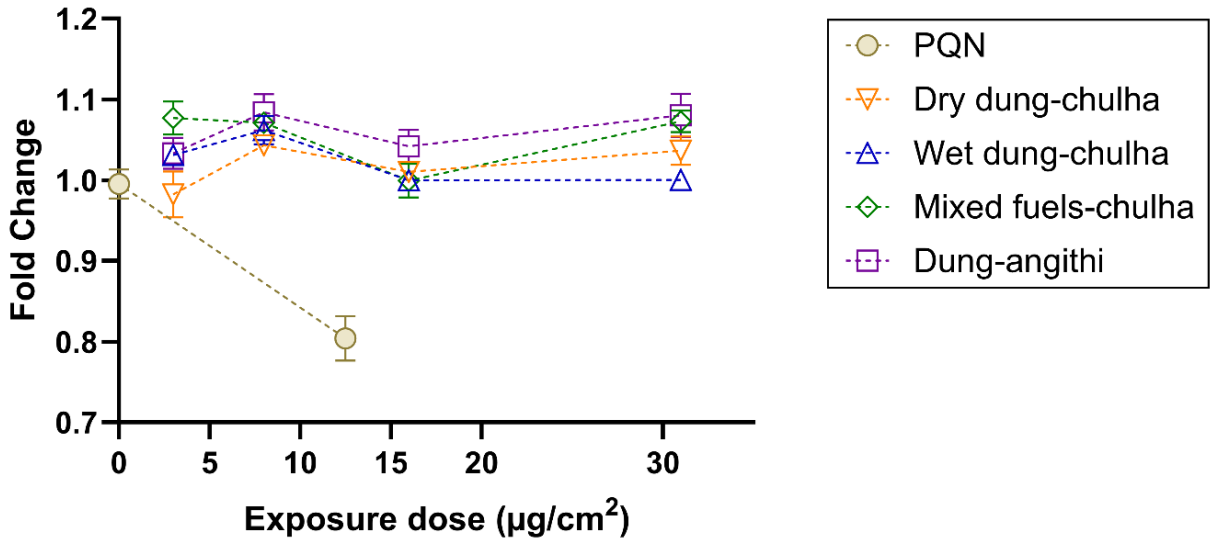

Figure 11: Dose response cell viability changes assessed by MTT metabolic assay. *Cells were exposed to SRM 1648a or biomass PM (3-31 µg/cm^2). Two concentrations of PQN were used (0.03 µg/ cm^2 or 12.5 µg/ cm^2) were used as a redox active positive control. Values expressed as mean fold change from mock treated controls (value of 1.0) ± SEM.*

4.3.4 Apoptosis analysis

To confirm whether cytotoxicity was contributing to changes in respiratory burst dynamics, the population of cells entering apoptotic pathways was also assessed using flow cytometry. Apoptosis was not a major pathway of cytotoxicity in cells following acute exposures to SRM1648a or solid biomass fuel emissions, as described in Figure 12A. Less than 2% of cells were apoptotic, which was comparable to mock treated cells, Figure 12 B.

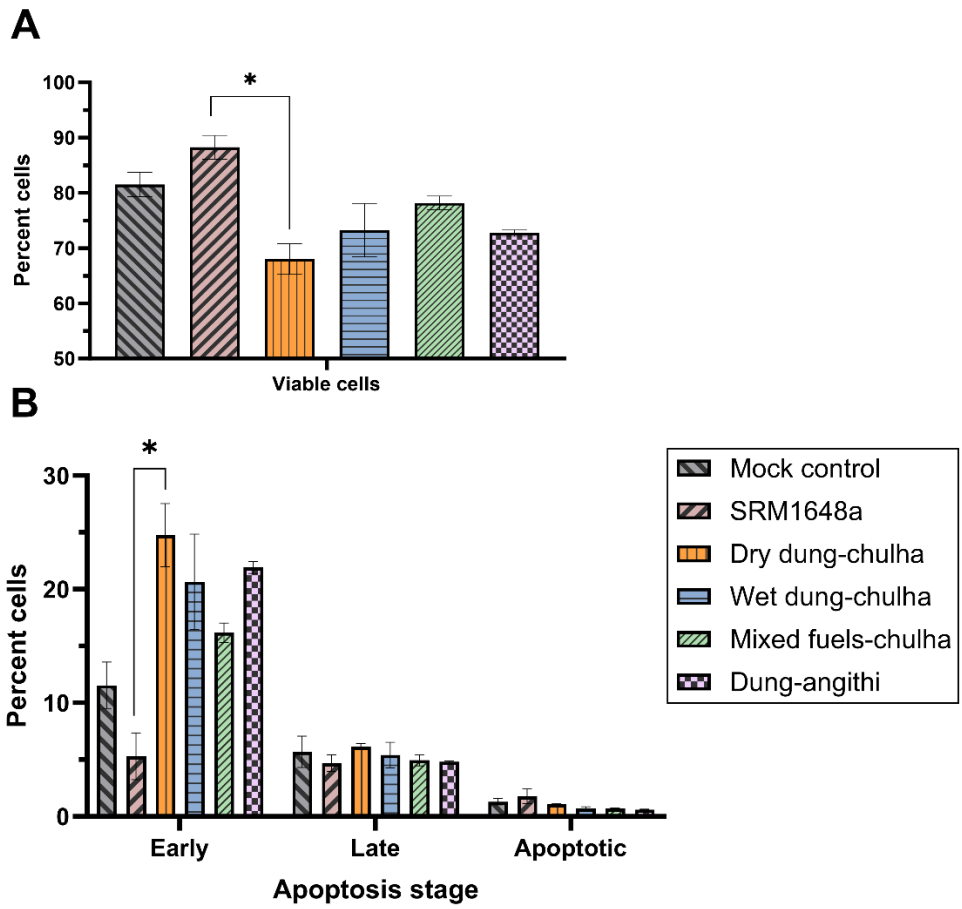

Figure 12: Percentage of cells entering apoptosis. *Cells were exposed to 14 µg/cm^2 PM for 4-hours before assessing percentage of viable and apoptotic cells by Annexin-V and PI staining. Two biological replicates for each individual PM filter sample were included to assess the mean values ± SEM. The percentage of (A) healthy viable cells or (B) cells entering apoptosis are illustrated. Less than 2% of all cells observed were apoptotic. * P <0.033, ** P <0.003, *** P <0.001.*

Interestingly, viability was higher in cells treated with urban dust SRM 1648a (mean = 88%) than in mock treated cells (mean = 81%). The lowest viability was observed in cells treated with dry dung from chulha (mean = 68%), which was significantly lower than SRM1648a treated cells (P =.05). While no significant differences in cells entering late apoptosis were observed among the different exposure groups compared to mock controls, the changes in the viable cell population corresponded with differences in the percentage of cells entering early apoptosis. For example, mock treated cells had a mean of 12% of cells entering early apoptosis, while cells treated with SRM 1648a had a mean of 5% of cells entering apoptosis. Cells treated with dry dung from chulha also had significantly higher proportion of cells in early apoptosis (mean = 25%) compared to SRM1648a treated cells (mean = 5%, P =.04). While not statistically significant, trends for biomass treated cells revealed a higher proportion of cells in early apoptosis compared to the mock controls.

4.4 Discussion

4.4.1 Macrophage respiratory burst is inhibited by sub-lethal doses of solid biomass fuel emissions

The results from this study demonstrate that a single acute 4-hour exposure to biomass particles alters respiratory burst dynamics, a critical innate immune function. Macrophage exposure to sublethal concentrations of solid biomass fuel PM resulted in modulated respiratory burst dynamics involving accelerated initial superoxide generation, yet diminished peak responses, and a decrease in the total amount of superoxide generated compared to mock controls. Respiratory burst inhibitions were captured 18-hours following the replacement of PM exposure media with

clean media, indicating that immunomodulatory effects of PM and PQN persist in macrophages even 22-hours after an initial 4-hour exposure to solid biomass fuel emissions.

Superoxide is a precursor to reactive oxygen species formation, while the extent of oxidative burst is a partial indicator of the immunocompetence and ROS accumulation in cells. While the results of this study indicate that cells are not generating excessive superoxide via NOX activation following acute 4-hour exposures to solid biomass PM, depressed respiratory burst following exposure to PM has been observed in other studies. One study showed that 24-hour exposures to $PM_{2.5}$ led to respiratory burst suppression in rabbit alveolar macrophages stimulated with zymosan, and particle number, mass, and metal content was associated with the inhibited response [84]. Various others studies have shown that wildfire, woodsmoke, and black carbon PM emissions deplete antioxidant enzymes, reduced respiratory burst responses, and impaired bacterial clearance following exposure to nonlethal doses of PM [42,85–90]. While the results in this study do not provide insight into the mechanism or specificity of altered macrophage respiratory burst response to specific fuel-stove combinations, these findings do indicate that the redox cycling capacity associated with PQN influences cellular toxicity in a manner that is different from solid biomass fuels.

Changes in cell respiratory burst dynamics were not due to cytotoxicity. The results of this study do not indicate any statistically significant changes in mitochondrial activity, cell membrane damage, and apoptosis following 4-hour exposures to solid biomass fuel PM emissions. Rather, PM exposed cells have non-significant increases in metabolic activity. This phenomenon of non-significant increased metabolic activity in PM exposed cells has been observed in other studies exposing cells *in vitro* to relatively low contractions or short exposure periods [91]. These viability results were confirmed by an additional assessment of intracellular ATP levels. Cells exposed to

the relatively lower concentration of PQN had a non-significant increase in intracellular ATP compared to mock controls, but a non-significant decrease in intracellular ATP were observed for solid fuel treated cells. These opposing trends in intracellular ATP were not considered to be indicative of cytotoxicity but indicate that PQN and solid biomass fuel emissions may have different impacts on cellular energy homeostasis (Appendix A1). While mitochondrial stress was not the focus of this study, mitochondrial proton and electron leaks could impact cellular superoxide production and minor fluctuations in mitochondrial respiration may also impact cellular energy homeostasis [92]. Such energy fluctuations could contribute to the ability for PQN treated cells to sustain respiratory burst responses and may explain the attenuated responses in biomass treated cells but warrants further investigation. Changes in apoptosis were not assessed in PQN treated cells. However, significant differences in the percent of viable cells and the initiation of apoptosis were observed between cells exposed to urban dust and cells exposed to PM emissions from chulha stoves. Together these findings provide valuable insight into macrophage respiratory burst functions alterations following exposures to sub-lethal concentration of solid biomass fuel emissions and indicate pollutants from diverse sources may have impacts immune cell function and viability via distinct mechanisms.

4.4.2 Limitations

There are several limitations that should be considered with the results of *in vitro* exposure studies. These results only reflect effects from a single 4-hour exposure and further studies containing additional time points should be used to verify these conclusions. Furthermore, studies using higher dosages of PM would provide insight into the concentrations needed to induce macrophage cell death. However, the sample volume that could be used for experiments was limited due to the finite number of solid biomass filters and PM mass attained from field

sampling. Finally, while the results of this study indicate that exposure to non-lethal concentrations of PM inhibits respiratory burst to modulate superoxide generation, a detailed molecular mechanism that explains the reduced superoxide generation capacity is not directly addressed in this study. Cellular redox status is not assessed in this study and the influence of reductive and oxidative stress is not directly addressed. These results should be replicated, and future studies should focus on understanding whether factors such as diminished expression of NOX, direct enzymatic inhibition of NOX by PM components, or changes in the expression of other antioxidant neutralizing proteins explain the observed effects in superoxide generation capacity in macrophages exposed to PM.

5. Gene expression alterations and cell cycle dynamics in macrophages exposed to solid biomass fuel PM

5.1 Regulation of antioxidant gene expression

ROS and electrophile compounds are recognized to activate nuclear factor (erythroid-derived 2)-like 2 (Nrf2) transcription factor and the subsequent transcription of antioxidants and cytoprotective genes. Nrf2 targets include antioxidants glutathione (GSH), glutathione reductase (Gsr), and glutathione peroxidase-1 (Gpx1), detoxification enzyme NAD(P)H: quinone oxidoreductase 1 (Nqo1), and metabolism gene glucose-6-phosphate dehydrogenase (G6pd), which facilitate cellular adaptation to toxic insults and maintain redox and metabolic homeostasis, illustrated in Figure 13.

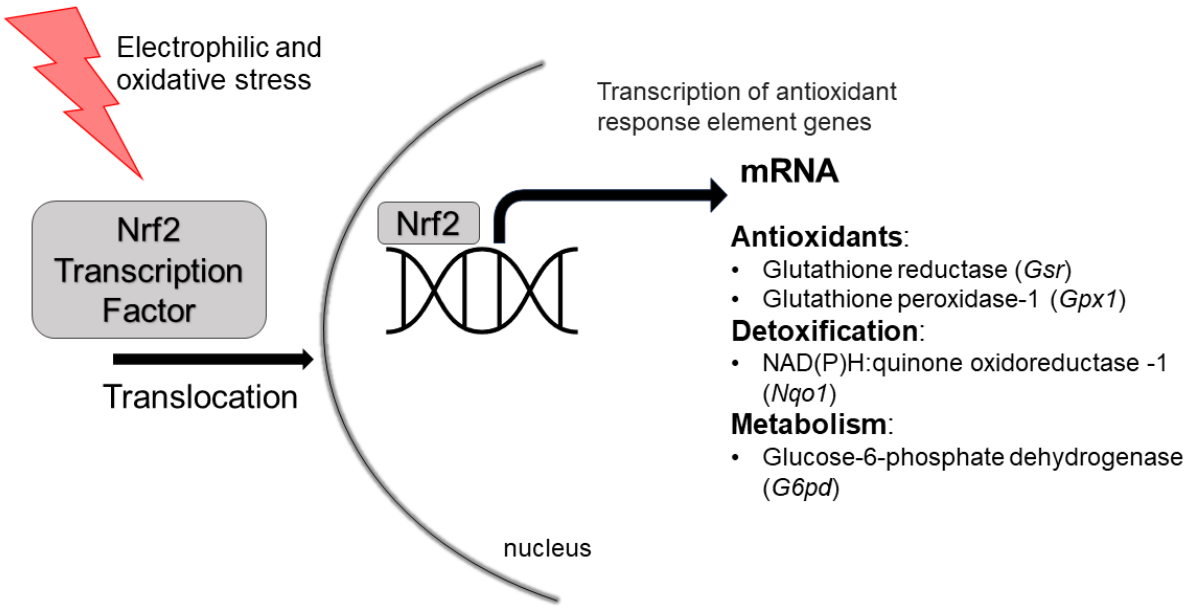

Figure 13: Exogenous and endogenous ROS and electrophile compounds activate the translocation of Nrf2 *, a transcription factor that regulates the transcription of various antioxidants and cytoprotective genes.*

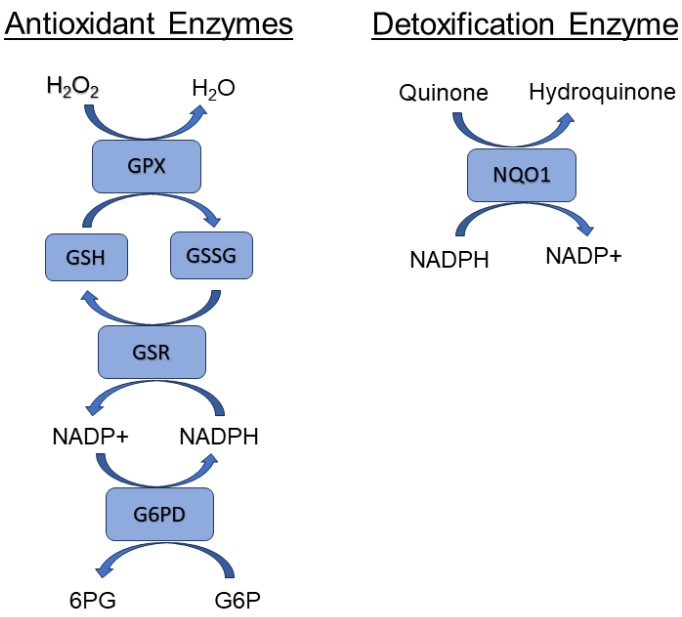

Figure 14: The glutathione antioxidant pathway defends against oxidative stress. *Oxidative stress promotes a cellular shift to the oxidized state of glutathione disulfide (GSSG). Nrf2 regulates the expression of genes involved in maintaining a reduced GSH pool and NADPH regeneration. Nrf2 also regulates the transcription of oxidant detoxification enzymes such Nqo1, which also depend on the availability of NADPH cofactors.*

GSH is an antioxidant containing a sulfhydryl group (-SH) which exists in two redox states, as it can participate in reduction and conjugation reactions to mitigate the effects of cellular reactive species such as peroxides. Oxidative stress shifts the ratio of reduced GSH and oxidized glutathione disulfide (GSSG). Multiple molecular players maintain GSH homeostasis during oxidative stress, including glutathione reductase (Gsr) which reduces oxidized glutathione disulfide (GSSG) back to its reduced GSH form using NADPH as a reducing cofactor. However, GSH also participates in the enzymatic activity of Gpx1, acting as a cofactor to catalyze the detoxification of hydrogen peroxide. Other Nrf2 targets such as Nqo1 detoxify toxic quinones into hydroquinone and utilize either NADH or NADPH as reducing cofactors. The levels reducing cofactors GSH and NADPH are maintained by G6pd, the rate-limiting enzyme of the fundamental pentose phosphate cellular metabolic pathway [93–95]. The interconnected relationship

between antioxidant and detoxifying enzyme activity, and energy-dependent processes is illustrated in Figure 14.

Dysregulation of *Nrf2* expression and function is implicated in PM induced lung injury and the exacerbation of respiratory diseases such as emphysema and COPD. Disruption of the GSH antioxidant system is implicated in the development and progression of respiratory diseases such as COPD and cardiovascular diseases including atherosclerosis [96,97]. PM can alter intracellular levels of GSH, GPx1 and Gsr and thereby modulate the cellular redox state and disrupt normal cell signaling processing. However, it remains unclear how different air pollutants drive changes in the regulation of the Nrf2 response pathway and dynamic antioxidant, detoxification, and metabolic adaptation gene responses. Several studies report that PM oxidants and electrophiles activate Nrf2 to induce the expression of antioxidants. For example, the PAH content and oxidative potential of diesel exhaust particles and ambient PM have been reported to play an important role in inducing Nrf2 activity and downstream antioxidants enzymes in macrophages following 6-hour *in vitro* exposures [98]. Similarly, *Nrf2* and downstream genes levels were upregulated in the blood sample from elderly people with coronary artery disease in response to traffic related population [99]. However, other patterns of *Nrf2* dysregulation have also been observed in studies using human alveolar macrophages from smokers, which show that basal *Nrf2* messenger RNA (mRNA) expression and its target genes is lower among older smokers, compared to younger smokers [100].

Women who cook exclusively with biomass fuels have been found to have higher protein expression of Nrf2 and NQO1 in sputum samples compared to LPG users [101]. While Nrf2 and NQO1 provide adaptive protection from PM elicited oxidative stress, *NQO1* overexpression has been linked to susceptibility to COPD and pulmonary cancer [102–104]. This may be explained by

the diverse functions of Nqo1 involving cell proliferation, cell cycle progression, and metabolic regulation [105]. To further understand the changes in macrophage respiratory burst which were seen after exposure to solid biomass fuel PM, the mRNA expression of transcription factor *Nrf2*, and the expression of downstream target genes, *Gpx1*, *Gsr*, *Nqo1*, and *G6pd* were assessed after an acute *in vitro* exposure using RAW 264.7 macrophages. Changes in cell cycle progression in cells exposed to biomass PM emissions were also explored to study the relationship between cellular redox state, metabolism, and changes in normal macrophage cell function.

5.2 Materials and methods

5.2.1 Gene expression analysis using Real-Time Polymerase Chain Reaction

Gene expression was assessed using quantitative real time polymerase chain reaction (qRT-PCR). RAW 264.7 cells were plated at a density of 2.5 x 10^5 cells per well on a 24-well plate and were treated with to 26 µg/cm^2 of PM extracts for four hours before harvesting total ribonucleic acid (RNA) using TRI reagent. A single dosage of a 0.3 µM PQN solution (0.1 µg/ mL; 0.005 µg/cm^2) was used as a positive control for a redox active compound. Sterile cell culture water was used as a mock treatment for all biological studies. RNA was isolated and purified using Directzol RNA microprep kit (Zymo Research) according to manufacturer's instructions. The quantity and quality of RNA was determined by measuring absorbance at 260 nm and 280 nm using a NanoDrop Lite spectrophotometer (ThermoFisher). Reverse transcription of 0.5 µg of total RNA to generate complementary deoxyribonucleic (cDNA) was performed using the iScript™ acid cDNA synthesis kit (Bio-Rad) using a single cycle reaction starting with priming at 24 ˚C for five minutes, reverse transcription at 46 ˚C for 20 minutes, and inactivation at 95 ˚C

for one minute to make cDNA. Synthesized cDNA was then diluted 1:5 and 1 uL was amplified per well on a BioRad CFX Connect thermocycler using the iTaq Universal SYBR green supermix (Bio-Rad). The qRT-PCR cycle conditions were initiated by an initial denaturation at 95˚C for three minutes, followed by 40 cycles of denaturing step (95 ˚C for 10 seconds), annealing step (60 ˚C for 60 seconds) and extension step (72 ˚C for 60 seconds). The BioRad CFX Manager software version 3.1 was used to determine Cq values. Primer sequences were selected from previously published sequences and are listed in Table 6. The relative expression levels of nuclear factor erythroid 2–related factor 2 (*Nrf2*) [106], glutathione peroxidase 1 (*Gpx1*) [107], NAD(P)H quinone dehydrogenase 1 (*Nqo1*) [108], glutathione reductase (*Gsr*) [109], and glucose-6-phosphate dehydrogenase (*G6pd*) [93] were calculated using the comparative Ct method (2^-ΔΔCt) [110] using glyceraldehyde 3-phosphate dehydrogenase (*Gapdh*) [111] as the reference gene. The specificity of the amplification products was confirmed by melting curve analysis.

Table 6: Primer sequences used for qRT-PCR

Nrf2 forward	5'-CTGAACTCCTGGACGGGACTA-3'
Nrf2 reverse	5'-CGGTGGGTCTCCGTAAATGG-3'
Gpx1 forward	5'- CCACCGTGTATGCCTTCTCC-3'
Gpx1 reverse	5'- AGAGAGACGCGACATTCTCAAT-3'
Nqo1 forward	5'- TTCTGTGGCTTCCAGGTCTT-3'
Nqo1 reverse	5'-TCCAGACGTTTCTTCCATCC -3'
Gsr forward	5'- CACGGCTATGCAACATTCGC -3'
Gsr reverse	5'- TGTGTGGAGCGGTAAACTTTT-3'
G6pd forward	5'- CCTACCATCTGGTGGCTGTT-3'
G6pd reverse	5'- CATTCATGTGGCTGTTGAGG-3'
Gapdh forward	5'-GAAGCCCATCACCATCTTCCA-3'
Gapdh reverse	5'-TTGGCTCCACCCTTCAAGTG-3'

5.2.2 Cell cycle analysis using BrdU FITC assay

Cells were seeded in 12-well plates at a density of 2.5 x 10^5 cells per well and exposed to 14 µg/cm^2 of biomass particulate extracts before quantifying cell cycle progression with immunofluorescent staining of incorporated bromodeoxyuridine (FITC BrdU Flow Kit; BD Sciences). A single dosage of a 0.3 µM PQN solution (0.1 µg/ mL; 0.003 µg/cm^2) was used as a positive control for a redox active compound. Sterile cell culture water was used as a mock treatment for all biological studies. Following exposure with PM, cells were incubated with 10 µL of 1 mM BrdU solution in PBS for 2-hours. Cells were harvested by scraping and washed with staining buffer (PBS + 2% FBS) and centrifuged at 1200 rpm (Allegra 6R Centrifuge) for five minutes before proceeding to fixation and permeabilization steps, as described by the manufacturer. Cells were treated with 30 µg of Deoxyribonuclease (DNase) diluted in phosphate buffered saline (PBS) for 45 minutes before proceeding to incubate the cells for 20 minutes with 1 µL of anti-bromodeoxyuridine (BrdU) antibody in 50 µL BD perm/wash buffer. Finally, cells were incubated with 50 µg propidium iodine (PI) resuspended in a total of 1 mL of staining buffer before acquiring cell staining data with a flow cytometer. Data was acquired using a BD Accuri C6 Flow cytometer and FlowJo software. Samples were measured in duplicate and represent two biological replicate values, while controls represent three biological replicate values.

5.2.3 Statistical analysis

All data were expressed as means ± SEM, unless otherwise stated. Different sample size filters (N) were used across experiments, due to sample volume limitations. For qRT-PCR experiments, N = 3 dry dung-chulha filters, N = 4 wet dung-chulha filters, N = 3 mixed fuels-chulha filters,

and N = 2 dung-angithi filters were used. Samples were measured in duplicate wells and represent two biological replicate values, while controls represent three biological replicate values. Gene expression data were normalized to *Gapdh* within each plate, and values are normalized to the fold-change of 1 for mock controls. For cell cycle analysis, values represent percentage of cells positive for the outcome evaluated, from the total cell population analyzed. For gene expression analysis, the statistical significance was assessed following a normality test using a Bonferroni-corrected one-way ANOVA and a significance level of a=0.05. For cell cycle experiments, N = 5 dry dung-chulha filters, N = 4 wet dung-chulha filters, N = 6 mixed fuels-chulha filters, and N = 3 dung-angithi filters were used. For cell cycle analysis, the statistical significance was assessed using the non-parametric Kruskal-Wallis test performed with Dunn's correction for multiple comparisons following a normality test using a significance level of a=0.05. All statistical analyses were performed using GraphPad Prism (version 10.1.0 for Windows, GraphPad Software, San Diego, CA, USA, www.graphpad.com).

5.3 Results

5.3.1 Particulate matter source-specific effects on mRNA expression of redox and metabolic homeostasis-related genes

Figure 15 shows the results of this study demonstrating that all PM treatments generally resulted in a downregulation of *Nrf2* and *Gpx1* gene transcription, and upregulation of *Nqo1*. However, different transcriptional response trends were observed for *Gsr* and *G6pd* among cells exposed to PM from varying sources. Statistically significant differences in mean fold change in *Nrf2* expression between groups ($F(6,34) = [5.0]$, $P < .001$) were observed. *Nrf2* mRNA levels are significantly downregulated after 4-hour exposures to all treatments, except chulha dry dung PM emissions, (Figure 15A). Macrophages exposed to SRM 1648a and PQN had significantly reduced expression of *Nrf2* by to almost half compared to those of mock treated cells (mean = 0.5-fold change, $P = .03$ and mean= 0.4-fold change, $P = .01$, respectively.) Cells exposed to solid biomass fuel emissions demonstrated similar statistically significant downregulation of *Nrf2*. Cells exposed to wet dung PM from chulha stoves showed a 0.6-fold reduction ($P = .01$), while cells exposed to mixed fuels PM from chulha stoves showed a 0.5-fold reduction ($P = .01$), and cells exposed to dung PM from angithi stoves showed a 0.6-fold reduction compared to mock treated controls ($P = .01$). Cells exposed to chulha dry dung PM exhibited a similar trend of reduced *Nrf2* expression of 0.8-fold compared to mock controls, but these effects did not reach statistical significance.

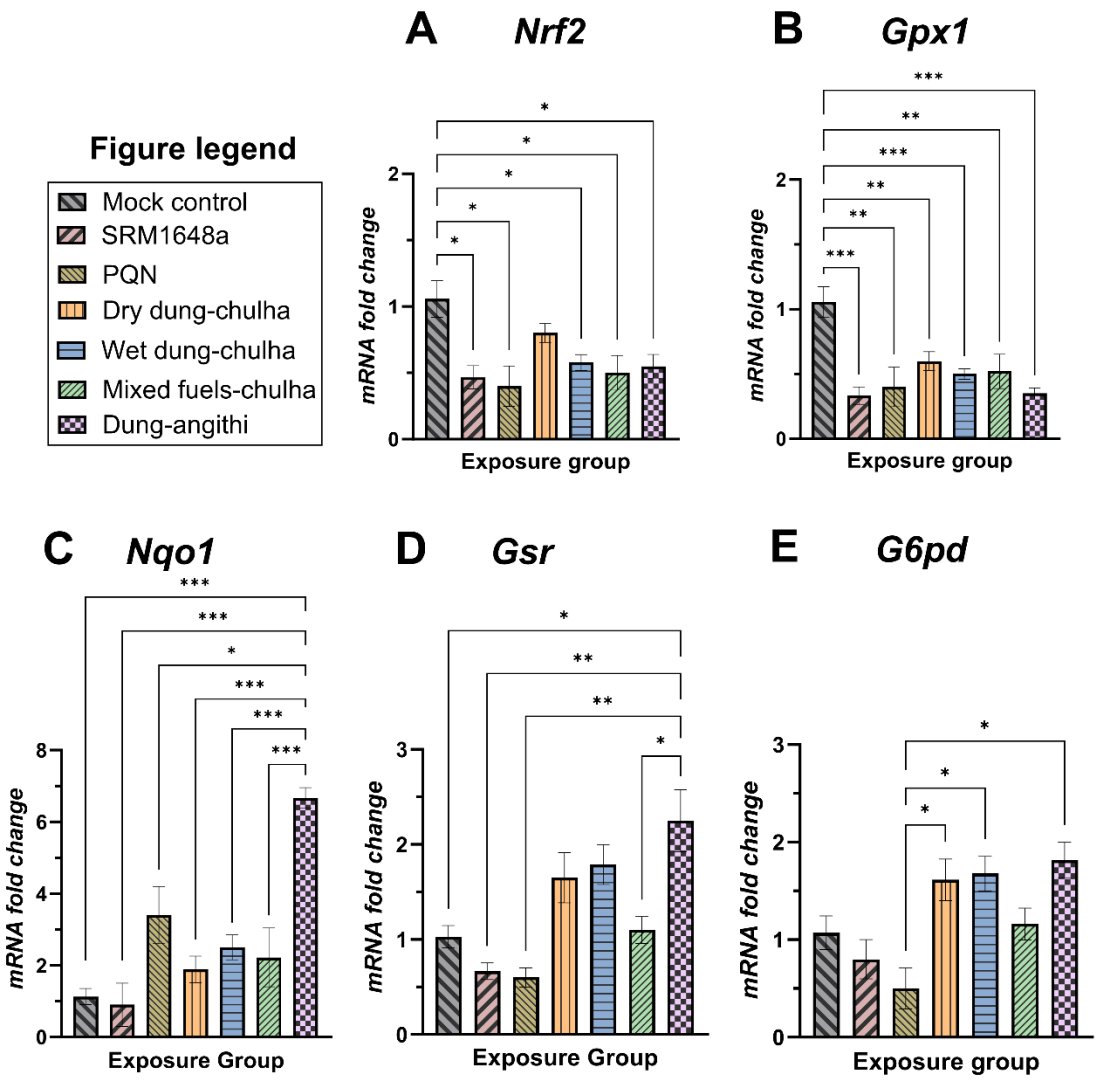

Figure 15: Gene expression of antioxidant and metabolic related genes in RAW 264.7 cells *exposed to 26 µg/cm2 of PM extracts or 0.005 µg/cm2 of PQN for four hours. The relative expression levels of (A) Nrf2, (B) Gpx1, (C) Nqo1, (D) Gsr, and (E) G6pd normalized to Gapdh mRNA were expressed as fold change from mock treated controls. * p <0.033, ** p <0.003, *** p <0.001.*

Statistically significant differences in mean fold change of *Gpx1* expression between groups were also observed (F (6,34) = [8.2], P <.001). The mRNA levels of *Gpx1* were downregulated by nearly half in PM exposed groups compared to mock treated controls (Figure 15B). Statistically significant downregulation of *Gpx1* mRNA levels were observed in SRM 1648a treated cells which had levels reduced by 0.33-fold (P <.001), while PQN treated cells had a

reduction of 0.4-fold (P =.002) compared to control cells. Angithi dung exposed cells showed a 0.35-fold reduction (P <.001) compared to untreated cells. Cells exposed to chulha emissions also demonstrated similar reductions in *Gpx1* expression with a 0.6-fold reduction observed in chulha dry dung exposed cells (P =.005), and a 0.5-fold reduction observed in both in chulha wet dung and mixed fuel exposed cells (P <.001, P =.003 respectively).

While *Nrf2* and *Gpx1* genes were downregulated following acute exposure to PM from various sources, the expression of antioxidant gene *Nqo1* was upregulated in macrophages treated with PQN and biomass fuel sources (Figure 15C). Statistically significant differences in mean fold change in *Nqo1* expression between groups (F (6,32) = [19.0], P <.001) were observed. Angithi dung exposure led to a significant upregulation of *Nqo1*, showing a remarkable 6.6-fold increase compared to untreated controls (P <.001). Furthermore, *Nqo1* gene expression levels of angithi dung exposed cells exceeded those observed in the other exposure groups and was statistically higher compared to PQN, SRM 1648a, and PM from chulha stoves (P <.001). Cells exposed to solid biomass fuel emissions or PQN exhibited a nearly 2-fold upregulation of *Nqo1* compared to mock controls, although the difference did not reach statistical significance. A 1.9-fold upregulation of *Nqo1* was observed in cells exposed to dry dung from chulha stoves, which was similar to the change observed in cells exposed to mixed fuels from chulha exhibiting a 2.2-fold upregulation, compared to untreated controls. A similar trend was also observed in cells exposed to wet dung from chulha stoves, with a 2.5-fold upregulation of *Nqo1* expression. This upregulation was comparable to the 2.4-fold upregulation observed in PQN exposed cells. In contrast, cells treated with SRM 1648a exhibited a 0.9-fold change in *Nqo1* expression.

The expression of *Gsr* and *G6pd* was also upregulated in cells exposed to solid biomass fuels. The changes in *Gsr* expression exhibited similar trends to the observed changes in *Nqo1* gene

expression following acute exposure to PM. Statistically significant differences in mean fold change in *Gsr* expression between groups (F (6,34) = [5.5], P <.001) were observed (Figure 15D) Exposure to dung-angithi PM resulted in a significant upregulation of *Gsr* expression of 2.3-fold compared to untreated cells (P =.01). Upregulation of *Gsr* expression in cells exposed to dung-angithi emissions surpassed the levels induced by other PM treatments and demonstrated statically significant differences compared to cells exposed to SRM 1648a (P =.01), PQN (P =.006), and chulha mixed fuels (P =.05). Cells exposed to wet or dry dung from chulha stoves also demonstrate a moderate but non-significant upregulation of *Gsr* by nearly 1.7-fold compared to untreated controls. Chulha mixed fuel exposed cells did not differ from mock controls (mean = 1.1-fold change). Cells exposed to SRM 1648a and PQN exposures exhibited downregulated *Gsr* gene expression by 0.7- and 0.6-fold, respectively, albeit not statistically significant.

Finally, statistically significant differences in mean fold change in *G6pd* expression between groups (F (6,34) = [4.7], P =.001) were observed (Figure 15E). Exposure to PQN also led to a downregulation of *G6pd* gene expression, with a notable decrease of 0.5-fold compared to untreated controls. This reduction was significantly lower than the groups exposed to dry dung from chulha (P =.04), mixed fuels from chulha (P =.02), and dung from angithi (P =.01). While statistical significance in *G6pd* expression was not achieved solid biomass fuel exposed cells against mock controls, these exposures resulted in relatively higher levels of *G6pd* mRNA compared to the controls. The *G6pd* mRNA levels in chulha dry dung and wet dung exposed cells were increased by 1.6- and 1.7-fold respectively, which was comparable to cells exposed to the 1.8-fold fold upregulation observed in macrophages exposed to dung PM from angithi stoves. *G6pd* mRNA levels in cells exposed to chulha mixed fuels did not differ from mock controls

(mean = 1.2-fold change). Macrophages exposed to SRM 1648a also exhibited a marginal decrease in *G6pd* mRNA levels, reaching approximately 0.8-fold relative to controls.

5.3.2 Cell cycle dynamics following exposure at non-lethal doses

Cell cycle progression and pro-apoptotic changes were assessed with intracellular staining paired with flow cytometry techniques. Minor differences in cell cycle progression were observed after acute exposures to PM from various sources, illustrated in Figure 16.

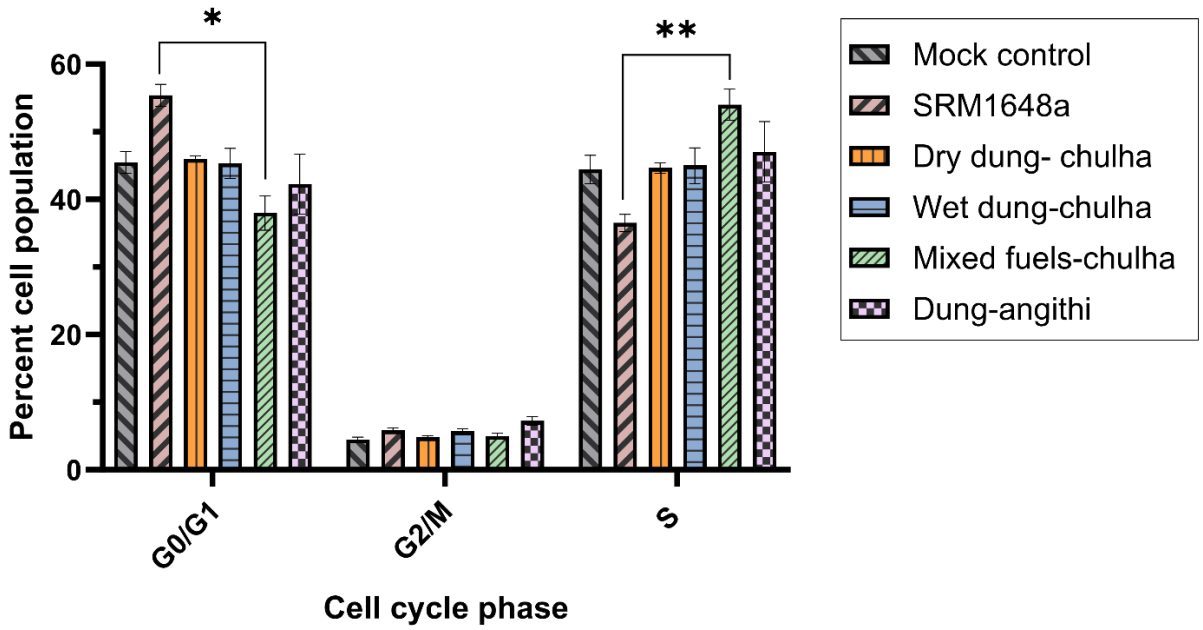

Figure 16: Acute PM exposure influences macrophage cell cycling dynamics. *Percentage of cells in G0/G1, G2/M, or S phase following exposure to 14 µg/cm^2 for 4-hours. Two biological replicates for each individual PM filter sample were included to assess the mean values. * P <0.033, ** P <0.003, *** P <0.001.*

The mean percentage of cells in G0/G1 phase was 45% for mock control cells, which was unchanged in cells exposed to dry dung PM from chulha (mean = 46%), wet dung PM from chulha (mean = 45%), and dung PM from angithi (mean = 42%). Cells treated with SRM 1648a had a higher percentage of cells in G0/G1 phase (mean = 55%) but did not reach statistical

significance. This increase in G0/G1 phase in SRM 1648a treated cells also corresponded to a reduced percentage of cells in the active division S-phase (mean = 34%). The mean percentage of cells in S-phase among mock controls was 41% and cells exposed to dry dung from chulha (mean = 42%), wet dung from chulha (mean = 38%), or dung from angithi (mean = 38%) did not differ significantly from control cells. Cells treated with mixed wood-dung fuel chulha PM had statistically significant reductions in the percentage of cells in G0/G1 phase compared to SRM 1648a treated cells (mean = 38%, P =.01). This corresponded with statistically significant difference of cells in S-phase, with mixed fuel treated cells having a higher percentage of cells actively dividing compared to SRM 1648a treated cells (mean = 54%, P =.008).

5.4 Discussion

5.4.1 Transcriptional modulation of redox and metabolic homeostasis-related genes by particles from distinct sources

The results in this study fall in line with previous scientific findings indicating that the expression of antioxidant related genes could be either upregulated or downregulated by PM from distinct sources. Unexpectedly, *Nrf2* and *Gpx1* gene expression was consistently downregulated in cells exposed to all PM treatments, but there were variable effects on the expression of other target genes downstream of *Nrf2* such as *Nqo1*, *Gsr*, and *G6pd* following exposure to either SRM 1648a, PQN, or biomass fuel emissions from distinct stove sources. It is possible that gene transcription studies do not reflect the protein levels activity and regulatory mechanistic changes impacted by PM exposure. A study by Li *et al*. demonstrated that Nrf2 protein accumulated in the nucleus in macrophages and epithelial cells following exposure diesel exhaust particles, but changes in Nrf2 protein activity were not accompanied by increased *Nrf2*

mRNA expression at any time point [98]. Their results indicated that diesel exhaust particles also had variable effects on the expression of specific antioxidants following acute 3-hour exposures, showing increased expression of heme oxygenase and *Nqo1*, but no changes in the levels of *Gpx1* and *Gsr* compared to controls. Studies comparing the effects of multiple air pollutants on antioxidant gene expression have also demonstrated that transcriptional responses are likely both cell specific and are differentially activated by different PM sources. Urban PM SRM 1648a and cigarette smoke extract have been shown to differentially alter the expression of genes encoding *Gpx1* and *Gsr* antioxidant enzymes in human epithelial cells. One study reported that 24-hour exposures to SRM 1648a resulted in the downregulation of both *Gpx* and *Gsr* genes, while exposure to cigarette smoke extract decreased *Gpx1* gene expression, but increased *Gsr* gene expression levels when compared to control cells [112].

While activation of the antioxidant response system has been extensively studied in cells exposure to PM sourced from urban environments, this study provides insight into the effects induced by exposure to dung and mixed biofuel PM emissions from traditional cookstoves. The results from this chapter indicate that *Gpx1* gene expression is significantly reduced by SRM 1648a, PQN, and solid fuel PM emissions when compared to mock controls. Nonsignificant downregulation of *Gsr* was observed in SRM 1648a and PQN treated cells compared to mock controls. On the other hand, *Gsr* upregulation was observed in biomass treated cells, with significant upregulation observed in cells exposed to PM from angithi stoves compared to cells exposed to SRM 1648a. These results indicate that PM particles from different sources contribute to oxidative stress by reducing the expression of antioxidant enzyme-encoding genes, such as *Gpx1*. However, chemical compounds unique to biomass combustion conductions play a

role in the differential transcriptional modulation of *Gsr*, with cells exposed to PM from angithi stoves exhibit a strong upregulation compared to other PM treatments

Exposure to SRM 1648a also resulted in decreased expression of *Nqo1*, and *G6pd* although these were not significant when compared to the mock control. However, the expression of *Nqo1* and *G6pd* were significantly higher in biomass PM treated cells when compared to SRM 1648a. Emissions from dung-angithi emissions exhibited the strongest upregulation response of these genes, further indicating that PM properties associated with combustion source properties contribute to the transcriptional modulations observed in this study. *Nqo1* was upregulated by all treatments except SRM 1648a. The expression of *Nqo1* was highly upregulated by the PQN, which was expected response to a quinone positive control. However, it is interesting to note that PQN treated cells also exhibited the strongest reduction in *G6pd* mRNA. Together these results indicate that PM emissions from distinct sources and with different chemical properties differentially influence the transcription of antioxidant and metabolic genes.

Some possible explanation for these findings may involve the intricate relationship between post-transcriptional regulation and post-translational regulation of these key enzymes. For example, studies using cell free approaches have shown that PM can deplete antioxidant enzymes and reduce activity of Gpx and GSH, which may in part be due to the reactive surface properties of PM [113]. In fact, compounds found in in aqueous cigarette smoke extracts and diesel exhaust particle extracts have been shown to modify enzymes via irreversible covalent modifications, likely through reaction with conjugated carbonyl compounds [114]. Disruptions of normal enzymatic processes by various sources of PM is known to contribute to cellular oxidative stress, however more studies should be conducted to explore how the direct modification of antioxidant enzymes related to transcriptional and translational level effects.

This study focused on genes that mitigate the cellular oxidative stress from PM, but Nqo1 and G6pd enzymes have multiple cellular roles. Nqo1 is also known to regulation of cell cycle progression at the G2/M phase and its overexpression is associated with increased cell proliferation in cancer cells [115]. Similarly, G6pd is involved in cellular carbohydrate metabolism, direct regeneration of pyridine nucleotide cofactors, and activation of pro-oncogenic pathways [116]. Various *in vitro* studies have demonstrated that PM may induce cell cycle alterations and therefore, changes in cell cycle were explored in this study. Some studies have shown that the percentage of human bronchial epithelial cells in S phase decreased and the percentage of cells in G2/M phase increased significantly after exposure to ambient urban $PM_{2.5}$ from winter seasons [117,118], whereas other studies have shown a delay in S-phase progression [119]. Changes in cell cycle dynamics are generally related to DNA damage and the complex activation of repair mechanism responses, which are influenced by the presence of specific PAHs adsorbed on the particle surface and cell specific metabolic capacity [120].

In this study, we observed that 4-hour exposures to PM induced minor effects on cell cycle progression compared to mock controls. The most striking changes differences in cycle progression patterns were observed between macrophages treated with SRM 1648a and cells exposed to mixed dung brushwood fuel from chulha stove, which had opposing effects. Cells treated with SRM 1648a, had more cells in G0/G1 phase, corresponding with less cells in S-phase, an effect that has previously reported in macrophages following acute exposure to SRM 1648a [121]. In contrast, cells exposed to mixed fuel emissions from chulha stoves demonstrated a higher percentage of cells in S-phase, which corresponded with less cells in the G0/G1 phase. The results from this study overall demonstrate that properties associated with PM source have

different effects on gene expression changes and cell cycle changes, and cells respond to biomass fuel PM in drastic different ways than responses observed for SRM 1648 a material.

5.3.1 Limitations

One of the main limitations of this study is the exploration of gene expression only at a single time point and at a single exposure dose. The exploration of gene expression at multiple time points and multiple doses would provide insight into the highly dynamic changes that may occur in a dose-dependent manner. Gene expression changes may be transient, and therefore a single time window may not capture delayed effects. The genes selected for this study may also be regulated by multiple overarching regulatory pathways, which were not explored in this study. For example, Nqo1 activation is regulated by multiple regulatory pathways and could be elicited by Aryl hydrocarbon receptor activity, an alternative stress response pathway that was not the focus of this study. Studies focusing on multiple regulatory pathways could provide further insight into the mechanistic changes that are relevant to disease initiating pathways. Additionally, this study would benefit from an additional exploration into the protein level changes occurring simultaneously, to further ascertain the mechanistic impact of gene expression changes.

6. Multivariate analysis: Relationship between biomass fuel combustion conditions and oxidative particle properties and cellular responses

6.1 Introduction

Various components of $PM_{2.5}$ have been linked with detrimental health outcomes [122,123]. For example, human exposure studies have found that ambient elemental carbon (EC) concentrations are strongly associated with changes in hospital admissions for cardiovascular health outcomes, while organic carbon (OC) has a greater impact on respiratory outcomes [124]. Combustion conditions play a pivotal role in the formation of emissions from biomass burning and differences in the chemical composition may have different levels of toxicity. In this study, we assessed how combustion processes influence particle oxidative potential properties and examine the relationship between emission factors and modulation of macrophage biological responses.

The combustion temperature and efficiency differences between smoldering and flaming fires are typically represented by MCE. MCE is derived from CO_2 and CO gases representing differences in flaming and non-pyrolysis smoldering combustion processes. Organic emissions from the combustion of woody materials such as levoglucosan have been found to be enhanced during flaming combustion and are reduced in the smoldering phase of combustion, when oxygenated organic species prevail [125]. However, emission factors (g emissions/ kg fuel burned) are dependent on various temperature driven chemical processes unique to fuel-stove combustion conditions. Dynamic changes in oxygenation, temperature of the fire, and surface area to volume ratio of the fuel also contribute to the formation of OC, and the generation of low molecular weight PAHS found in the vapor phase versus high molecular weight PAHS adsorbed on to particulates [126]. MCE, driven by emission factors predominantly emitted during the flaming

phase of combustion, only partially explains the total variations in emission factors for PM, OC, EC, and PAHs [127]. Pyrolysis (the thermal decomposition of organic materials in the absence of oxygen) is an important factor driving the solid biomass fuel emission factors. Pyrolysis temperature influences the VOC profile of biomass fires and the formation of PAHs, which is represented by a high temperature to low temperature VOC ratio (high/low VOC ratio) [128]. The high/low VOC ratio is derived from the proportion of ethyne to furan emissions reflects the relative contribution of high and low temperature processes to combustion emissions, and has been shown to best predict VOC emissions profiles [129].

Particulate matter from different sources and distinct composition have been shown to differently influence cell viability and transcriptional changes, with urban, fine, and diesel exhaust reference particles inducing different levels of responses in human bronchial epithelial cells [130]. PM matter from mobile sources, coal combustion, and wood combustion sources have also been previously found to differentially modulate the gene expression of antioxidants heme oxygenase [131]. Assessing how combustion processes that influence PM composition contribute to cellular toxicity can provide insight into how cellular adaptations, such as oxidative stress responses, are influenced by particles from different sources. Here, we assess how solid biomass fuel emission factors related to MCE, high/low VOC ratios, and OC influenced particle OP, and how these particle properties correlated with macrophage respiratory burst and transcription of oxidative stress and metabolic response genes.

6.2 Methods

Mean emission factors for each individual combustion event are presented on a gram per kilogram of dry fuel basis ± SEM unless otherwise noted. For PAH emissions, we use the summed 16 PAH assessment (ΣPAH) representing ubiquitous environmental PAHs. Samples include dry dung-chulha (N = 5), wet dung -chulha (N = 4), mixed (wood-dung) fuels-chulha (N = 6), and dung- angithi (N = 3) fuel stove combinations. To determine the statistical significance of the differences in the mean emission factors results among independent groups, a one-way ANOVA was performed using a Bonferroni correction for repeated measures using a significance level of a=0.05. Biological endpoints are normalized to the mock control sample value of 1 for each individual combustion event sample. Bivariate and multivariate analysis were performed by Spearman's nonparametric correlation to assess the correlation coefficient r. Different sample sizes (N) were used across experiments and are listed in the figure legends. The null hypothesis that there is no correlation between the two variables (r = 0). The variables with evidence of a two-tailed P <.05 association were considered significant. All statistical analyses were performed using GraphPad Prism (version 10.1.0 for Windows, GraphPad Software, San Diego, CA, USA, www.graphpad.com).

6.3 Results

6.3.1 Differences in emission characteristics between chulha and angithi stoves

The 18 filter samples from this study are a subset of a larger set of samples sourced from individual combustion events. Significant differences in the mean emission factors were observed between mixed fuel-chulha stove emissions and dung-angithi stove emissions, but no significant differences in the emission factors for chulha stoves used with wet or dry dung, or mixed dung-brushwood fuels, as described in Figure 17. Significant differences for emission factors were observed for the larger dataset used for chemical analysis, but statistically significant differences in this study were limited by the smaller sample size of samples available for the toxicological analyses (data not shown.) The samples used in this study showed major differences between the angithi stoves used with dung and the chulha stoves used with mixed brushwood-dung fuels. Angithi stoves were characterized by a lower MCE and higher OC emissions compared to chulha stoves, corresponding with a higher emission of $PM_{2.5}$, which are characteristic of highly polluting traditional Angithi stoves. A borderline significant difference (P =.054) in the high/low VOC ratio was also observed between angithi stoves and mixed fuels chulha stoves, with angithi stove emissions having the lowest high/low VOC ratio.

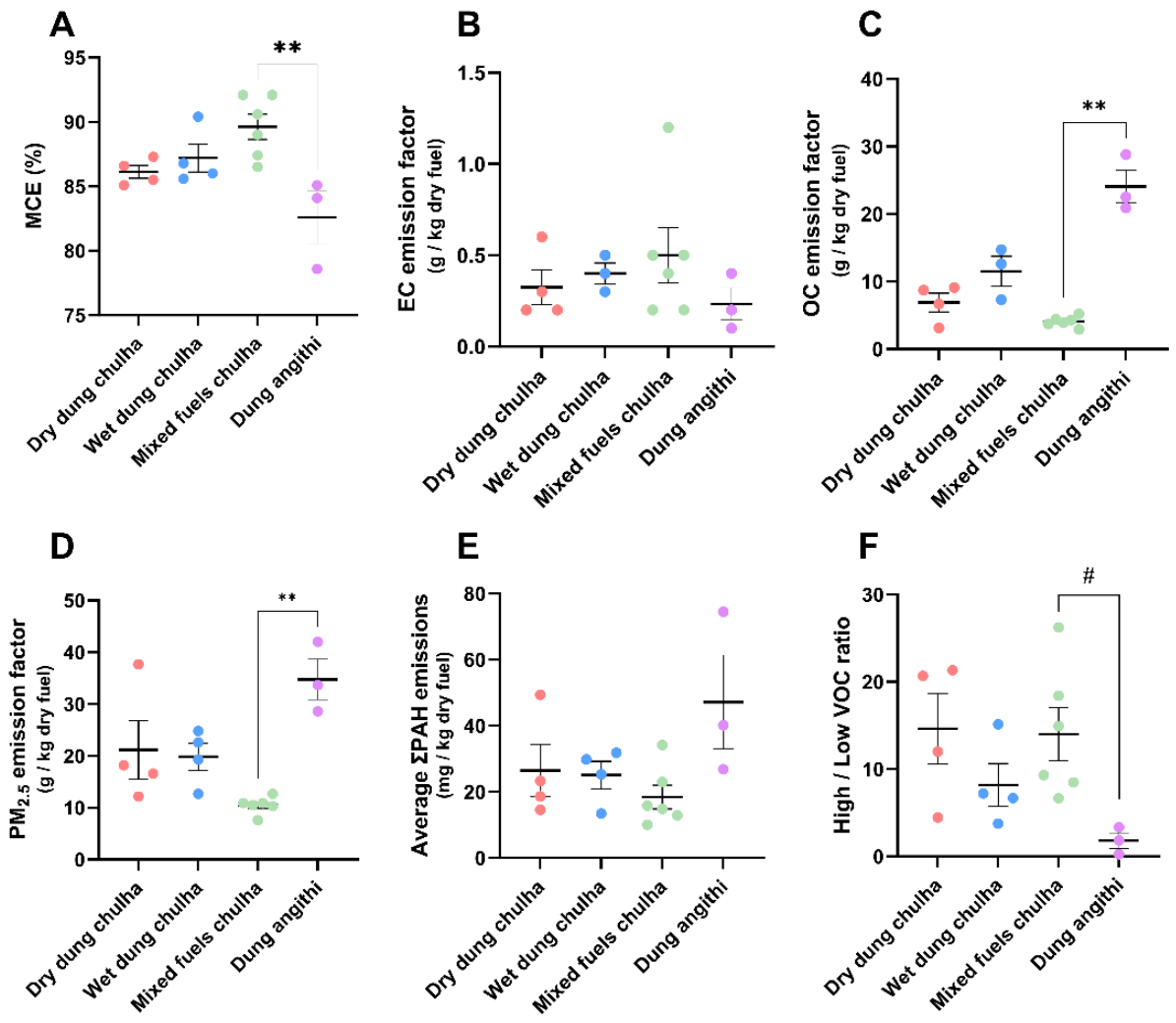

Figure 17: Comparison of average emission factors from chulha and angithi stoves. *Fuel and stove combinations influence (A) MCE, (B) elemental carbon, (C) organic carbon, (D) $PM_{2.5}$, (E) ΣPAH, and (F) the high/low VOC emission profile (F). * P <0.033, ** P <0.003, *** P <0.001, # = a borderline significant difference.*

6.3.2 Temperature dependent combustion properties influence macrophage oxidative stress responses.

To assess how solid biofuel PM emission factor characteristics influence macrophage cell function, associations with biological outcomes including superoxide generation dynamics from respiratory burst assessments and gene expression of antioxidant and metabolic related genes were explored. The combustion properties and particle properties significantly associated with *in*

vitro biological outcomes include MCE, OC, high/low VOC ratio, and DTT OP, as summarized in Figure 18.

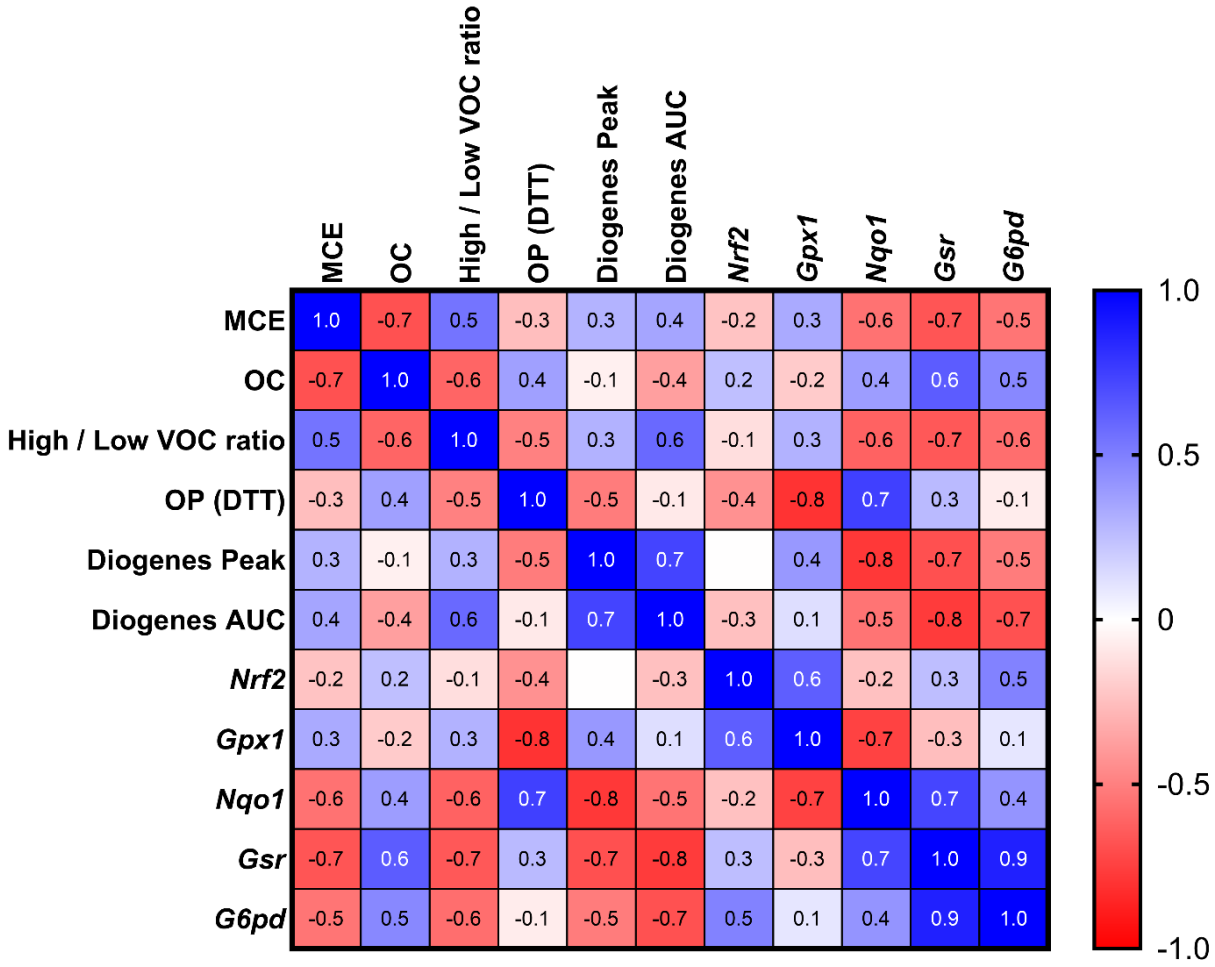

Figure 18: Associations of combustion PM emissions properties and biological outcomes. *Spearman correlation coefficients (r) for associations of combustion emissions factors, particle oxidative potential (OP) properties from DTT assay assessment, and biological outcomes including respiratory burst function assessment with the Diogenes assay and changes in gene expression of antioxidant and metabolic related genes.*

Emission factors were highly variable among stove-fuel combinations and no significant associations between *in vitro* biological outcomes and $PM_{2.5}$, EC, or ΣPAH were found. Particle OP had statistically significant negative associations macrophage peak superoxide levels (Figure 19A), significant positive associations with *Nqo1* gene expression (Figure 19B), and significant

negative associations with *Gpx1* gene expression (Figure 19C). In other words, exposure to particles with a high oxidative capacity correlated with an attenuated accumulation of superoxide generation during respiratory burst, downregulation of antioxidant *Gpx1*, yet upregulation of detoxifying enzyme *Nqo1*. In general, *Gpx1* expression is negatively associated with *Nqo1* expression, but positively associated with *Nrf2* expression, but changes in the *Nrf2* gene expression is not associated with the any other endpoint (Figure 18).

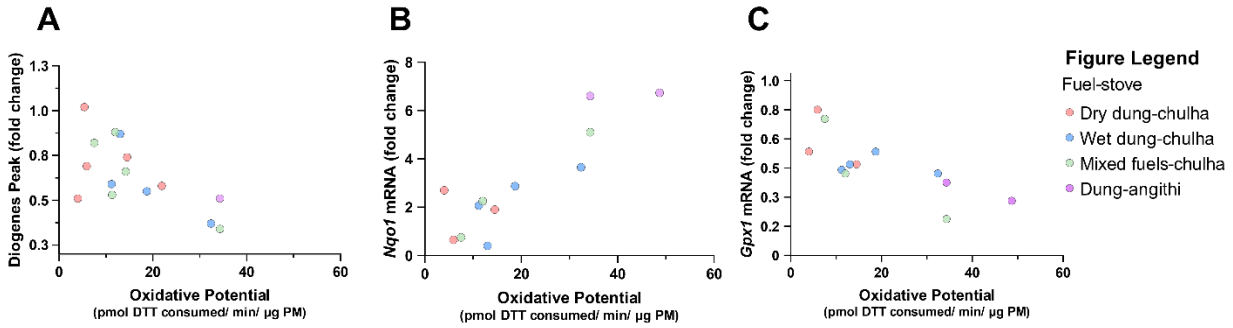

Figure 19: Significant associations of particle OP properties and in vitro biological outcomes. *Associations with (A) peak superoxide levels reflect Diogenes values from N = 5 dry dung-chulha, N = 4 wet dung-chulha, N = 5 mixed fuels-chulha, and N = 1 dung-angithi samples. Associations with (B) Nqo1 gene expression and (C) Gpx1 gene expression reflect gene expression values from N=3 dry dung-chulha, N = 4 wet dung-chulha, N = 3 mixed fuels-chulha, and N = 2 dung-angithi samples.*

While both high/low VOC ratio and MCE factors are influenced by complex temperature dependent combustion process, MCE had statistically significant negative associations with *Gsr* and *Nqo1* expression only, but no significant associations with particle OP (Figure 18). The high/low VOC ratio factor had statistically significant negative associations with particle OP (Figure 20A), significant positive associations with macrophage total superoxide generation assessed by Diogenes AUC (Figure 20B), statistically significant negative associations with *Nqo1* (Figure 20C) and *Gsr* (Figure 20D) gene expression. These results indicate that particles with lower values for high/low VOC ratio were correlated with higher particle redox activity,

stronger inhibition of macrophage superoxide generation during respiratory burst, and upregulation of antioxidant gene expression compared to particles with elevated high/low VOC ratio values.

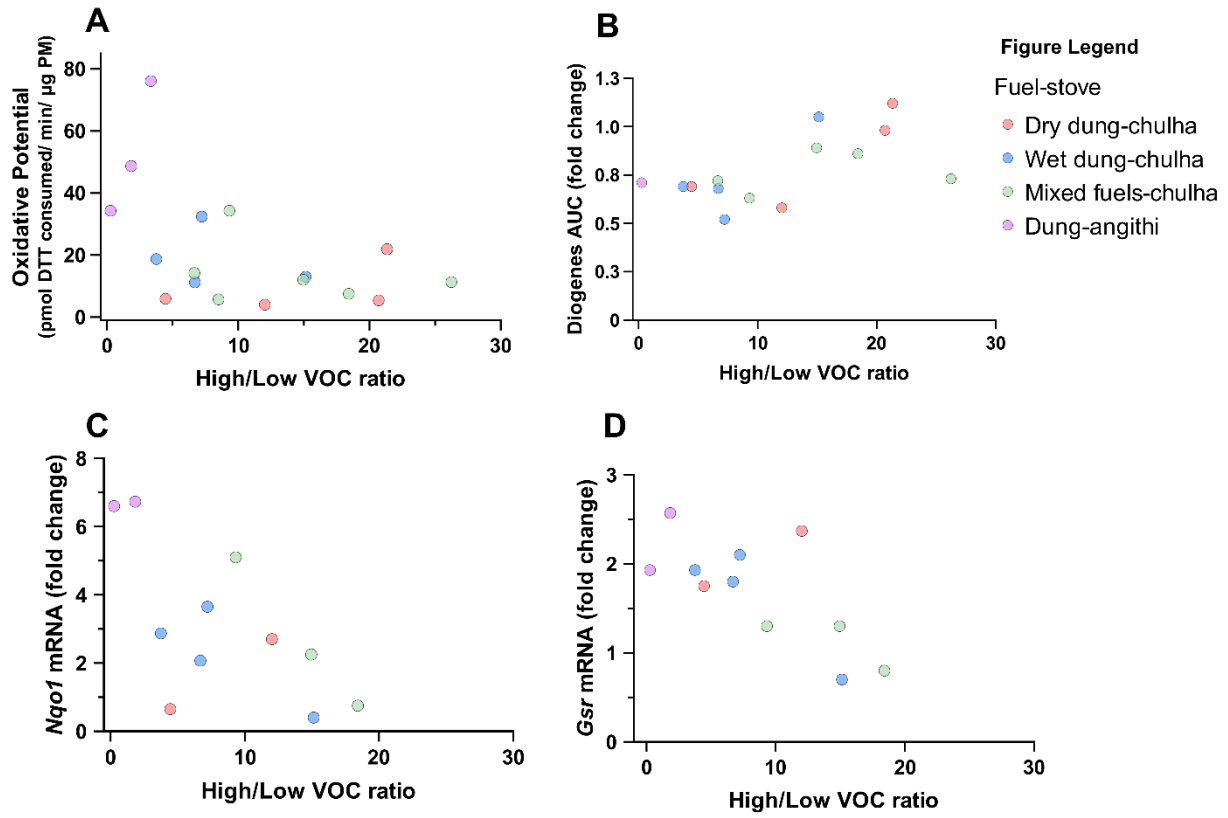

Figure 20: Significant associations of high/low VOC ratio and in vitro biological outcomes. *The high/low VOC ratio was missing for N = 1 dry dung-chulha sample. Associations with (A) oxidative potential reflect N = 4 dry dung-chulha, N = 4 wet dung-chulha, N = 6 mixed fuels-chulha, and N = 3 dung- angithi samples. Associations with (B) total superoxide generation reflect Diogenes values from N=4 dry dung-chulha, N = 4 wet dung-chulha, N = 5 mixed fuels-chulha, and N = 1 dung-angithi samples. Associations with (C) Nqo1 and (D) Gsr gene expression values represent N=2 dry dung-chulha, N=4 wet dung-chulha, N = 3 mixed fuels-chulha, and N = 2 dung- angithi samples.*

Gsr expression had statistically significant negative associations with both peak (Figure 21A) and total superoxide levels during macrophage respiratory burst and statistically significant positive with metabolic-related *G6pd* gene expression (Figure 21C). *G6pd* gene expression also had statistically significant negative associations with macrophage total superoxide generation

(Figure 21B). These findings indicate that the ability of macrophages to rapidly accumulate endogenous superoxide and sustain superoxide production for extended periods is linked to an intricate relationship between the expression of genes related to antioxidant capacity and cellular energy maintenance. Together these findings from this study indicate that changes in gene expression of antioxidant can be both up and downregulated by particles from difference combustion sources, and the extent of macrophage respiratory burst inhibition is influenced by cellular redox and energy transcriptional adaptions in response to exposure to particles with distinct chemical profiles.

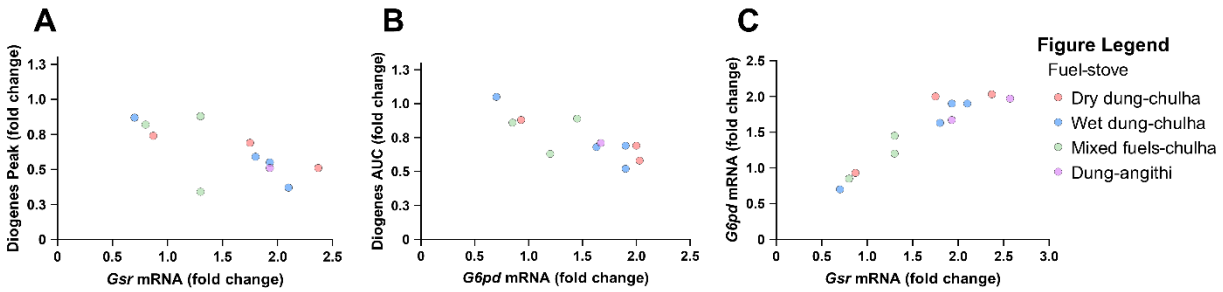

Figure 21: Significant associations between gene expression and respiratory burst responses. *Associations between Gsr and peak superoxide levels (A), total superoxide generation B), and G6pd gene expression (C) reflect N = 4 dry dung-chulha, N = 4 wet dung-chulha, N = 3 mixed fuels-chulha samples. Figures (A) and (B) include N = 1 dung- angithi sample, and (C) which includes N = 2 dung-angithi samples.*

6.4 Discussion

6.4.1 Possible mechanisms underlying particulate source driven immune cell function modulation

This study assessed the how solid biomass fuel combustion conditions that contribute to the differences in PM emissions and chemical composition, influence the oxidative potential of particles and their associations with macrophage respiratory burst and gene expression changes.

Particles with a lower value of high/low VOC ratios were found to have a higher OP, which indicates that pyrolysis-driven combustion processes contribute to the generation of organic compounds with electrophilic and highly redox properties, yet no association between MCE and particle OP were found. Emissions characterized by reactive particle surface properties and lower high/low VOC ratios were associated with alterations in macrophage respiratory burst dynamics, overall resulting in inhibited superoxide peak responses and total superoxide generation in activated macrophages. Reduction in superoxide production could be partially explained by increased expression of antioxidant genes that mitigate the accumulation of ROS. Emissions from dung-angithi fuel-stove combinations had lower MCE and high/low VOC ratios compared to any other fuel-stove combination and these temperature-dependent combustion processes were shown to influence macrophage gene expression. Particles from combustion processes characterized by lower MCE and high/low VOC ratios were correlated with a higher upregulation of *Gsr* antioxidant and *Nqo1* detoxification enzymes compared to particles from combustion processes with higher MCE and higher values of high/low VOC ratios. However, fluctuating cellular energy demands via changes in NADPH cofactor pools associated with NOX, Gsr, and Nqo1 enzyme activity may also play a role, which are typically maintained by G6pd rate-limiting enzyme. The results from this study show significant associations between *Gsr* gene expression and *G6pd* expression, indicating that cellular redox homeostasis and respiratory burst are intricately linked.

Differences in particle-mediated biological responses by solid biomass fuel emissions is likely influenced by the presence of aromatic compounds and constituents with unsaturated bonds with the ability to participate oxidizing and electrophilic reactions, typically generated during inefficient combustion processes. While this study suggests that redox imbalance and cellular

stress response activation are differentially induced by combustion processes characterized by lower MCE and high/low VOC ratios, it is unlikely that a singular mechanism or pathway is solely accountable for the changes in innate immune cell functional reported here. Nrf2 activation mechanisms and antioxidant induction pathways are known to be activated in response to PM, yet this study shows *Nrf2* and *Gpx1* genes were downregulated following exposure to all solid biomass fuel PM. Disruptions of normal enzymatic processes by various components of PM or complex transcriptional regulation processes may contribute to the downregulation of specific antioxidant genes. There are known complex interactions and feedback loops between the many cellular stress response signaling cascades, promoting diverse intracellular changes relating to cell function. For example, *Nqo1* expression is also influenced by Aryl Hydrocarbon Receptor signaling pathway, which regulates the catabolism of PAHs [108]. The contribution of PAHs to overall cellular toxicity was expected to be minimal in this study due to their low aqueous solubility and use of aqueous filter extract samples for this study. However, PAHs bound to the particle surface may influence particle reactivity and their overall biological effects. Overall, in this study PM with low oxidative properties resulted in less adverse outcomes, sustained intracellular redox homeostasis, and low induction of stress-response genes. These findings overall support the mounting evidence that particles from distinct sources induce cellular toxicity via different mechanisms.

7. Summary Discussion

7.1 Summary of key findings

The experiments and findings in this study described within this dissertation describe how temperature-dependent combustion processes from the use of dung and mixed dung-brushwood fuels with traditional Indian cookstoves influence the OP of $PM_{2.5}$ emissions. An *in vitro* innate immune cell exposure model was used for toxicological assessments and to explore how PM from distinct sources affect macrophage viability, respiratory burst, cell cycle dynamics, and the expression of important antioxidants and energy-related gene targets. Correlation analyses revealed particle OP and biological effects were related to the emission factors emitted during individual combustion events.

Differences between the oxidative potential of $PM_{2.5}$ emissions from chulha stoves, angithi stoves, and urban dust were observed. $PM_{2.5}$ emissions from angithi smoldering combustion cookstoves were found to have a higher oxidative potential than PM emissions from chulha flaming combustion cookstoves, urban dust and the single diesel quinone compound PQN, whereas the OP of chulha stoves emissions was lower than both reference compounds. While no statistically significant differences in OP were observed among the chulha cookstoves flaming combustion used with fuels of varying moisture levels, a trend of higher OP was observed for wet dung and mixed fuels compared to dry dung fuels. While smoldering and flaming processes that contribute to stove MCE was initially considered to be the main driving factor influencing OP, multivariate analysis revealed that high/low VOC ratio was correlated OP. However, both MCE and high/low VOC were associated with multiple biological endpoints. Overall, pyrolysis processes are an important factor driving OP and particle redox activity.

Toxicology assessments were conducted using submerged culture exposure with the RAW 264.7 macrophage cell line. The overall findings from biological studies support the growing scientific evidence that distinct combustion sources alter innate immune cell functions through different molecular mechanisms. Cell viability was assessed through various approaches and no significant reductions were observed after 4-hour exposures to PM from different sources. Acute exposure to solid biomass fuels PM emissions did not reduce metabolic activity in macrophages immediately following exposure. Sustained viability was confirmed 18-hours post exposure using an additional evaluation of cytotoxicity measuring LDH secretion by cells with damaged cell membranes and no statistically significant differences were observed for cells exposed to urban dust, PQN, or solid biofuel emissions compared to mock controls (Appendix A2).

Cell death from apoptotic mechanisms was also assessed using staining with PI, which binds to the double stranded DNA of cells with damaged plasma membranes (such as in late apoptotic or necrotic cells) and with recombinant annexin V staining, which binds to the outer plasma membrane in apoptotic cells. Apoptosis was not identified as a major pathway of cytotoxicity in cells following acute exposures, with viability ranging between 68%-88% across all groups. Significant differences in viability and entry into apoptosis were observed only between urban dust and dry dung chulha emissions. Viability was moderately higher in cells treated with urban dust compared to mock controls, whereas viability was lowest in cells treated with dry dung from chulha. Cells treated with dry dung from chulha also had a significantly higher proportion of cells in early apoptosis compared to cells exposed to urban dust. Together these findings indicate that macrophages do not exhibit major differences in viability following acute exposure to solid biomass fuels, urban dust, or PQN.

The main biological effects observed in this study following macrophage exposure to air pollutants included inhibited respiratory burst and altered gene expression of metabolic and glutathione maintenance genes responses. Respiratory burst dynamics affected by solid biomass fuels include reduced peak levels of superoxide accumulated in the initial stage, accelerated rate of superoxide generation characterized by a faster time to reach superoxide generation peak, and diminished overall superoxide generation throughout the response period compared to mock controls. These effects did not exhibit a linear dose response. Additionally, the effects induced by solid biomass fuels differed from PQN, with PQN overall having no effect on total amount of superoxide generated, did not exhibit accelerated rate of superoxide generation compared to mock controls, and had increased overall superoxide generation compared to mock controls. Changes in respiratory burst were associated with particle OP and high/low VOC ratio, but not with MCE indicating that pyrolysis processes and combustion efficiency influence the redox activity of particles, and the severity of biological impacts. Overall, acute macrophage exposures to solid biomass fuel stove emissions resulted in differential impacts on cellular oxidative stress and innate immune cell function compared to PQN and urban dust.

Macrophages exposed to all solid biofuel emissions, urban dust, and PQN exhibited under expression of gene *Nrf2* (encoding the important transcription factor for activation of the antioxidant response element) and *Gpx1* (encoding the antioxidant involved in hydroperoxides in a GSH dependent manner). Increased expression of *Nqo1* (encoding the enzyme involved in detoxifying quinones) was observed in cells exposed to solid biofuel emissions and PQN, but not urban dust. Differential gene expression patterns were observed for *Gsr* (encoding the antioxidant involved in GSH regeneration) and *G6pd* (encoding the housekeeping enzyme providing cofactor substrates for antioxidants) among solid fuels, urban dust, and PQN. These

gene expression changes were also associated with high/low VOC ratio factor and particle OP, and to a lesser extent MCE. Due to the changes in oxidative and electrophilic stress responses observed following exposure to air pollutants, cell cycle dynamics were expected to be affected. However, the effects on cell cycle progression compared to mock controls were minimal, with significant differential patterns in cell cycle progression observed only between SRM 1648a and mixed fuels PM emissions from chulha stoves.

7.2 Key limitations

The results in this dissertation reflect macrophage effects from PM samples collected during household cooking events, which provides a more realistic insight into the how fuel-stove combinations influence particle toxicity compared to laboratory generated particles. However, a major limitation of this approach is the restricted sample size of the filters available for the studies in this investigation, especially for the dung-angithi fuel-stove combination. The number of filters used across experimental studies varied due to limitations in the sample volumes and extract concentration following extraction of PM from filters. The effects from filters from any single fuel-stove combination are highly variable, and further evaluation with a higher sample size is needed to ascertain if the values from these studies represent outliers. Overall, chulha and angithi cookstoves were shown to have different OP and distinct biological effects. However, the low number of samples used in this study limits the conclusions that can be made regarding the associations between fuel mixtures and OP. The moisture content in the brushwood-dung fuel combinations and angithi-dung samples likely influences emission composition, but their effect on OP remains ambiguous given the variability in the results. Furthermore, these studies were conducted with aqueous filter extracts, which do not fully reflect the full impact of other toxic

pollutants created during combustion such as water insoluble compounds, compounds in the volatile phase, and less polar PAHs.

The results in this study indicate that multiple regulatory pathways may contribute to the acute biological effects observed. In this study, we observed how acute 4-hour exposures resulted in immune cell dysfunction many hours after the PM was removed from cell culture media. However, a major limitation of the biological studies here is the use of the immortalized mouse macrophage cell line RAW 264.7. The use of primary cells harvested from rodents, or the use of human cell lines would provide more relevant insight into the molecular mechanistic changes relevant to human disease models. Given the limited sample size of this study, we were not able to validate our findings in multiple cell lines, include multiple exposure dosages, and include multiple time points, which would also provide insight into the dynamic processes that contribute to cellular dysfunction. Additionally, some of these mechanistic details could be explored with the use of inhibitors to identify the role of mitochondria, NOX, and other molecular proteins. The contribution of multiple regulatory pathways could be ascertained by measuring protein level changes through various time points or with inhibitors to block activation of specific pathways such as negative inhibitors of Nrf2. Overall, the implication of these effects over extended periods and in models of chronic exposure warrants further investigation.

7.3 Overall significance

This study provides insight into the toxicity of solid biomass fuels. We show differences in toxicity from air pollutants generated by the combustion of dung fuels and dung-brushwood mixtures commonly used with chulha and angithi cookstoves, adding to the limited information that exists about air pollutants from specific fuel-stove combinations. The limited studies that

have explored the effects of dungs have primarily focused on lab generated particles and dung fuels only. While prior research has predominantly focused on the impact of dung and other solid biomass fuels on epithelial cells, this study highlights notable effects on normal macrophage function and varying impacts from air pollutants originating from different combustion sources and mixed fuel sources. The biological effects of solid biofuels have been previously shown to be cell specific. Changes in macrophages function and oxidative stress response are known to contribute to various cardiopulmonary diseases, such as atherosclerosis. Therefore, the results in this study provide valuable insight into how innate immune cell dysfunction contributes to overall detrimental pulmonary and cardiovascular health outcomes from solid fuel exposure.

BIBLIOGRAPHY

1. World Health Organization. *Burning Opportunity: Clean Household Energy for Health, Sustainable Development, and Wellbeing of Women and Children.* WHO; 2016. https://apps.who.int/iris/handle/10665/204717

2. World Health Organization. Household air pollution. *World Health Organization*. https://www.who.int/news-room/fact-sheets/detail/household-air-pollution-and-health. Published November 28, 2022. Accessed July 20, 2023.

3. Frostad JJ, Nguyen QP, Baumann MM, et al. Mapping development and health effects of cooking with solid fuels in low-income and middle-income countries, 2000–18: a geospatial modelling study. *Lancet Glob Health*. 2022;10(10):e1395-e1411. doi:10.1016/S2214-109X(22)00332-1

4. Schilmann A, Ruiz-García V, Serrano-Medrano M, et al. Just and fair household energy transition in rural Latin American households: are we moving forward? *Environ Res Lett*. 2021;16(10):105012. doi:10.1088/1748-9326/ac28b2

5. Bonjour S, Adair-Rohani H, Wolf J, et al. Solid Fuel Use for Household Cooking: Country and Regional Estimates for 1980–2010. *Environ Health Perspect*. 2013;121(7):784-790. doi:10.1289/ehp.1205987

6. Smith KR, Apte MG, Yuqing M, Wongsekiarttirat W, Kulkarni A. Air pollution and the energy ladder in asian cities. *Energy*. 1994;19(5):587-600. doi:10.1016/0360-5442(94)90054-X

7. Chafe ZA, Brauer M, Klimont Z, et al. Household Cooking with Solid Fuels Contributes to Ambient PM $_{2.5}$ Air Pollution and the Burden of Disease. *Environ Health Perspect*. 2014;122(12):1314-1320. doi:10.1289/ehp.1206340

8. Fuller R, Landrigan PJ, Balakrishnan K, et al. Pollution and health: a progress update. *Lancet Planet Health*. 2022;6(6):e535-e547. doi:10.1016/S2542-5196(22)00090-0

9. Chafe ZA, Brauer M, Klimont Z, et al. Household Cooking with Solid Fuels Contributes to Ambient PM $_{2.5}$ Air Pollution and the Burden of Disease. *Environ Health Perspect*. 2014;122(12):1314-1320. doi:10.1289/ehp.1206340

10. Rao V, Somers JH. Black carbon as a short-lived climate forcer: A profile of emission sources and co-emitted pollutants. *19th Annu Int Emiss Inventory Conf San Antonio Tex*. Published online 2010. https://www3.epa.gov/ttnchie1/conference/ei19/session5/rao.pdf

11. Trevor J, Antony V, Jindal SK. The effect of biomass fuel exposure on the prevalence of asthma in adults in India – review of current evidence. *J Asthma*. 2014;51(2):136-141. doi:10.3109/02770903.2013.849269

12. Prasad R. Biomass fuel exposure and respiratory diseases in India. *Biosci Trends*. 2012;6(5):219-228. doi:10.5582/bst.2012.v6.5.219

13. Gautam S, Edwards R, Yadav A, et al. Probe-based measurements of moisture in dung fuel for emissions measurements. *Energy Sustain Dev*. 2016;35:1-6. doi:10.1016/j.esd.2016.09.003

14. Chen R, Hu B, Liu Y, et al. Beyond PM2.5: The role of ultrafine particles on adverse health effects of air pollution. *Biochim Biophys Acta - Gen Subj*. 2016;1860(12):2844-2855. doi:10.1016/j.bbagen.2016.03.019

15. Wilson SJ, Miller MR, Newby DE. Effects of Diesel Exhaust on Cardiovascular Function and Oxidative Stress. *Antioxid Redox Signal*. 2018;28(9):819-836. doi:10.1089/ars.2017.7174

16. Dutta A, Ray MR, Banerjee A. Systemic inflammatory changes and increased oxidative stress in rural Indian women cooking with biomass fuels. *Toxicol Appl Pharmacol*. 2012;261(3):255-262. doi:10.1016/j.taap.2012.04.004

17. Dutta A, Roychoudhury S, Chowdhury S, Ray MR. Changes in sputum cytology, airway inflammation and oxidative stress due to chronic inhalation of biomass smoke during cooking in premenopausal rural Indian women. *Int J Hyg Environ Health*. 2013;216(3):301-308. doi:10.1016/j.ijheh.2012.05.005

18. Mukherjee S, Roychoudhury S, Siddique S, et al. Respiratory symptoms, lung function decrement and chronic obstructive pulmonary disease in pre-menopausal Indian women exposed to biomass smoke. *Inhal Toxicol*. 2014;26(14):866-872. doi:10.3109/08958378.2014.965560

19. World Health Organization. *WHO Global Air Quality Guidelines: Particulate Matter (PM2.5 and PM10), Ozone, Nitrogen Dioxide, Sulfur Dioxide and Carbon Monoxide.* WHO; 2021.

20. Reisen F, Meyer CP, Weston CJ, Volkova L. Ground-Based Field Measurements of PM $_{2.5}$ Emission Factors From Flaming and Smoldering Combustion in Eucalypt Forests. *J Geophys Res Atmospheres*. Published online August 9, 2018. doi:10.1029/2018JD028488

21. Bølling A, Totlandsdal A, Sallsten G, et al. Wood smoke particles from different combustion phases induce similar pro-inflammatory effects in a co-culture of monocyte and pneumocyte cell lines. *Part Fibre Toxicol*. 2012;9(1):45. doi:10.1186/1743-8977-9-45

22. Kim YH, Warren SH, Krantz QT, et al. Mutagenicity and Lung Toxicity of Smoldering vs. Flaming Emissions from Various Biomass Fuels: Implications for Health Effects from Wildland Fires. *Environ Health Perspect*. 2018;126(1):017011. doi:10.1289/EHP2200

23. Kim YH, King C, Krantz T, et al. The role of fuel type and combustion phase on the toxicity of biomass smoke following inhalation exposure in mice. *Arch Toxicol*. 2019;93(6):1501-1513. doi:10.1007/s00204-019-02450-5

24. Hargrove MM, Kim YH, King C, et al. Smoldering and flaming biomass wood smoke inhibit respiratory responses in mice. *Inhal Toxicol*. 2019;31(6):236-247. doi:10.1080/08958378.2019.1654046

25. Atwi K, Mondal A, Pant J, et al. Physicochemical properties and cytotoxicity of brown carbon produced under different combustion conditions. *Atmos Environ*. 2021;244:117881. doi:10.1016/j.atmosenv.2020.117881

26. Antiñolo M, Willis MD, Zhou S, Abbatt JPD. Connecting the oxidation of soot to its redox cycling abilities. *Nat Commun*. 2015;6(1):6812. doi:10.1038/ncomms7812

27. Niranjan R, Thakur AK. The Toxicological Mechanisms of Environmental Soot (Black Carbon) and Carbon Black: Focus on Oxidative Stress and Inflammatory Pathways. *Front Immunol*. 2017;8:763. doi:10.3389/fimmu.2017.00763

28. Hakimzadeh M, Soleimanian E, Mousavi A, et al. The impact of biomass burning on the oxidative potential of PM2.5 in the metropolitan area of Milan. *Atmos Environ*. 2020;224:117328. doi:10.1016/j.atmosenv.2020.117328

29. Calas A, Uzu G, Besombes JL, et al. Seasonal Variations and Chemical Predictors of Oxidative Potential (OP) of Particulate Matter (PM), for Seven Urban French Sites. *Atmosphere*. 2019;10(11):698. doi:10.3390/atmos10110698

30. Cesari D, Merico E, Grasso FM, et al. Source Apportionment of PM2.5 and of its Oxidative Potential in an Industrial Suburban Site in South Italy. *Atmosphere*. 2019;10(12):758. doi:10.3390/atmos10120758

31. Bates JT, Weber RJ, Abrams J, et al. Reactive Oxygen Species Generation Linked to Sources of Atmospheric Particulate Matter and Cardiorespiratory Effects. *Environ Sci Technol*. 2015;49(22):13605-13612. doi:10.1021/acs.est.5b02967

32. Beig G, Chate DM, Ghude SD, et al. Evaluating population exposure to environmental pollutants during Deepavali fireworks displays using air quality measurements of the SAFAR network. *Chemosphere*. 2013;92(1):116-124. doi:10.1016/j.chemosphere.2013.02.043

33. Arbex MA, Saldiva PHN, Pereira LAA, Braga ALF. Impact of outdoor biomass air pollution on hypertension hospital admissions. *J Epidemiol Community Health*. 2010;64(7):573-579. doi:10.1136/jech.2009.094342

34. Arbex MA, Martins LC, De Oliveira RC, et al. Air pollution from biomass burning and asthma hospital admissions in a sugar cane plantation area in Brazil. *J Epidemiol Community Health*. 2007;61(5):395-400. doi:10.1136/jech.2005.044743

35. Park M, Joo HS, Lee K, et al. Differential toxicities of fine particulate matters from various sources. *Sci Rep*. 2018;8(1):17007. doi:10.1038/s41598-018-35398-0

36. Mudway IS, Duggan ST, Venkataraman C, Habib G, Kelly FJ, Grigg J. Combustion of dried animal dung as biofuel results in the generation of highly redox active fine particulates. *Part Fibre Toxicol*. 2005;2(1):6. doi:10.1186/1743-8977-2-6

37. Kurmi OP, Dunster C, Ayres JG, Kelly FJ. Oxidative potential of smoke from burning wood and mixed biomass fuels. *Free Radic Res*. 2013;47(10):829-835. doi:10.3109/10715762.2013.832831

38. McCarthy CE, Duffney PF, Wyatt JD, Thatcher TH, Phipps RP, Sime PJ. Comparison of in vitro toxicological effects of biomass smoke from different sources of animal dung. *Toxicol In Vitro*. 2017;43:76-86. doi:10.1016/j.tiv.2017.05.021

39. Fullerton DG, Jere K, Jambo K, et al. Domestic smoke exposure is associated with alveolar macrophage particulate load: Domestic smoke and macrophage particulate load. *Trop Med Int Health*. 2009;14(3):349-354. doi:10.1111/j.1365-3156.2009.02230.x

40. Bai Y, Brugha RE, Jacobs L, Grigg J, Nawrot TS, Nemery B. Carbon loading in airway macrophages as a biomarker for individual exposure to particulate matter air pollution — A critical review. *Environ Int*. 2015;74:32-41. doi:10.1016/j.envint.2014.09.010

41. Kulkarni NS, Prudon B, Panditi SL, Abebe Y, Grigg J. Carbon loading of alveolar macrophages in adults and children exposed to biomass smoke particles. *Sci Total Environ*. 2005;345(1-3):23-30. doi:10.1016/j.scitotenv.2004.10.016

42. Rylance J, Fullerton DG, Scriven J, et al. Household Air Pollution Causes Dose-Dependent Inflammation and Altered Phagocytosis in Human Macrophages. *Am J Respir Cell Mol Biol*. 2015;52(5):584-593. doi:10.1165/rcmb.2014-0188OC

43. Adaji EE, Ekezie W, Clifford M, Phalkey R. Understanding the effect of indoor air pollution on pneumonia in children under 5 in low- and middle-income countries: a systematic review of evidence. *Environ Sci Pollut Res*. 2019;26(4):3208-3225. doi:10.1007/s11356-018-3769-1

44. Yee J, Cho YA, Yoo HJ, Yun H, Gwak HS. Short-term exposure to air pollution and hospital admission for pneumonia: a systematic review and meta-analysis. *Environ Health*. 2021;20(1):6. doi:10.1186/s12940-020-00687-7

45. McCarthy CE, Duffney PF, Nogales A, et al. Dung biomass smoke exposure impairs resolution of inflammatory responses to influenza infection. *Toxicol Appl Pharmacol*. 2022;450:116160. doi:10.1016/j.taap.2022.116160

46. Weltman RM. *In-Field Emissions from Cookstoves in Rural Indian Households*. University of California Irvine; 2017. https://escholarship.org/uc/item/22f2g0r3#main

47. Fleming LT. *Molecular Composition, Optical Properties, and Chemical Aging of Primary and Secondary Organic Aerosol*. University of California Irvine; 2019. https://escholarship.org/uc/item/2kr287vs

48. Fleming LT, Weltman R, Yadav A, et al. Emissions from village cookstoves in Haryana, India, and their potential impacts on air quality. *Atmospheric Chem Phys*. 2018;18(20):15169-15182. doi:10.5194/acp-18-15169-2018

49. Fleming LT, Lin P, Laskin A, et al. Molecular composition of particulate matter emissions from dung and brushwood burning household cookstoves in Haryana, India. *Atmospheric Chem Phys*. 2018;18(4):2461-2480. doi:10.5194/acp-18-2461-2018

50. Weltman RM, Edwards RD, Fleming LT, et al. Emissions Measurements from Household Solid Fuel Use in Haryana, India: Implications for Climate and Health Co-benefits. *Environ Sci Technol*. 2021;55(5):3201-3209. doi:10.1021/acs.est.0c05143

51. Jayarathne T, Stockwell CE, Bhave PV, et al. Nepal Ambient Monitoring and Source Testing Experiment (NAMaSTE): emissions of particulate matter from wood- and dung-fueled cooking fires, garbage and crop residue burning, brick kilns, and other sources. *Atmospheric Chem Phys*. 2018;18(3):2259-2286. doi:10.5194/acp-18-2259-2018

52. Smith KR, Aust AE. Mobilization of Iron from Urban Particulates Leads to Generation of Reactive Oxygen Species *in Vitro* and Induction of Ferritin Synthesis in Human Lung Epithelial Cells. *Chem Res Toxicol*. 1997;10(7):828-834. doi:10.1021/tx960164m

53. Mitkus RJ, Powell JL, Zeisler R, Squibb KS. Comparative physicochemical and biological characterization of NIST Interim Reference Material PM2.5 and SRM 1648 in human A549 and mouse RAW264.7 cells. *Toxicol In Vitro*. 2013;27(8):2289-2298. doi:10.1016/j.tiv.2013.09.024

54. Cho AK, Di Stefano E, You Y, et al. Determination of Four Quinones in Diesel Exhaust Particles, SRM 1649a, and Atmospheric PM $_{2.5}$ Special Issue of *Aerosol Science and Technology* on Findings from the Fine Particulate Matter Supersites Program. *Aerosol Sci Technol*. 2004;38(sup1):68-81. doi:10.1080/02786820390229471

55. Yang M, Ahmed H, Wu W, Jiang B, Jia Z. Cytotoxicity of Air Pollutant 9,10-Phenanthrenequinone: Role of Reactive Oxygen Species and Redox Signaling. *BioMed Res Int*. 2018;2018:1-15. doi:10.1155/2018/9523968

56. Cho AK, Sioutas C, Miguel AH, et al. Redox activity of airborne particulate matter at different sites in the Los Angeles Basin. *Environ Res*. 2005;99(1):40-47. doi:10.1016/j.envres.2005.01.003

57. Gao D, Godri Pollitt KJ, Mulholland JA, Russell AG, Weber RJ. Characterization and comparison of $PM_{2.5}$ oxidative potential assessed by two acellular assays. *Atmospheric Chem Phys*. 2020;20(9):5197-5210. doi:10.5194/acp-20-5197-2020

58. Conte E, Canepari S, Frasca D, Simonetti G. Oxidative Potential of Selected PM Components. In: *Proceedings of the 2nd International Electronic Conference on Atmospheric Sciences*. MDPI; 2017:108. doi:10.3390/ecas2017-04131

59. Eiguren-Fernandez A, Shinyashiki M, Schmitz DA, et al. Redox and electrophilic properties of vapor- and particle-phase components of ambient aerosols. *Environ Res*. 2010;110(3):207-212. doi:10.1016/j.envres.2010.01.009

60. Gao D, Fang T, Verma V, Zeng L, Weber RJ. A method for measuring total aerosol oxidative potential (OP) with the dithiothreitol (DTT) assay and comparisons between an urban and roadside site of water-soluble and total OP. *Atmospheric Meas Tech*. 2017;10(8):2821-2835. doi:10.5194/amt-10-2821-2017

61. Bates JT, Fang T, Verma V, et al. Review of Acellular Assays of Ambient Particulate Matter Oxidative Potential: Methods and Relationships with Composition, Sources, and Health Effects. *Environ Sci Technol*. 2019;53(8):4003-4019. doi:10.1021/acs.est.8b03430

62. Fang T, Verma V, Bates JT, et al. Oxidative potential of ambient water-soluble $PM_{2.5}$ in the southeastern United States: contrasts in sources and health associations between ascorbic acid (AA) and dithiothreitol (DTT) assays. *Atmospheric Chem Phys*. 2016;16(6):3865-3879. doi:10.5194/acp-16-3865-2016

63. Fang T, Verma V, Guo H, King LE, Edgerton ES, Weber RJ. A semi-automated system for quantifying the oxidative potential of ambient particles in aqueous extracts using the dithiothreitol (DTT) assay: results from the Southeastern Center for Air Pollution and Epidemiology (SCAPE). *Atmospheric Meas Tech*. 2015;8(1):471-482. doi:10.5194/amt-8-471-2015

64. Chen LWA, Verburg P, Shackelford A, et al. Moisture effects on carbon and nitrogen emission from burning of wildland biomass. *Atmospheric Chem Phys*. 2010;10(14):6617-6625. doi:10.5194/acp-10-6617-2010

65. Verma V, Fang T, Xu L, et al. Organic Aerosols Associated with the Generation of Reactive Oxygen Species (ROS) by Water-Soluble $PM_{2.5}$. *Environ Sci Technol*. 2015;49(7):4646-4656. doi:10.1021/es505577w

66. Tuet WY, Chen Y, Xu L, et al. Chemical oxidative potential of secondary organic aerosol (SOA) generated from the photooxidation of biogenic and anthropogenic volatile organic compounds. *Atmospheric Chem Phys*. 2017;17(2):839-853. doi:10.5194/acp-17-839-2017

67. Charrier JG, Richards-Henderson NK, Bein KJ, McFall AS, Wexler AS, Anastasio C. *Oxidant Production from Source-Oriented Particulate Matter – Part 1: Oxidative Potential Using the Dithiothreitol (DTT) Assay*. Aerosols/Field Measurements/Troposphere/Chemistry (chemical composition and reactions); 2014. doi:10.5194/acpd-14-24149-2014

68. McWhinney RD, Badali K, Liggio J, Li SM, Abbatt JPD. Filterable Redox Cycling Activity: A Comparison between Diesel Exhaust Particles and Secondary Organic Aerosol Constituents. *Environ Sci Technol*. 2013;47(7):3362-3369. doi:10.1021/es304676x

69. Bamford HA, Bezabeh DZ, Schantz MM, Wise SA, Baker JE. Determination and comparison of nitrated-polycyclic aromatic hydrocarbons measured in air and diesel

particulate reference materials. *Chemosphere*. 2003;50(5):575-587. doi:10.1016/S0045-6535(02)00667-7

70. De Jesus R, Mosca A, Guarieiro A, Da Rocha G, De Andrade J. In vitro Evaluation of Oxidative Stress Caused by Fine Particles (PM2.5) Exhausted from Heavy-Duty Vehicles Using Diesel/Biodiesel Blends under Real World Conditions. *J Braz Chem Soc*. Published online 2017. doi:10.21577/0103-5053.20170223

71. Daher N, Saliba NA, Shihadeh AL, et al. Oxidative potential and chemical speciation of size-resolved particulate matter (PM) at near-freeway and urban background sites in the greater Beirut area. *Sci Total Environ*. 2014;470-471:417-426. doi:10.1016/j.scitotenv.2013.09.104

72. Crobeddu B, Baudrimont I, Deweirdt J, et al. Lung Antioxidant Depletion: A Predictive Indicator of Cellular Stress Induced by Ambient Fine Particles. *Environ Sci Technol*. 2020;54(4):2360-2369. doi:10.1021/acs.est.9b05990

73. Fujitani Y, Furuyama A, Tanabe K, Hirano S. Comparison of Oxidative Abilities of PM2.5 Collected at Traffic and Residential Sites in Japan. Contribution of Transition Metals and Primary and Secondary Aerosols. *Aerosol Air Qual Res*. 2017;17(2):574-587. doi:10.4209/aaqr.2016.07.0291

74. Dou J, Lin P, Kuang BY, Yu JZ. Reactive Oxygen Species Production Mediated by Humic-like Substances in Atmospheric Aerosols: Enhancement Effects by Pyridine, Imidazole, and Their Derivatives. *Environ Sci Technol*. 2015;49(11):6457-6465. doi:10.1021/es5059378

75. Yadav S, Kapoor TS, Vernekar P, Phuleria HC. Examining the Chemical and Optical Properties of Biomass-burning Aerosols and their Impact on Oxidative Potential. *Aerosol Air Qual Res*. 2023;23:230102. doi:10.4209/aaqr.230102

76. Zhang H hui, Li Z, Liu Y, et al. Physical and chemical characteristics of PM2.5 and its toxicity to human bronchial cells BEAS-2B in the winter and summer. *J Zhejiang Univ-Sci B*. 2018;19(4):317-326. doi:10.1631/jzus.B1700123

77. Hiraiwa K, Van Eeden SF. Contribution of Lung Macrophages to the Inflammatory Responses Induced by Exposure to Air Pollutants. *Mediators Inflamm*. 2013;2013:1-10. doi:10.1155/2013/619523

78. Barnes PJ. Oxidative Stress in Chronic Obstructive Pulmonary Disease. *Antioxidants*. 2022;11(5):965. doi:10.3390/antiox11050965

79. Cohen H, Newburger P, Chovaniec M, Whitin J, Simons E. Opsonized zymosan-stimulated granulocytes-activation and activity of the superoxide-generating system and membrane potential changes. *Blood*. 1981;58(5):975-982. doi:10.1182/blood.V58.5.975.975

80. Becker S, Soukup JM, Gallagher JE. Differential particulate air pollution induced oxidant stress in human granulocytes, monocytes and alveolar macrophages. *Toxicol In Vitro*. 2002;16(3):209-218. doi:10.1016/s0887-2333(02)00015-2

81. Taciak B, Białasek M, Braniewska A, et al. Evaluation of phenotypic and functional stability of RAW 264.7 cell line through serial passages. Roberts DD, ed. *PLOS ONE*. 2018;13(6):e0198943. doi:10.1371/journal.pone.0198943

82. Yang M, Ahmed H, Wu W, Jiang B, Jia Z. Cytotoxicity of Air Pollutant 9,10-Phenanthrenequinone: Role of Reactive Oxygen Species and Redox Signaling. *BioMed Res Int*. 2018;2018:1-15. doi:10.1155/2018/9523968

83. Tuet WY, Fok S, Verma V, et al. Dose-dependent intracellular reactive oxygen and nitrogen species (ROS/RNS) production from particulate matter exposure: comparison to oxidative potential and chemical composition. *Atmos Environ*. 2016;144:335-344. doi:10.1016/j.atmosenv.2016.09.005

84. Labedzka M, Gulyas H, Gercken G. Zymosan-induced chemiluminescence of alveolar macrophages: Depression by inorganic dust constituents. *Arch Environ Contam Toxicol*. 1991;21(1):51-57. doi:10.1007/BF01055555

85. Sada-Ovalle I, Chávez-Galán L, Vasquez L, et al. Macrophage Exposure to Polycyclic Aromatic Hydrocarbons From Wood Smoke Reduces the Ability to Control Growth of Mycobacterium tuberculosis. *Front Med*. 2018;5:309. doi:10.3389/fmed.2018.00309

86. Dong TTT, Hinwood AL, Callan AC, Zosky G, Stock WD. In vitro assessment of the toxicity of bushfire emissions: A review. *Sci Total Environ*. 2017;603-604:268-278. doi:10.1016/j.scitotenv.2017.06.062

87. Franzi LM, Bratt JM, Williams KM, Last JA. Why is particulate matter produced by wildfires toxic to lung macrophages? *Toxicol Appl Pharmacol*. 2011;257(2):182-188. doi:10.1016/j.taap.2011.09.003

88. Kubátová A, Dronen LC, Picklo, MJ, Hawthorne SB. Midpolarity and Nonpolar Wood Smoke Particulate Matter Fractions Deplete Glutathione in RAW 264.7 Macrophages. *Chem Res Toxicol*. 2006;19(2):255-261. doi:10.1021/tx050172f

89. Jalava PI, Salonen RO, Hälinen AI, et al. In vitro inflammatory and cytotoxic effects of size-segregated particulate samples collected during long-range transport of wildfire smoke to Helsinki. *Toxicol Appl Pharmacol*. 2006;215(3):341-353. doi:10.1016/j.taap.2006.03.007

90. Tao F, Gonzalez-Flecha B, Kobzik L. Reactive oxygen species in pulmonary inflammation by ambient particulates. *Free Radic Biol Med*. 2003;35(4):327-340. doi:10.1016/S0891-5849(03)00280-6

91. Valderrama A, Ortiz-Hernández P, Agraz-Cibrián JM, et al. Particulate matter (PM10) induces in vitro activation of human neutrophils, and lung histopathological alterations in a mouse model. *Sci Rep*. 2022;12(1):7581. doi:10.1038/s41598-022-11553-6

92. Jastroch M, Divakaruni AS, Mookerjee S, Treberg JR, Brand MD. Mitochondrial proton and electron leaks. Brown GC, Murphy MP, eds. *Essays Biochem*. 2010;47:53-67. doi:10.1042/bse0470053

93. Ham M, Lee JW, Choi AH, et al. Macrophage Glucose-6-Phosphate Dehydrogenase Stimulates Proinflammatory Responses with Oxidative Stress. *Mol Cell Biol*. 2013;33(12):2425-2435. doi:10.1128/MCB.01260-12

94. Singh A, Happel C, Manna SK, et al. Transcription factor NRF2 regulates miR-1 and miR-206 to drive tumorigenesis. *J Clin Invest*. 2013;123(7):2921-2934. doi:10.1172/JCI66353

95. Polat IH, Tarrado-Castellarnau M, Benito A, et al. Glutamine Modulates Expression and Function of Glucose 6-Phosphate Dehydrogenase via NRF2 in Colon Cancer Cells. *Antioxidants*. 2021;10(9):1349. doi:10.3390/antiox10091349

96. Drost EM. Oxidative stress and airway inflammation in severe exacerbations of COPD. *Thorax*. 2005;60(4):293-300. doi:10.1136/thx.2004.027946

97. Qiao M, Kisgati M, Cholewa JM, et al. Increased Expression of Glutathione Reductase in Macrophages Decreases Atherosclerotic Lesion Formation in Low-Density Lipoprotein Receptor–Deficient Mice. *Arterioscler Thromb Vasc Biol*. 2007;27(6):1375-1382. doi:10.1161/ATVBAHA.107.142109

98. Li N, Alam J, Venkatesan MI, et al. Nrf2 Is a Key Transcription Factor That Regulates Antioxidant Defense in Macrophages and Epithelial Cells: Protecting against the Proinflammatory and Oxidizing Effects of Diesel Exhaust Chemicals. *J Immunol*. 2004;173(5):3467-3481. doi:10.4049/jimmunol.173.5.3467

99. Wittkopp S, Staimer N, Tjoa T, et al. Nrf2-related gene expression and exposure to traffic-related air pollution in elderly subjects with cardiovascular disease: An exploratory panel study. *J Expo Sci Environ Epidemiol*. 2016;26(2):141-149. doi:10.1038/jes.2014.84

100. Suzuki M, Betsuyaku T, Ito Y, et al. Down-Regulated NF-E2–Related Factor 2 in Pulmonary Macrophages of Aged Smokers and Patients with Chronic Obstructive Pulmonary Disease. *Am J Respir Cell Mol Biol*. 2008;39(6):673-682. doi:10.1165/rcmb.2007-0424OC

101. Mondal NK, Saha H, Mukherjee B, Tyagi N, Ray MR. Inflammation, oxidative stress, and higher expression levels of Nrf2 and NQO1 proteins in the airways of women chronically exposed to biomass fuel smoke. *Mol Cell Biochem*. 2018;447(1-2):63-76. doi:10.1007/s11010-018-3293-0

102. Zhang H, Guan R, Zhang Z, et al. LncRNA Nqo1-AS1 Attenuates Cigarette Smoke-Induced Oxidative Stress by Upregulating its Natural Antisense Transcript Nqo1. *Front Pharmacol*. 2021;12:729062. doi:10.3389/fphar.2021.729062

103. Li Z, Zhang Y, Jin T, et al. NQO1 protein expression predicts poor prognosis of non-small cell lung cancers. *BMC Cancer*. 2015;15(1):207. doi:10.1186/s12885-015-1227-8

104. Kaghazchi B, Um IH, Elshani M, Read OJ, Harrison DJ. Spatial Analysis of NQO1 in Non-Small Cell Lung Cancer Shows Its Expression Is Independent of NRF1 and NRF2 in the Tumor Microenvironment. *Biomolecules*. 2022;12(11):1652. doi:10.3390/biom12111652

105. Dinkova-Kostova AT, Talalay P. NAD(P)H:quinone acceptor oxidoreductase 1 (NQO1), a multifunctional antioxidant enzyme and exceptionally versatile cytoprotector. *Arch Biochem Biophys*. 2010;501(1):116-123. doi:10.1016/j.abb.2010.03.019

106. Quiles JM, Narasimhan M, Shanmugam G, Milash B, Hoidal JR, Rajasekaran NS. Differential regulation of miRNA and mRNA expression in the myocardium of Nrf2 knockout mice. *BMC Genomics*. 2017;18(1):509. doi:10.1186/s12864-017-3875-3

107. Kumar RR, Narasimhan M, Shanmugam G, et al. Abrogation of Nrf2 impairs antioxidant signaling and promotes atrial hypertrophy in response to high-intensity exercise stress. *J Transl Med*. 2016;14(1):86. doi:10.1186/s12967-016-0839-3

108. Kimura A, Kitajima M, Nishida K, et al. NQO1 inhibits the TLR-dependent production of selective cytokines by promoting IκB-ζ degradation. *J Exp Med*. 2018;215(8):2197-2209. doi:10.1084/jem.20172024

109. Vankova D, Kiselova-Kaneva Y, Ivanova D. Uric acid effects on glutathione metabolism estimated by induction of glutamate-cysteine ligase, glutathione reductase and glutathione synthetase in mouse J744A.1 macrophage cell line. *Folia Med (Plovdiv)*. 2022;64(5):762-769. doi:10.3897/folmed.64.e65507

110. Rao X, Huang X, Zhou Z, Lin X. An improvement of the 2ˆ(-delta delta CT) method for quantitative real-time polymerase chain reaction data analysis. *Biostat Bioinforma Biomath*. 2013;3(3):71-85.

111. Lim SL, Tran DN, Zumkehr J, et al. Inhibition of hematopoietic cell kinase dysregulates microglial function and accelerates early stage Alzheimer's disease-like neuropathology. *Glia*. 2018;66(12):2700-2718. doi:10.1002/glia.23522

112. Hur J, Rhee CK, Jo YS. Effects of Antioxidant on Oxidative Stress and Autophagy in Bronchial Epithelial Cells Exposed to Particulate Matter and Cigarette Smoke Extract. *Tuberc Respir Dis*. 2022;85(3):237-248. doi:10.4046/trd.2021.0152

113. Hatzis C, Godleski JJ, González-Flecha B, Wolfson JM, Koutrakis P. Ambient Particulate Matter Exhibits Direct Inhibitory Effects on Oxidative Stress Enzymes. *Environ Sci Technol*. 2006;40(8):2805-2811. doi:10.1021/es0518732

114. Staimer N, Nguyen TB, Nizkorodov SA, Delfino RJ. Glutathione peroxidase inhibitory assay for electrophilic pollutants in diesel exhaust and tobacco smoke. *Anal Bioanal Chem*. 2012;403(2):431-441. doi:10.1007/s00216-012-5823-z

115. Oh ET, Kim HG, Kim CH, et al. NQO1 regulates cell cycle progression at the G2/M phase. *Theranostics*. 2023;13(3):873-895. doi:10.7150/thno.77444

116. Yang, Wu, Yen, et al. The Redox Role of G6PD in Cell Growth, Cell Death, and Cancer. *Cells*. 2019;8(9):1055. doi:10.3390/cells8091055

117. Jalava PI, Salonen RO, Pennanen AS, et al. Heterogeneities in Inflammatory and Cytotoxic Responses of RAW 264.7 Macrophage Cell Line to Urban Air Coarse, Fine, and Ultrafine Particles From Six European Sampling Campaigns. *Inhal Toxicol*. 2007;19(3):213-225. doi:10.1080/08958370601067863

118. Wu J, Shi Y, Asweto CO, et al. Fine particle matters induce DNA damage and G2/M cell cycle arrest in human bronchial epithelial BEAS-2B cells. *Environ Sci Pollut Res*. 2017;24(32):25071-25081. doi:10.1007/s11356-017-0090-3

119. Abbas I, Badran G, Verdin A, et al. In vitro evaluation of organic extractable matter from ambient PM2.5 using human bronchial epithelial BEAS-2B cells: Cytotoxicity, oxidative stress, pro-inflammatory response, genotoxicity, and cell cycle deregulation. *Environ Res*. 2019;171:510-522. doi:10.1016/j.envres.2019.01.052

120. Longhin E, Holme JA, Gutzkow KB, et al. Cell cycle alterations induced by urban PM2.5 in bronchial epithelial cells: characterization of the process and possible mechanisms involved. *Part Fibre Toxicol*. 2013;10(1):63. doi:10.1186/1743-8977-10-63

121. Roman A, Korostyński M, Jankowska-Kieltyka M, Piechota M, Hajto J, Nalepa I. Gene Expression Changes Induced by Exposure of RAW 264.7 Macrophages to Particulate Matter of Air Pollution: The Role of Endotoxins. *Biomolecules*. 2022;12(8):1100. doi:10.3390/biom12081100

122. Park S, Ku J, Lee SM, et al. Potential toxicity of inorganic ions in particulate matter: Ion permeation in lung and disruption of cell metabolism. *Sci Total Environ*. 2022;824:153818. doi:10.1016/j.scitotenv.2022.153818

123. Wyzga RE, Rohr AC. Long-term particulate matter exposure: Attributing health effects to individual PM components. *J Air Waste Manag Assoc*. 2015;65(5):523-543. doi:10.1080/10962247.2015.1020396

124. Levy JI, Diez D, Dou Y, Barr CD, Dominici F. A Meta-Analysis and Multisite Time-Series Analysis of the Differential Toxicity of Major Fine Particulate Matter Constituents. *Am J Epidemiol*. 2012;175(11):1091-1099. doi:10.1093/aje/kwr457

125. Weimer S, Alfarra MR, Schreiber D, Mohr M, Prévôt ASH, Baltensperger U. Organic aerosol mass spectral signatures from wood-burning emissions: Influence of burning conditions and wood type. *J Geophys Res Atmospheres*. 2008;113(D10):2007JD009309. doi:10.1029/2007JD009309

126. Jones JM, Ross AB, Mitchell EJS, Lea-Langton AR, Williams A, Bartle KD. Organic carbon emissions from the co-firing of coal and wood in a fixed bed combustor. *Fuel*. 2017;195:226-231. doi:10.1016/j.fuel.2017.01.061

127. Shen G, Xue M, Wei S, et al. Influence of fuel moisture, charge size, feeding rate and air ventilation conditions on the emissions of PM, OC, EC, parent PAHs, and their derivatives from residential wood combustion. *J Environ Sci*. 2013;25(9):1808-1816. doi:10.1016/S1001-0742(12)60258-7

128. Greenberg JP, Friedli H, Guenther AB, Hanson D, Harley P, Karl T. Volatile organic emissions from the distillation and pyrolysis of vegetation. *Atmospheric Chem Phys*. 2006;6(1):81-91. doi:10.5194/acp-6-81-2006

129. Sekimoto K, Koss AR, Gilman JB, et al. High- and low-temperature pyrolysis profiles describe volatile organic compound emissions from western US wildfire fuels. *Atmospheric Chem Phys*. 2018;18(13):9263-9281. doi:10.5194/acp-18-9263-2018

130. Engels SM, Kamat P, Pafilis GS, et al. *Particulate Matter Composition Drives Differential Molecular and Morphological Responses in Lung Epithelial Cells*. Systems Biology; 2023. doi:10.1101/2023.05.17.541204

131. Graff DW, Schmitt MT, Dailey LA, Duvall RM, Karoly ED, Devlin RB. Assessing the Role of Particulate Matter Size and Composition on Gene Expression in Pulmonary Cells. *Inhal Toxicol*. 2007;19(sup1):23-28. doi:10.1080/08958370701490551

Appendix A: Supporting Material for Chapter 4

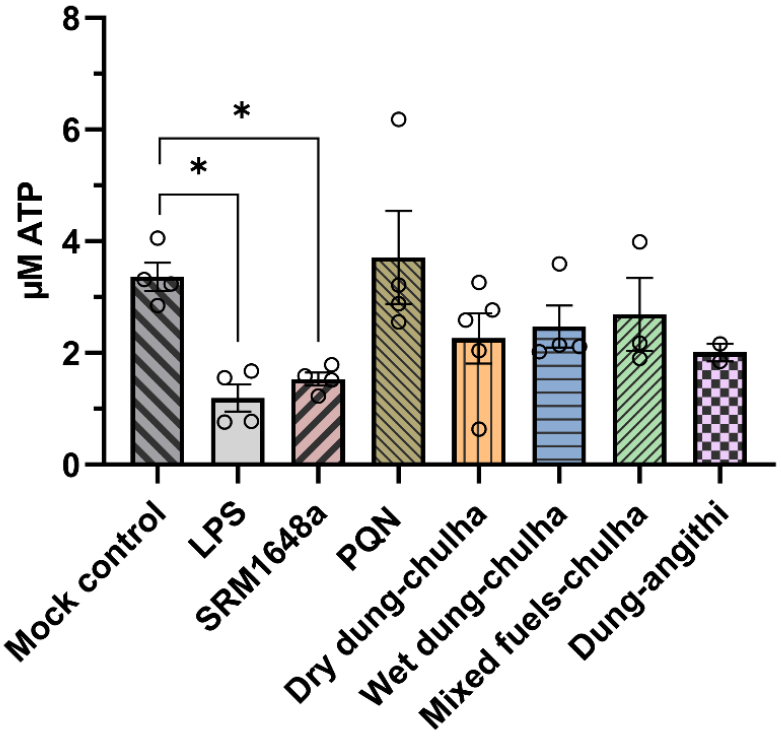

Figure A1: Intracellular ATP levels in macrophages following 4-hour exposure to PM. *RAW 264.7 cells were seeded at a concentration of 1.5 x 10^4 cells per well in a 96 well plate and exposed to 50 µg of PM per well (16 µg/cm^2) for four hours before assessing intracellular adenosine triphosphate (ATP) levels with the Luminescent ATP Detection Kit (Abcam) according to the manufacturer's instructions using a Centro LB 960 Chemiluminescent Instrument (Berthold Technologies, Bad Wildbad, Germany). Intracellular ATP levels were determined by linear regression from an ATP standard curve (0-10 µM). A total of N = 5 dry dung-chulha filters, N = 4 wet dung-chulha filters, N = 3 mixed fuels-chulha filters, N = 2 dung-angithi filters were used in this experiment. Two biological replicates for each individual PM filter sample were included to assess the mean intracellular ATP concentration. SRM1648a and PQN were included to compare the effects of PM from different sources. Lipopolysaccharide (LPS) was used as positive control for ATP depletion, with cells being exposed to 1µg of LPS (3.1 µg/cm^2). All data were expressed as means ± SEM. Statistical significance was assessed at P <0.05 using the nonparametric Mann-Whitney compared to mock control cells. The LPS positive control and the SRM1648a treated cells showed statistically significant reductions in intracellular ATP compared to mock treated controls (P =.029 got both samples). No statistically significant differences in intracellular ATP were observed for cells exposed to solid biofuel PM emissions compared to mock controls.*

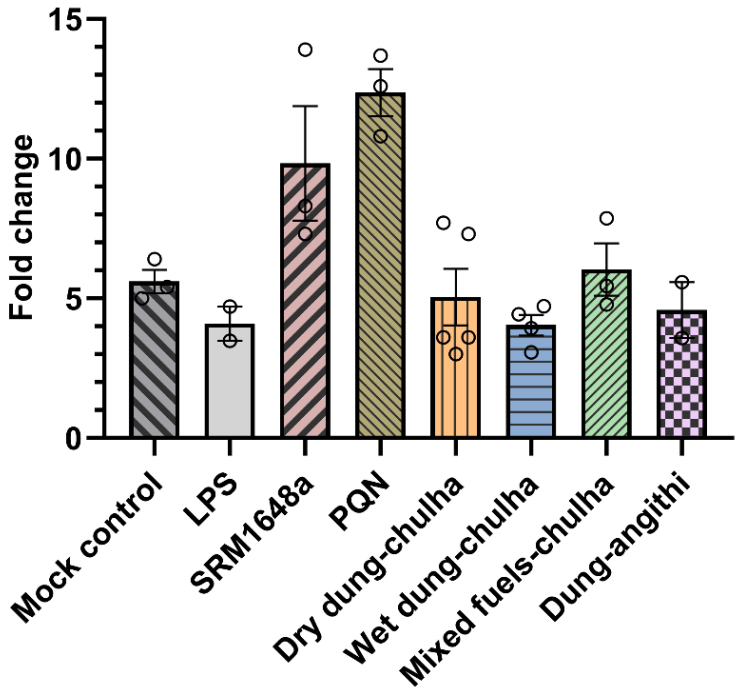

Figure A2: Lactate dehydrogenase cytotoxicity assay. *Cell viability was determined by measuring the cellular release of LDH from the cytosol into the extracellular cell media* 22*-hours after initial acute exposure to PM, using the Pierce LDH Cytotoxicity Kit (Thermo Fisher) according to manufacturer's instructions. RAW 264.7 cells were plated at a density of 2.5 x* 10^5 *cells per well on a 24-well plate and were treated with 100 µL of PM extracts in a total of 500 µL media for four hours. Macrophages rested in clean media after the 4-hour exposure to PM. Cells were exposed to lipopolysaccharide bacteria membrane (LPS, 13 µg/cm*^{2}*), SRM 1648a, biomass PM (26 µg/cm*^{2}*), or PQN (0.003 µg/cm*^{2}*) and then allowed to rest in clean media for 18-hours before accessing LDH secretion. Values represent the mean percent of cell with excess LDH secretion normalized to the mock control of 1 ± SEM. A minimum of two biological replicates for each exposure sample was used to assess the mean values. A total of N = 5 dry dung-chulha filters, N = 4 wet dung-chulha filters, N = 3 mixed fuels-chulha filters, N = 2 dung-angithi filters were used in this experiment. Statistical significance was assessed at P <0.05 using the nonparametric Mann-Whitney compared to mock control cells. Increased secretion of LDH indicates cell membrane damage, and these results confirm that cells treated with biomass emissions did not exhibit any cytotoxicity when compared to mock controls. Cells exposed to SRM1648a or PQN demonstrated a higher percentage of cytotoxic cells compared to mock control cells, but effects were not statistically significant.*